PHOTOPHYSICS AND PHOTOCHEMISTRY OF PHENANTHRENE, 1,3-DIKETONATOBORON DIFLUORIDES

by

Susan Pin Wu

B.Sc., Sichuan Normal University, 1983

THESIS SUBMITTED IN PARTIAL FULFILLMENT OF

THE REQUIREMENTS FOR THE DEGREE OF

MASTER OF SCIENCE

in the Department

of

Chemistry

© Susan Pin Wu 1994

SIMON FRASER UNIVERSITY

May 1994

APPROVAL

Name: Susan Pin Wu

Degree: Master of Science

Title of Thesis: Photophysics and Photochemistry of Phenanthrene, 1,3-Diketonatoboron Difluorides.

Examining Committee:

Chair: Dr. F.W.B. Einstein

Dr. Y.L. Chow
Senior Supervisor

Dr. A.S. Tracey
Committee Member

Dr. R.H. Hill,
Committee Member

Internal Examiner: Dr. S. Holdcroft

Date Approved: _____ May 5 / 94 _____

PARTIAL COPYRIGHT LICENSE

I hereby grant to Simon Fraser University the right to lend my thesis, project or extended essay (the title of which is shown below) to users of the Simon Fraser University Library, and to make partial or single copies only for such users or in response to a request from the library of any other university, or other educational institution, on its own behalf or for one of its users. I further agree that permission for multiple copying of this work for scholarly purposes may be granted by me or the Dean of Graduate Studies. It is understood that copying or publication of this work for financial gain shall not be allowed without my written permission.

Title of Thesis/Project/Extended Essay:

photophysics and Photochemistry of Phenanthrene , 1,3 - Diketonatoboron Difluorides

Author:

_____
(signature)

Susan Pin Wu
(name)

May 6 / 94
(date)

Abstract

Photocycloaddition of phenanthrene (PN) with acetylacetonatoboron difluoride (AABF$_2$) was studied. The reaction yields 1,5-diketone products in dioxane and diethyl ether, but not in acetonitrile. Mechanistic studies were carried out. The quantum yields of the products are only dependent on the concentration of AABF$_2$, not the concentration of PN. This indicates that an excited state PN is the initial excited species. Triplet sensitization by acetophenone or benzophenone does not induce a photocycloaddition, implying the singlet mechanism. Fluorescence quenching studies showed that singlet excited PN was quenched by AABF$_2$ and formed an emissive exciplex with a well defined isoemissive point in the low concentration range, [AABF$_2$] ≤ 0.03 M. The results of this work demonstrate unambiguously that this exciplex is the intermediate for photocycloaddition. In contrast, the excitation of AABF$_2$ in the presence of PN gives neither exciplex emission nor any products. The dipole moment of the PN/AABF$_2$ exciplex was estimated based on its static property to give 11.6 D, reflecting the strong electron transfer character. Steady state and time-resolved fluorimetry were used to investigate the kinetics of the interaction of the singlet excited state PN and the exciplex with ground state AABF$_2$ in dioxane. Many rate constants for the formation and decay of the photochemically reactive exciplex were measured. Quenching of the exciplex by ground state AABF$_2$ occurs, and the quantum yield conveys dependency on the square of its concentrations that would fit a nonlinear relation in the double reciprocal plot of $1/\Phi$ vs $1/$[AABF$_2$]. The plot started to curve upward at [AABF$_2$] = 0.025 M owing to simultaneous complication from quenching of exciplex by AABF$_2$ and unproductive absorption by AABF$_2$, particularly at a high concentration range. Experimentally, the isoemissive point is unfocused

at [AABF2] $\geq$ 0.025 M, indicating the effect of exciplex quenching.   In acetonitrile, singlet excited PN preferentially undergoes electron transfer to give the PN cation radical without causing a cycloaddition.

Preliminary investigations of the photophysics of the 4-tert-butyl 4'-methoxy-dibenzoylmethanatoborodifluoride (MBDBF$_2$) and photocycloaddition of MBDBF$_2$ to several olefins were carried out. Fluorescence studies showed that the monomer of MBDBF$_2$ was quenched by norbornylene, 1,3-pentadiene, methyl methacrylate and cyclohexene when the concentration of MBDBF$_2$ was low (10^{-6} M) and excimer of MBDBF$_2$ was formed when the concentration of MBDBF$_2$ was high (10^{-2} M). MBDBF$_2$ was irradiated in the presence of several olefins including norbornylene, 1,3-pentadiene, methyl methacrylate and cyclohexene. In the presence of these olefins, 1:1 adducts of 1,5 diketones were obtained, which were assumed to be formed by a [2+2] photoaddition followed by cyclobutane ring opening to give 1,2-addition products. Irradiations of MBDBF$_2$ to 1,3-pentadiene and methyl methacrylate give only head to head adducts. Photoaddition preferentially occurs at the carbon-carbon double bond adjacent to the *p*-methoxyphenyl side with high regioselectivity.

.

Dedication

To my parents

To Yan Kang

Acknowledgments

The author wishes to express her gratitude to:

Table of Contents

Table of Figures

Table of Tables

CHAPTER 1   INTRODUCTION

1-1   1,3-Diketonatoboron Difluorides

β-diketonatoboron difluoride complexes have been known since 1924[1]. Since then the number of BF_2 complexes have been synthesized using the reaction of 1,3-diketones with BF_3[2,3]. Spectroscopic evidence suggests that the chelat ring system is stabilized by resonance. The chemical shifts of the two methyl groups of acetylacetonatoboron difluoride ($AABF_2$) are identical in both ^1H and ^{13}C NMR spectra, indicating that the methyl groups are chemically and magnetically equivalent[3,4]. X-ray crystallographic analysis of benzoylacetonatoboron difluoride ($BABF_2$) clearly shows that the two B-O bond lengths (1.488$\overset{0}{A}$) are identical as well as two C-O bond lengths (1.304$\overset{0}{A}$)[5]. The UV absorption of BF_2 complex shows a marked bathochromic shift of the absorption maximum, accompanied by an enhancement of extinction coefficient relative to the parent β-diketone which suggest π-π* transition in the delocalized π electron system in the chelating ligand[6]. Also, the IR spectra are different from that of free ligand. The C=C and C=O stretching vibrations shift to lower frequencies, therefore, no free carbonyl groups are present which is consistent with the chelated structure[7]. The high dipole moment results from the extensive resonance involved in the intramolecular charge transfer. For instance, $AABF_2$ and dibenzoylmethanatoboron difluoride ($DBMBF_2$) have dipole moments of 7.6 and 6.7 D, respectively[8]. In these chelate BF_2 complexes, the polarization of electron density results in a partial negative charge at the boron and a partial positive one at the ligand (scheme 1-1).

Scheme 1-1
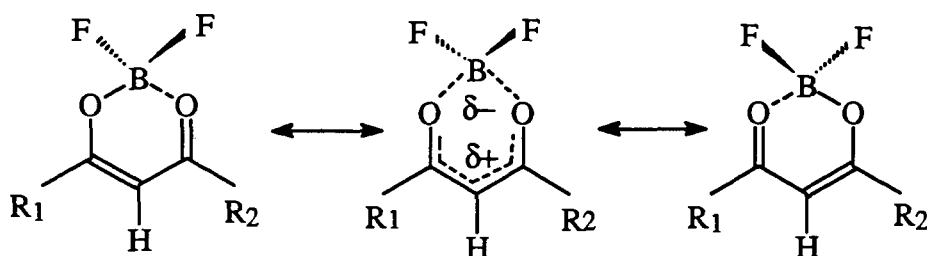
	R_1	R_2	Abbreviation
1	CH_3	CH_3	$AABF_2$
2	CH_3	C_6H_5	$BABF_2$
3	C_6H_5	C_6H_5	$DBMBF_2$

The reduction potentials of BF_2 complexes are 0.6 volt lower than their parent β-diketones. These BF_2 complexes have been used as electron acceptors in the design of photoconducting materials[9].

1-2 Photochemistry of 1,3-diketones

The [2+2] photocycloaddition of β-diketones with simple olefins was discovered by de Mayo, which is well known as the de Mayo reaction (Scheme

1-2). The reaction has been suggested to take place from the triplet state of the β-diketones[10]. This reaction gives an effective method for constructing carbon skeletons, but it suffers from a low quantum efficiency. Recently, the photocycloaddition of the BF_2 complexes of β-diketones have been investigated by Chow's group and it has been found to give a photoadduct pattern which is similar to those obtained from the de Mayo reaction. However, the reaction occurs from the singlet state of BF_2 β-diketone with an improved quantum efficiency[11, 12].

Scheme 1-2

The de Mayo Reaction
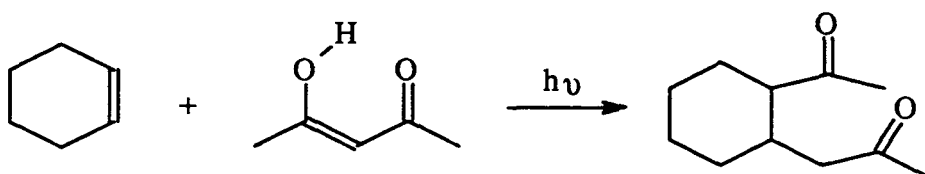
The dibenzoylmethanatoboron difluoride (DBMBF$_2$) has been chosen as a model compound to study the photophysics and photochemistry of these BF_2 complexes. It has been found that the logarithm of the observed quenching constant (k_q) of DBMBF$_2$ fluorescence by olefins correlates with the ionization potentials (IP) of the olefins. This correlation between log k_q and IP suggest that the interaction of singlet excited DBMBF$_2$ with olefins involve some degree of electron transfer in which DBMBF$_2$ acts as electron acceptor. The interaction of DBMBF$_2$ with various simple olefin gives regiospecific and highly stereospecific photocycloadducts of 1,5-diketones which are assumed to form by

3

a [2+2] photocycloaddition followed by hydrolysis in which the cyclobutane ring is opened (scheme 1-3).[13, 14]

Scheme 1-3
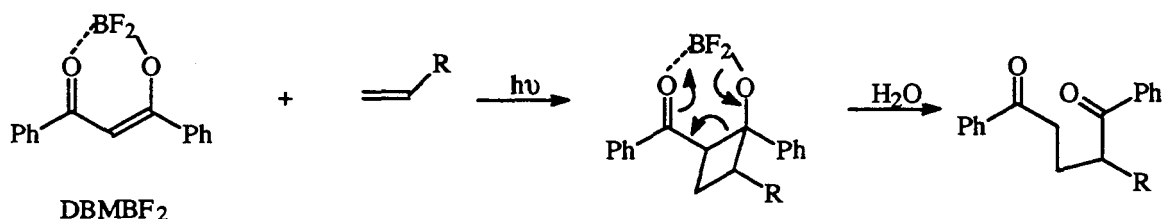
DBMBF$_2$

R	yield (%)
CH$_3$(CH$_2$)$_3$	78
(CH$_3$)$_3$C	69
CH$_2$=CH(CH$_2$)$_2$	92

A more favorable electron-transfer interaction is indicated in the photoreaction involving electron rich olefins. It is also found that DBMBF$_2$ sensitized some of the electron rich olefins to yield cation radical olefins that undergo dimerization with another ground state olefin and rearrangement[15] as illustrated in Scheme 1-4. This evidence suggested photoinduced electron transfer (PET).

Scheme 1-4

(endo)		(exo)
Major		Minor

4
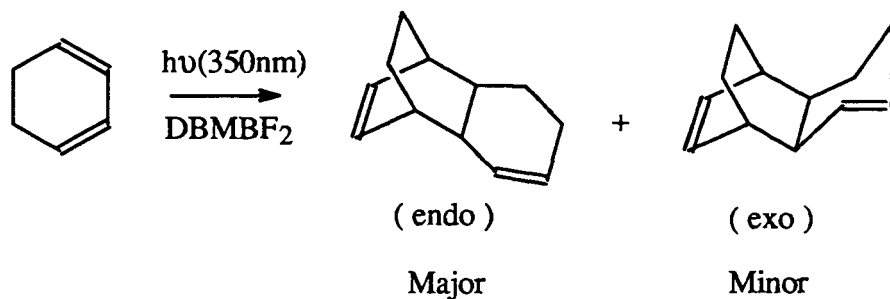
The strong exciplex emission of DBMBF$_2$ with methylated benzene have been observed, but no photocycloaddition products were detective[16]. In contrast, when the weak exciplex emission of AABF$_2$ with benzene derivatives is observed, alkyl-type 1,3-diketonatoboron difluorides such as AABF$_2$ react with benzene derivatives to give primarily [2+2] cycloaddition products[17]. This is consistent with the following rule of thumb: strong exciplex emission does not lead to products while weak exciplex emission does[18].

1-3 Phenanthrene

The photocycloaddition of phenanthrene (PN) to several electron-poor ethylenes, including maleic and fumaric acid derivatives, chloroethylenes and acrylonitrile, has been studied[19, 20]. The addition always occurs at the 9,10-position of PN to yield cyclobutane derivatives, except for the oxetane formed from dimethyl fumarate. Reaction of various derivatives of PN with different olefins does not fit to a single mechanism. For instance, the photocycloaddition of PN with dimethyl fumarate shows that the products of cyclobutane derivatives obtain either from direct irradiation or triplet sensitized irradiation. The product of oxetane is only observed on direct irradiation, which implies that oxetane is from the singlet state, while the formation of the cyclobutane adducts is preceded by a triplet state (*via* triplet exciplex as well as *via* triplet PN)[21].

The photocycloaddition of 9-cyanophenanthrene (9-CNPN) to several styrene derivatives has also been described (Scheme 1-5)[21].

5

Scheme1-5

9-CNPN   *trans*-anethole   (8)
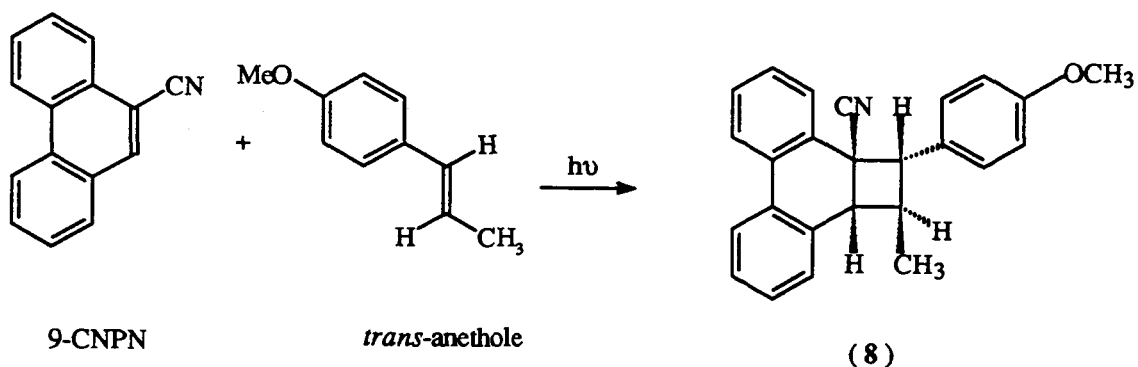
In several cases, exciplex emission was observed between 9-CNPN with styrene derivatives where an emissive exciplex offers a handle to link the photophysical and photochemical processes. In cases of photocycloaddition of 9-CNPN with substituted β-methylstyrenes, the emissive exciplex of 9-CNPN with *trans*-anethole was demonstrated to be a precursor of photocycloaddition[22]. These photoreactions have served as models among others, to connect the concept of exciplexes in photophysics and photochemistry. The investigation of intermediates in photocycloadditions is an intriguing area of photochemistry.

The previous experiments in our laboratory have shown that irradiation of a solution containing PN and AABF$_2$ gives *cis*- and *trans*-1,5-diketone isomers. The isolated yields are 46% and 5.6%, respectively (Scheme 1-6).[23a]

Scheme 1-6

(PN) (AABF$_2$) (9) (10)
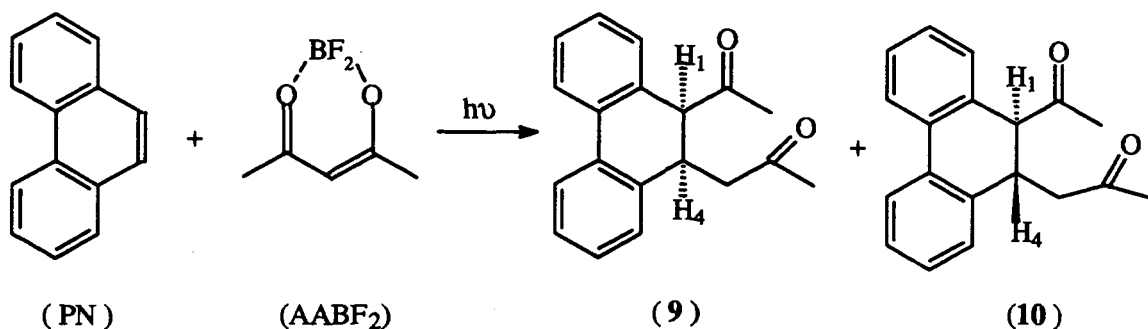
1-4   Research Proposal

DBMBF$_2$ and AABF$_2$ have been studied in Chow's group as a new type of electron acceptors.   Both were found to add to simple olefins but only AABF$_2$ added to methylated benzene and phenanthrene[23a]. The mechanism of photocycloaddition of AABF$_2$ with PN has not been explored yet. We decided to investigate the mechanism involved in this cycloaddition. The photophysical studies of new BF$_2$ complex (MBDBF$_2$) have been carried out in Chow's group.[23b] The photochemical behavior of new BF$_2$ complex (MBDBF$_2$) is still unknown. . We were interesting in the photochemical reaction of MBDBF$_2$ and photophysical behavior in corresponding solvent.   These decisions were based on the following considerations:

(1)   The BF$_2$ complexes are easily synthesized and purified.

(2)   The BF$_2$ complexes have high extinction coefficients (such as AABF$_2$ ε_{max} =16800 in ether), therefore they absorb light very efficiently.

(3)   1,3-diketonatoboron difluorides are better electron acceptors compared with the parent 1,3-diketones.

(4)   The BF_2 complexes are fairly stable, both thermally and towards the light.

(5)   The photochemistry of $MBDBF_2$ with the various types of olefins is unknown.

(6)   The photocycloaddition of PN with $AABF_2$ has considerable interests from the synthetic and the mechanistic point of view.

The aim of this research can be outlined as follows:

(1) To investigate the mechanism of the photocycloaddition of $AABF_2$ and PN involved in following:

        (i)   To determine the reactive species and the multiplicity of the reactive excited species involved in the photocycloaddition;

        (ii)   To explore the type of intermediate(s) involved;

        (iii)   To study the kinetics of the photocycloaddition by using quantum yield measurements, fluorescence quenching, and time-resolved fluorescence decay.

(2) To examine the absorption and fluorescence emission of $MBDBF_2$;

(3) To conduct $MBDBF_2$ fluorescence quenching with various types of olefins;

(4) To explore the photocycloaddition of $MBDBF_2$ with olefins.

CHAPTER 2   RESULTS

2-1   Mechanistic Studies for the Photocycloaddition of PN and AABF$_2$

2-1.1 Product Studies

AABF$_2$ undergoes a relatively efficient [2+2] photocycloaddition with PN as shown in Scheme 1-6.   The photoaddition was found to be solvent dependent; the reaction occured only in weakly polar solvents (ether and dioxane) , but not in a polar solvent (acetronitrile).

The material balance of this reaction was determined by GC analysis and plotted in Fig.2-1.   The formation of *trans*-product (10) was detectable but insignificant, not exceeding 5 % after six hours irradiation.   This *trans*-product is likely a secondary product.
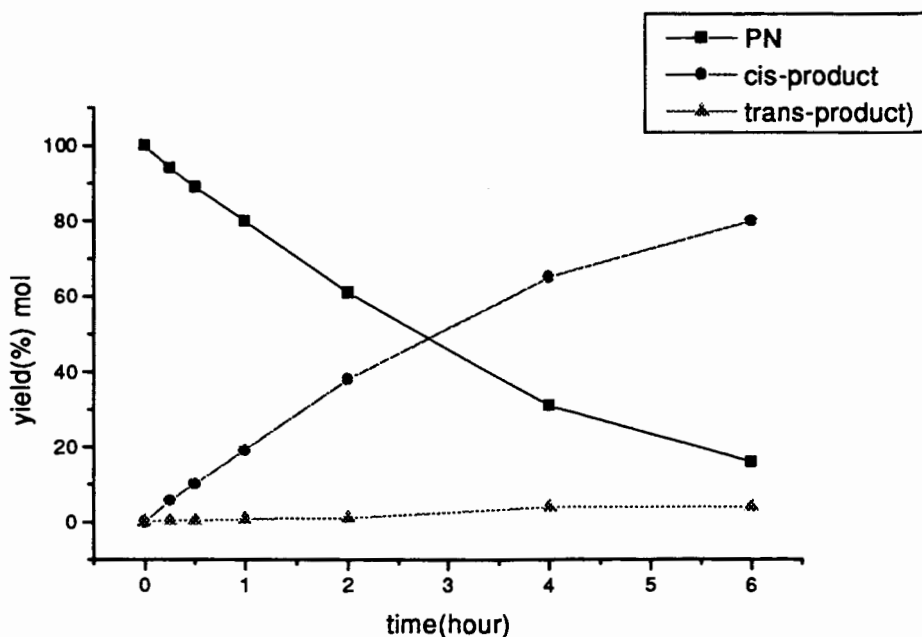
Fig. 2-1   Material balance in the photoaddition

of PN (0.02 M) with AABF$_2$(0.04 M)

In 0.1 N H_2SO_4 / CH_3OH solution, the *cis*-product (**9**) was slowly isomerized to the *trans*-product (**10**) with a low yield (5-6 % in 10 hours). However, treatment of the *cis* and *trans* mixture with a 0.2 N $NaOCH_3$-CH_3OH solution at room temperature, the trans-product (**10**) kept unchanged and the *cis*-product (**9**) underwent aldol condensation to give enones (**11**) and (**12**) with ratio of 99% to 1%, both enones showed the similar MS pattern, with the $M^+ + 1$ peak at 261 in GC-MS by electron impact ionization (EI) and chemical ionization (CI) mode. The major enone was isolated by flash chromatography. The structure (**11**) was identified based on the spectral data (IR, MS, ^1H NMR, ^{13}C NMR listed in Table 4-6 to Table 4-9). This is consistent with Ouyang's results[23]. The further confirmation of structue of (**11**) carried out by decoupling experiments. Structure (**11**) was favored on the basis that (i) a small coupling (J = 0.5 Hz) between the CH_3 and CH_2 groups and (ii) one aromatic proton at a relatively high chemical shift (7.05 ppm) arising from anisotropy of the nearby carbonyl group.

Scheme 2-1

(9) → H+ → (10)

NaOCH3   NaOCH3

(11)   (12)
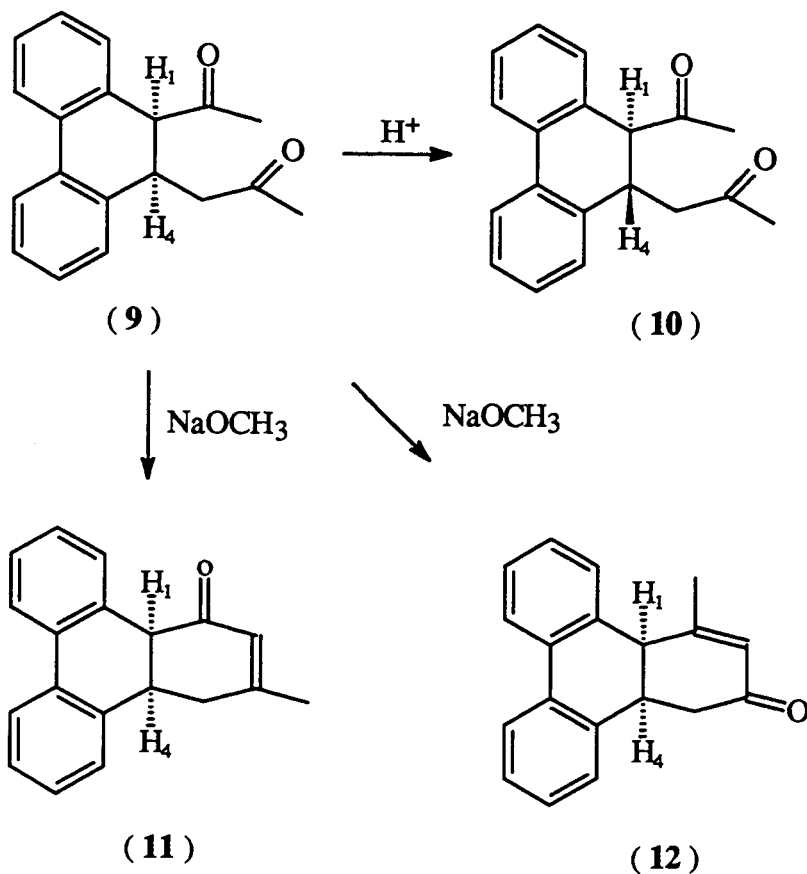
2-1.2 Quantum Yield Studies

The quantum yield is defined as following:

$$\Phi_{product} = \frac{\text{number of moles (molecules) of product formed}}{\text{number of einstein (photons) of radiation absorbed}}$$

$$= \frac{\text{rate of formation of product}}{\text{intensity of absorbed radiation}}$$

Important information concerning the kinetics of photocycloaddition can be obtained from the quantum yield of product formation as a function of reactant concentration.[24] In order to demonstrate which excited state initiates photocycloaddition, a series of the photoadditions was run either at a constant concentration of $AABF_2$ with increasing amounts of PN or vice versa in dioxane using RPR 3500A as the light source. Product quantum yields were determined under two sets of conditions. Firstly, when the $AABF_2$ concentration was held fixed at 0.02M, the quantum yield of product was found to be independent of the PN concentration, within experimental error. Secondly, the quantum yield of product formation for photocycloaddition was determined in the $AABF_2$ concentration in the range of 0.008-0.04 M, while the PN concentration was held fixed at 0.02 M. The quantum yield increased with increasing concentration of $AABF_2$ (0.008 M to 0.025 M) where a plot of reciprocal of quantum yield *versus* reciprocal of $AABF_2$ concentration gave a reasonable linear correlation (Fig.2-2). However, the experiment points started to curve upward at $[AABF_2] > 0.025$ M in dioxane; i.e., the quantum yield decreased with increasing $AABF_2$ concentration (Table 2-1 and Fig. 2-2). The linear portion could be extrapolated to the limit to give Ksv ($k_q\tau$ = intercept /slope) = 460 ± 140 M^{-1} in dioxane according to Eq.2-1. Such double reciprocal plots generally involve large error margins.

$$1 \,/\, \Phi = 1 \,/\, \beta + 1 \,/\, \beta K_{sv}[\, A \,] \qquad\qquad (2\text{-}1)$$

$$K_{sv} = \text{intercept} \,/\, \text{slope}$$

Table (2-1) Quantum Yield as a Function of the Concentration in Photocycloaddition of PN and AABF2

.# of Expt	$[AABF_2]$ (M)	R_f	Φ	$1/[AABF_2]$	$1/\Phi$
1	0.0064	0.165	0.0887	156	11.27
2	0.0080	0.166	0.0892	125	11.21
3	0.0088	0.177	0.0952	114	10.50
4	0.0104	0.181	0.0972	96	10.29
5	0.0120	0.180	0.0969	83	10.32
6	0.0140	0.184	0.0991	71	10.09
7	0.0160	0.189	0.102	63	9.80
8	0.0200	0.188	0.101	50	9.90
9	0.0240	0.183	0.0983	42	10.17
10	0.0400	0.153	0.0820	25	12.20

Notes:

a.   The 10 x 5mL sample solutions (pyrex tubes) containing PN (0.02 M), $C_{16}H_{34}$ (0.01 M ; as I.S.) and various of concentrations of $AABF_2$ were purged with N_2 for 10 minutes and irradiated for 14 minutes with RPR-350nm lamps.

b.   The quantum yields (Φ) were determined by a standard method (detail see experimental section).

c.   Percent conversion of PN were controlled under 10%.
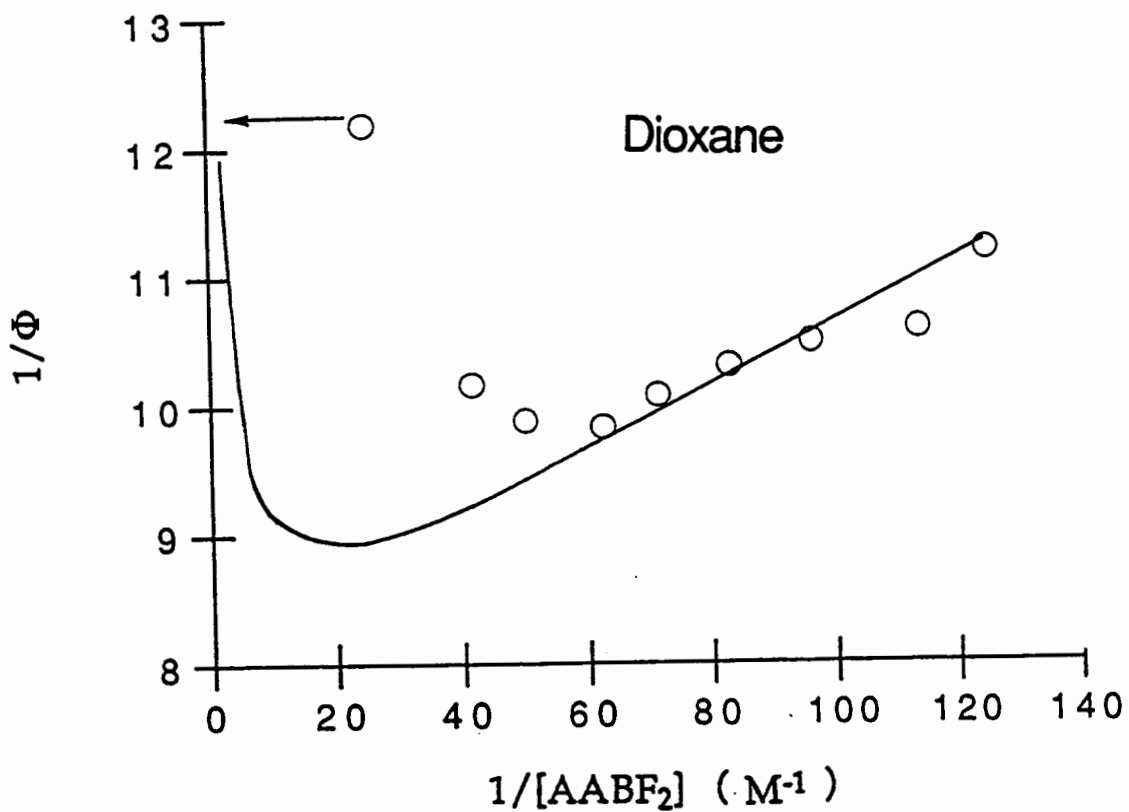
Fig. 2-2 Plot of $1/\Phi$ *versus* $1/$ $AABF_2$. The points are experimentally determined and the solid line is that computed from Eq. 3-1 and the rate constants given in Table 2-7

14

2-1.3 Triplet Sensitization

In order to investigate the possibility of a triplet state reaction between PN (E_S = 83 kcal / mol, E_T = 62 kcal / mol) and AABF$_2$ (E_S = 92 kcal / mol, E_T = 64 kal / mol), triplet sensitization experiments were carried out using acetophenone (E_S = 79 kcal / mol, E_T = 74 kcal / mol) and benzophenone (E_S = 74 kcal / mol, E_T = 69 kcal /mol) as triplet sensitizers. High concentrations (0.20 M) of sensitizers were used to ensure that most incident light had been absorbed (>90%) by the sensitizers. The concentration of PN and AABF$_2$ were 0.02 M. GC analysis showed no detectable cycloaddition products in the presence of triplet sensitizers, while the corresponding control experiment (in the absence of sensitizers) resulted in 20% yield of cycloaddition products.

2-1.4 Quenching of PN Fluorescence:

(a)   Quenching by AABF$_2$

PN exhibits strong fluorescence peaks and also phosphorescence in 2-propanol / ether at 77K (liquid nitrogen). The emissions were not affected by AABF$_2$ at 77K even when the concentration of AABF$_2$ was 0.025 M.   At room temperature, PN also showed strong fluorescence in most solvents.   PN's fluorescence was systematically reduced in the prescence of AABF$_2$. Quenching of PN (5 x 10^{-4} M) fluorescence intensity by AABF$_2$ (0-0.024 M) was examined in dioxane at room temperature. (Fig.2-3). The interaction in the low range of [AABF$_2$] < 0.025 M was analyzed according to the standard Stern-Volmer

equation (Eq. 2-2) where the Stern-Volmer constants K_{sv} ($kq\tau$) were found to be 120 M^{-1} (under air) and 276 M^{-1} (under argon) in dioxane (Fig. 2-4).

$$I^0 / I = 1 + K_{sv} [Q] = 1 + kq\tau [Q] \qquad (2\text{-}2)$$

The reduction of PN fluorescence intensity by AABF$_2$ was accompanied by the appearance of a new red-shifted and structureless emission band which showed the maximum at 480 nm and an isoemissive point at 438 nm in dioxane. The new emission was uncharacteristic of either PN's fluorescence or phosphorescence. AABF$_2$ does not show any detectable luminescence. It should be pointed out that neither the ground state complex of PN and AABF$_2$ nor the excimer of PN was observed under the experimental conditions similar to those of observing of new emission. Therefore, this new emission must be due to an excited state complex (exciplex) formed between singlet excited PN and a ground state AABF$_2$. This exciplex emission could only be observed in medium polarity solvents (such as, ether and dioxane), but not in acetonitrile. This isoemissive point started to lose at higher [AABF$_2$] of 0.035 M; the intensity of exciplex emission ceased to increase regardless of further quenching of PN fluorescence.
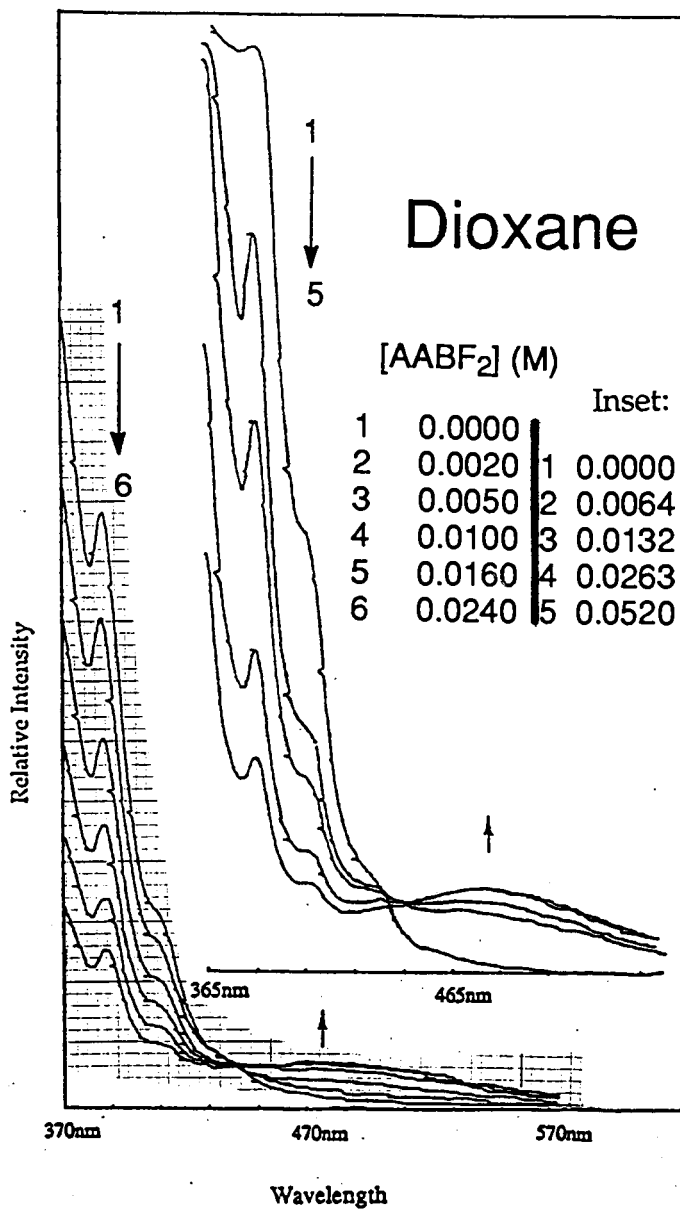
Fig. 2-3 Quenching of PN (5×10^{-4} M) fluorescence by $AABF_2$ (0 - 0.024 M) with $\lambda_{ex} = 350$ nm in dioxane. Inset: Similar quenching at higher $AABF_2$ concentration

17
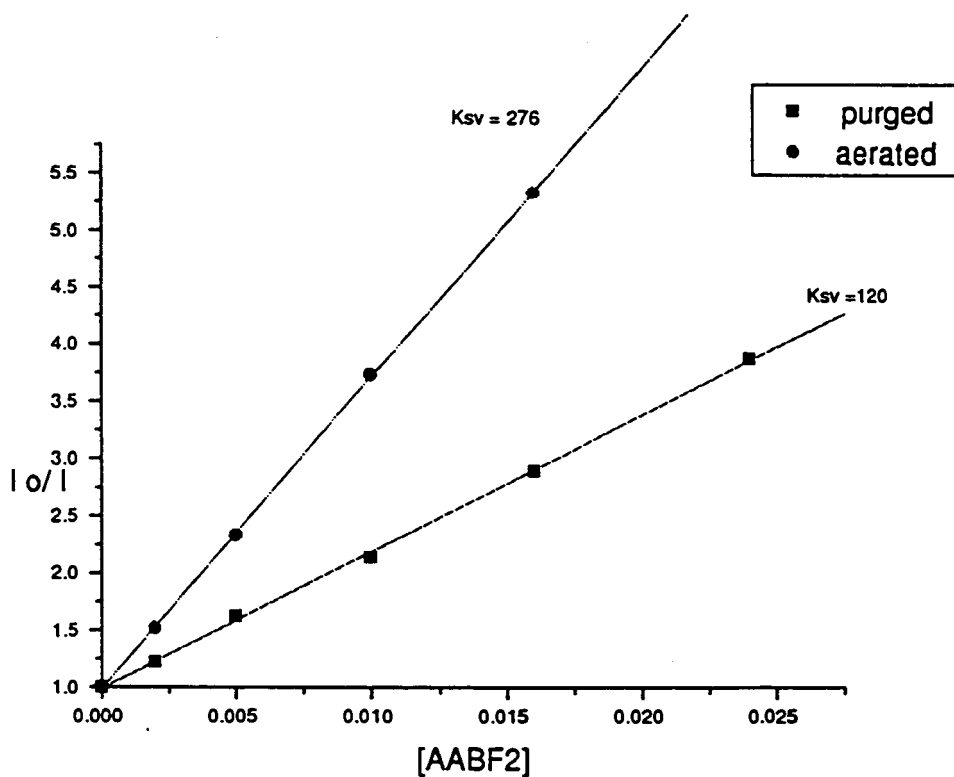
Fig. 2-4 The Stern-Volmer plot of quenching of PN (5×10^{-4} M)

by $AABF_2$ in dioxane

A PN fluorescence quenching study was also carried out in acetonitrile under argon. The result showed that PN fluorescence was reduced in the presence of $AABF_2$ (0 - 0.002 M) (Fig.2-5), however, no exciplex emission

could be detected in acetonitrile. This interaction was also analyzed by the Stern-Volmer equation to give a Stern-Volmer constant K_{sv} 538 M^{-1} .
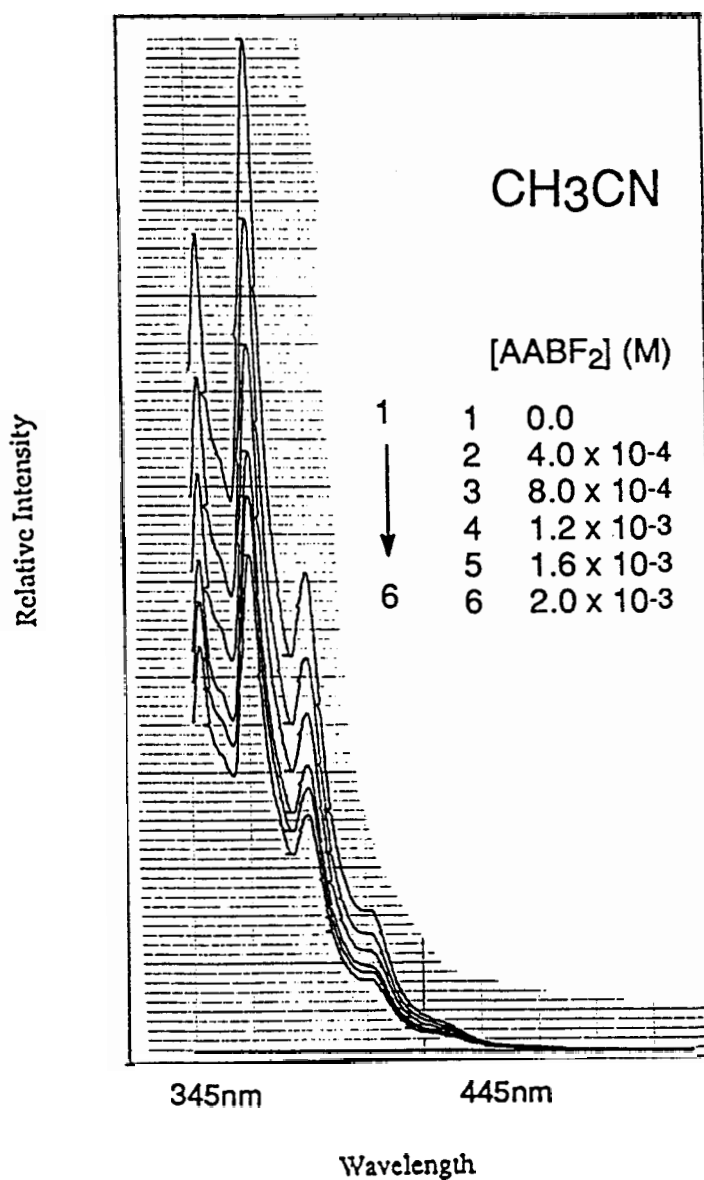
Fig. 2-5 Quenching of PN (5 ×10^{-4} M) fluorescence by AABF$_2$ (0 - 0.002 M)
with λex = 335 nm in CH$_3$CN
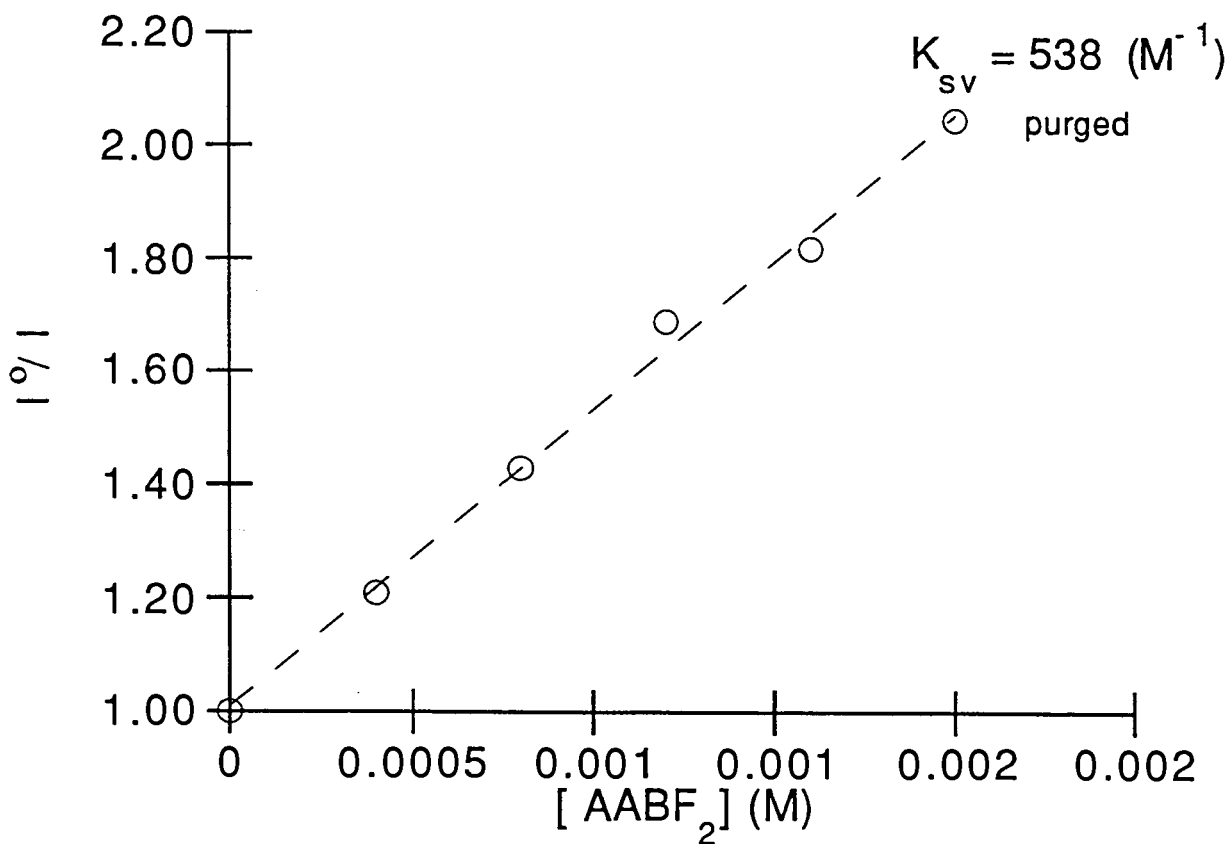
Fig. 2-6   The Stern-Volmer plot of quenching of PN (5×10^{-4} M) by $AABF_2$ in CH_3CN

(b)   Quenching by other quenchers

Fluorescence quenching of PN were also carried out in the absence of $AABF_2$ using the other quenchers, 1,3-pentadiene, 3,3-dimethylbutene and anisole. A stock solution of PN (2.0×10^{-5} M) in dioxane was made. The quenchers were directly injected into 3.0 ml of PN solution. The concentration of PN was changed upon the addition of quencher. Therefore, a correction for

dilution was made when the direct injection method was used to add quencher. The experimental data are listed in Table 2-2. The Stern-Volmer constants were estimated by Eq.2-2 (Fig. 2-7). PN fluorescence intensity at 370 nm was quenched feebly by 3,3-dimethlybutene (K_{sv} = 0.41 M^{-1}), by 1,3-pentadiene (K_{sv} = 0.41 M^{-1}), and by anisole (K_{sv} < 0.2 M^{-1}).

Table (2-2): Quenching of PN Fluorescence by olefins

[1,3-pentadiene] (M)	I^0/ I (uncorrected)	I^0/ I (corrected)
0.00	1.00	1.00
0.0493	1.02	1.02
0.0981	1.05	1.04
0.1940	1.13	1.10
0.3810	1.19	1.14
kqτ	0.62	0.41
[3,3-dimethylbutene](M)	I^0/ I (uncorrected)	I^0/ I (corrected)
0.00	1.00	1.00
0.0391	1.03	1.03
0.0779	1.07	1.06
0.1543	1.10	1.08
0.3026	1.19	1.14
kqτ		0.46
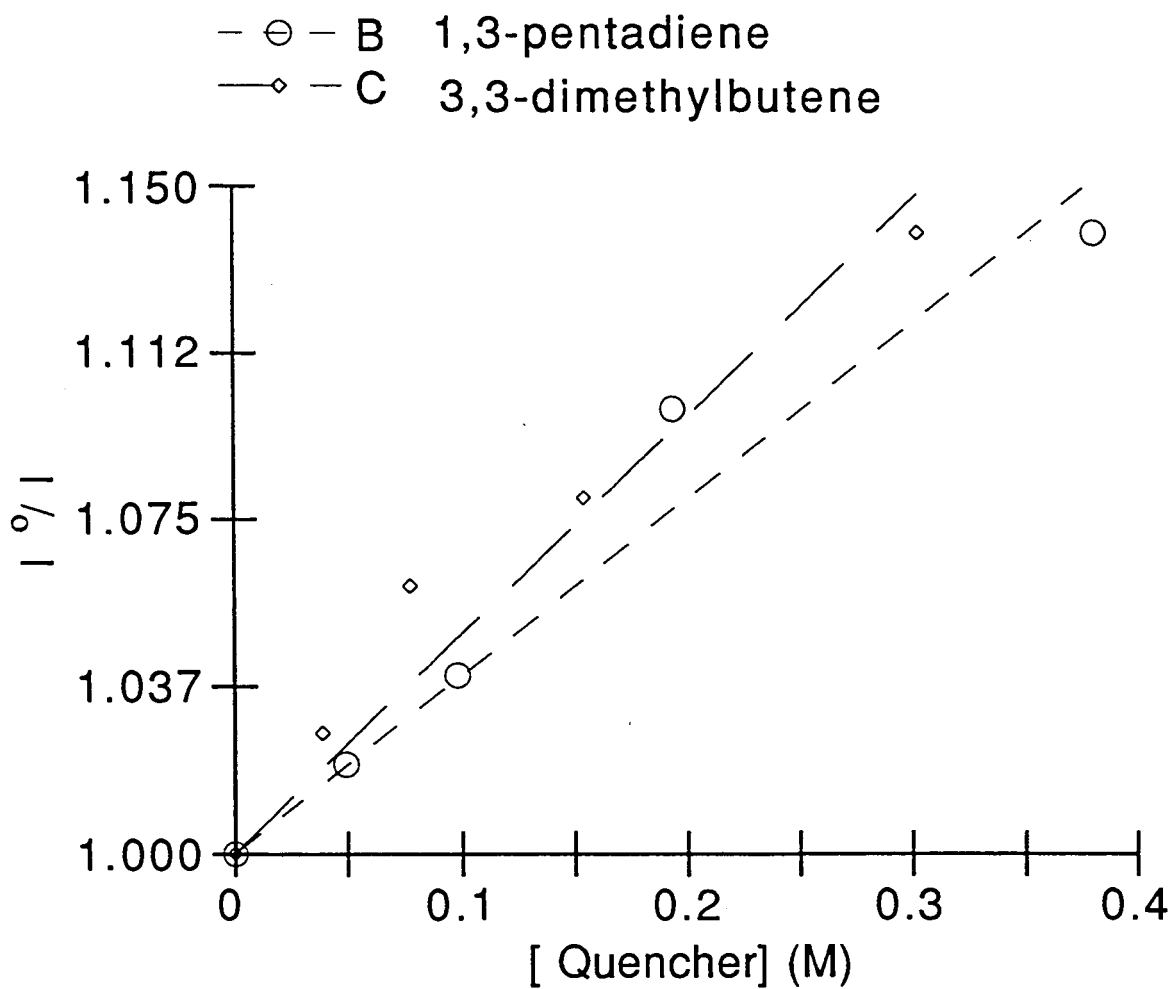
Fig. 2-7 Stern-Volmer plots for PN fluorescence quenching by olefins

2-1.5 Exciplex Characterization

Changing solvent polarity usually results in a shift in the λ_{max} of absorption and emission spectra. This shift is interpreted as a measure of the ground and excited state dipole moment difference (μ_g - μ_c). Upon increasing

the solvent polarity, the PN/AABF$_2$ exciplex emission maximum shifted to longer wavelengths. This indicated that this exciplex had some charge transfer character. The dipole moment of PN/AABF$_2$ exciplex was determined by emission solvatochromic analysis according to equation 2-3 where the experimental data are listed in Table 2-3. The similar approaches have appeared in the literature.[25,26]

$$\bar{v}_c^{max} = \bar{v}_{c(0)}^{max} - \frac{2\mu_c^2}{hc\rho^3}(\frac{\varepsilon-1}{2\varepsilon+1} - \frac{1}{2}\frac{n^2-1}{2n^2+1})$$

(2-3)

Where $\bar{v}_{c(0)}$:   ground state gas phase emission frequency

μ_c :   dipole moment

ρ :   the solvent cavity radius

h :   Planck's constant

ε :   dielectric constant

n :   refractive index of the solvent

A large scatter was found by plotting $\bar{v}_c^{max}$ versus $\frac{\varepsilon-1}{2\varepsilon+1} - \frac{1}{2}\frac{n^2-1}{2n^2+1}$. Such scatter is known and believed to be a result of failure of $\frac{\varepsilon-1}{2\varepsilon+1} - \frac{1}{2}\frac{n^2-1}{2n^2+1}$ to represent the microscopic solvent polarity and specific solvent-solute interactions. The scatter prevented evaluation of μ_c by equation 2-3 hence an alternative method was used. It is known that a plot of the exciplex emission maximum of PN/AABF$_2$ versus that of a standard in the same solvents gives a relative value of dipole moment as given by Equation (2-4)[27]. The dibenzoylmethanetoboron difluoride (MBDBF$_2$)/ p-xylene exciplex was chosen as standard where this exciplex has a known diople moment of 11.1 ± 0.5 D.[28]

23

$$v_u = \frac{\mu_u^2 \rho_s^3}{\mu_s^2 \rho_u^3} v_s + \text{constant}$$

(2-4)

In equation (2-4), the subscripts s and u represents the standard and unknown exciplex, respectively and ρ is the solvent cavity with respect to Onsager's dielectric theory. It is assumed that the solvent cavities of both system are equal ($\rho_s \approx \rho_u$) since the van der Waals volumes of the standard and PN/AABF$_2$ exciplex are about equal. Therefore a plot of v_u *versus* v_s gives the ratio of exciplex dipole moment from the slope (shown in Fig. 2-8). The PN/AABF$_2$ exciplex dipole moment is calculated to be 11.6 D. From the work of Weller's group, full electron transfer within an exciplex gives a dipole moment in the range of 12 - 14 D [29].

Table (2-3)   Solvent Effects on Exciplex Fluorescence

Solvent	n	ε	λ_{max}(nm)
Et$_2$O	1.3624	4.335	470±4
CHCl$_3$	1.4459	4.806	482±4
CCl$_4$	1.4601	2.238	495±4
CH$_2$Cl$_2$	1.4242	8.930	494±4
CH$_3$COOC$_2$H$_5$	1.4601	2.238	495±4
Dioxane	1.4224	6.020	474±4
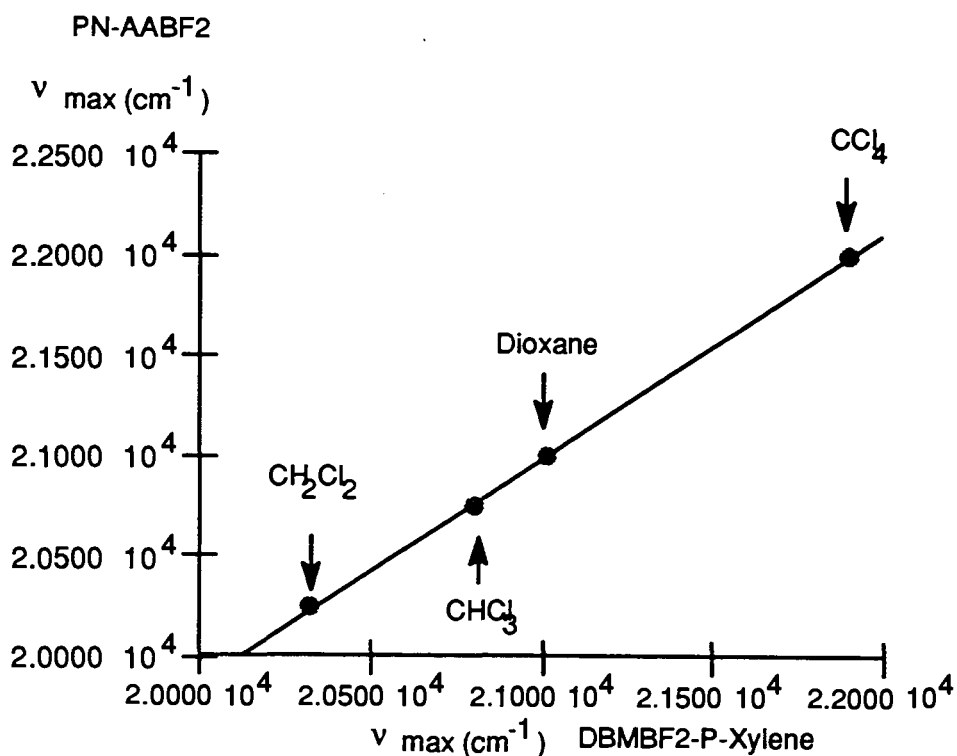
PN-AABF2

Fig. 2-8   Plot of fluorescence maxima (v_{max}) of the PN/AABF$_2$ exciplex

against the those of DBMBF$_2$/p-xylene exciplex

2-1.6 Exciplex Fluorescence Quenching By 1,3-Pentadiene And Anisole

The solution containing PN (5.0×10^{-4} M) and AABF$_2$ (0.02 M), where exciplex emission was reasonably strong, were used to examine exciplex emission quenching by 1,3-pentadiene (0-0.08179 M) (Fig.2-9) and anisole (0-0.0579 M) (Fig.10 and Fig.11).   It was found that exciplex fluorescence was preferentially quenched over PN fluorescence by those two quenchers. Exciplex quenching was analysed by Eq.(2-5) derived previously by Caldwells group,[30, 31, 32] where the ratio I_m^0/I_m corrects for Q$_2$ quenching the PN.

$$\frac{I_{ex}^0}{I_{ex}} + \frac{I_m^0}{I_m} = 1 + k_q^{ex} \tau_{ex}[Q_2]$$

(2-5)

The exciplex quenching by 1,3-pentadiene and anisole give $kq^{ex}\tau$ = 2.2 M^{-1}(under Ar) shown in Fig.12 and $kq^{ex}\tau$ = 6.8 M^{-1} (under air), 10.1 M^{-1} (under Ar) shown in Fig. 12, respectively.
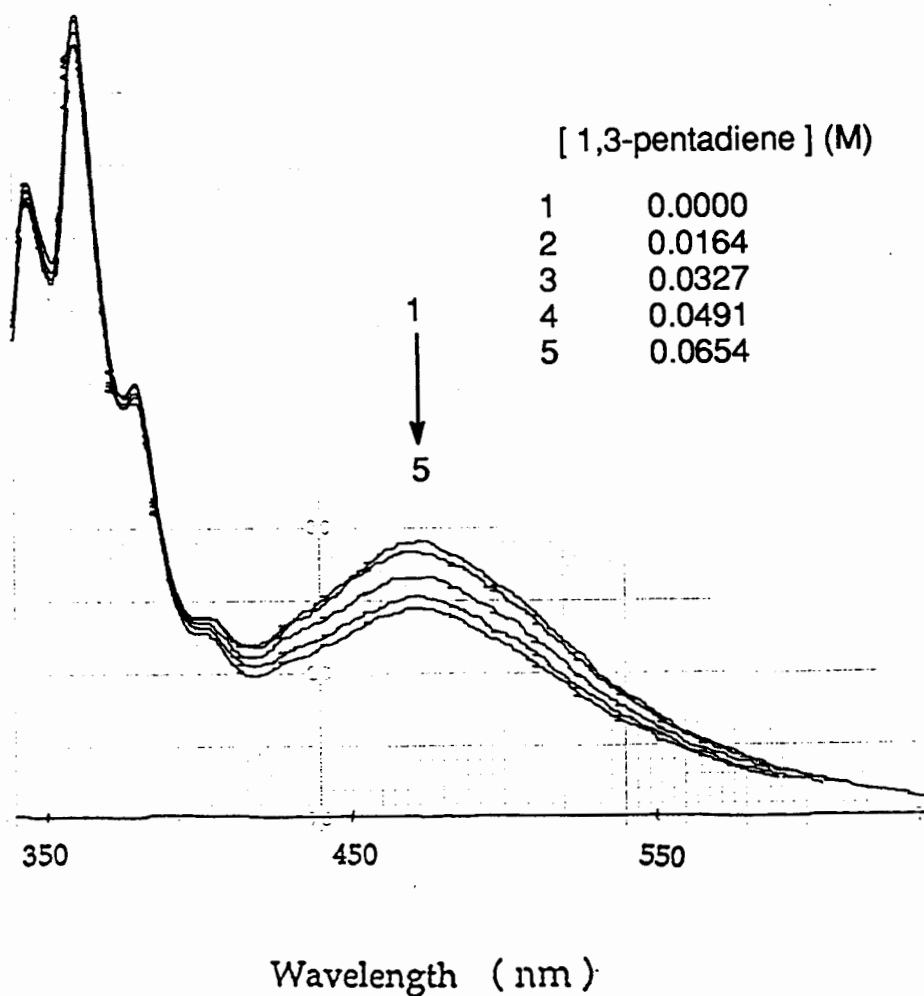
Fig. 2-9 Quenching of PN/AABF$_2$ Exciplex Fluorescence Intensity by 1,3-pentadiene with λex = 335 nm in Dioxane: (298 K)

	[anisole] (M)
1	0.0000
2	0.0146
3	0.0291
4	0.0435
5	0.0579

Wavelength (nm)
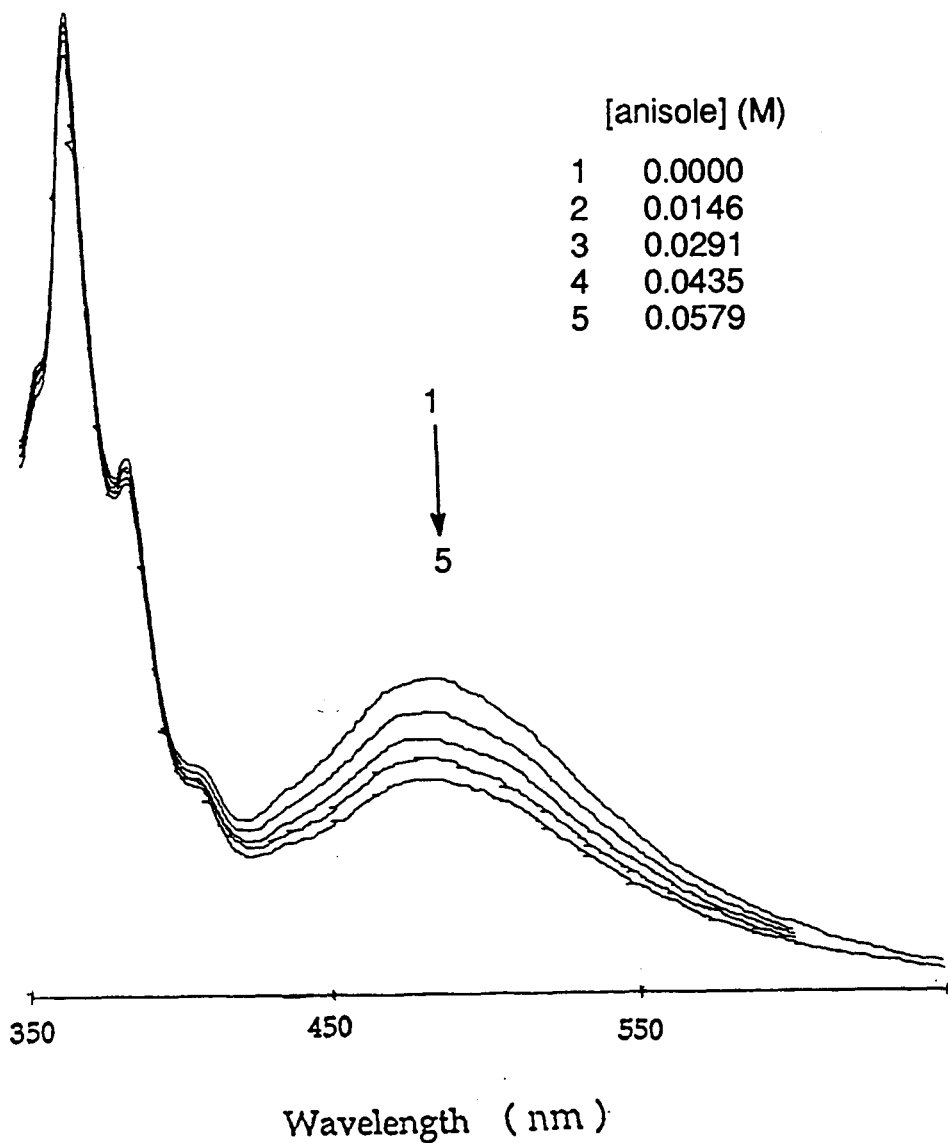
Fig. 2-10   The Quenching of Exciplex of PN/AABF$_2$ Emissive by Anisole

with λex = 335 nm in Dioxane under air

27
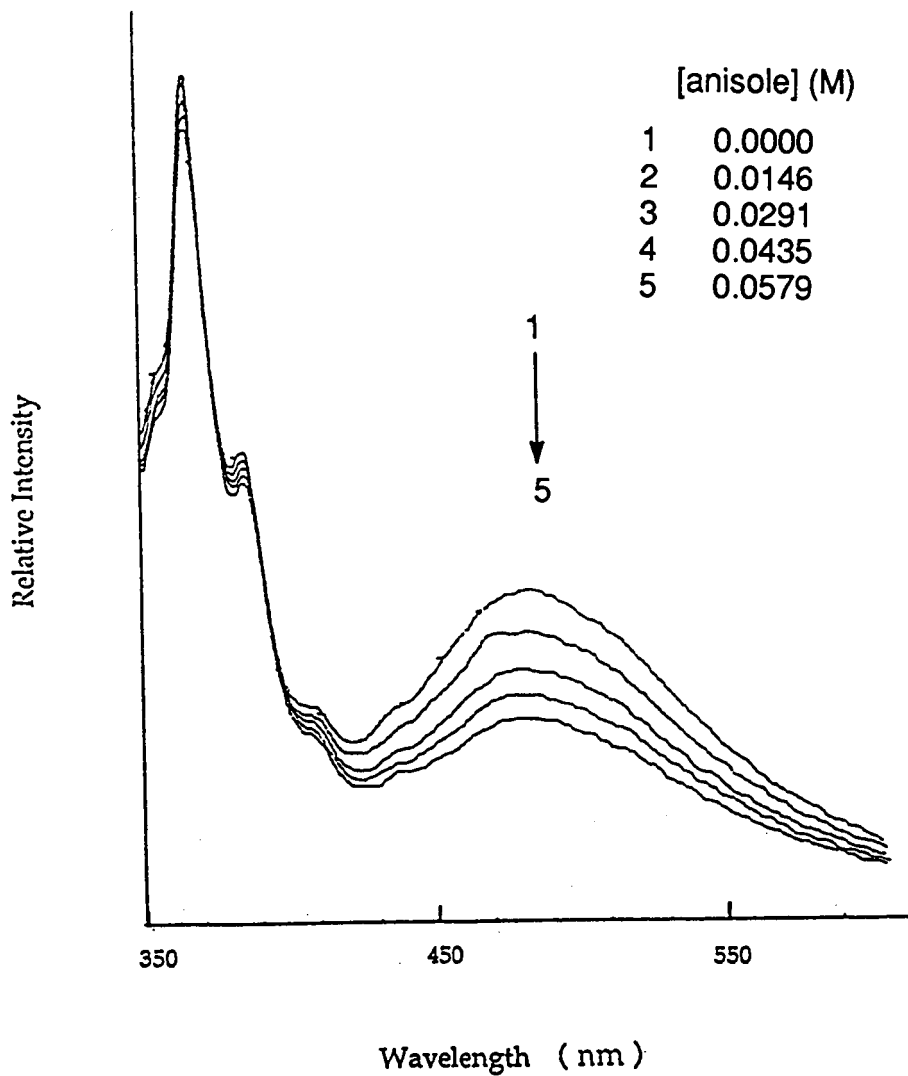
Fig. 2-11   The Quenching of Exciplex of PN/AABF$_2$ Fluorescence by
Anisole with λex = 335 nm in Dioxane under Argon
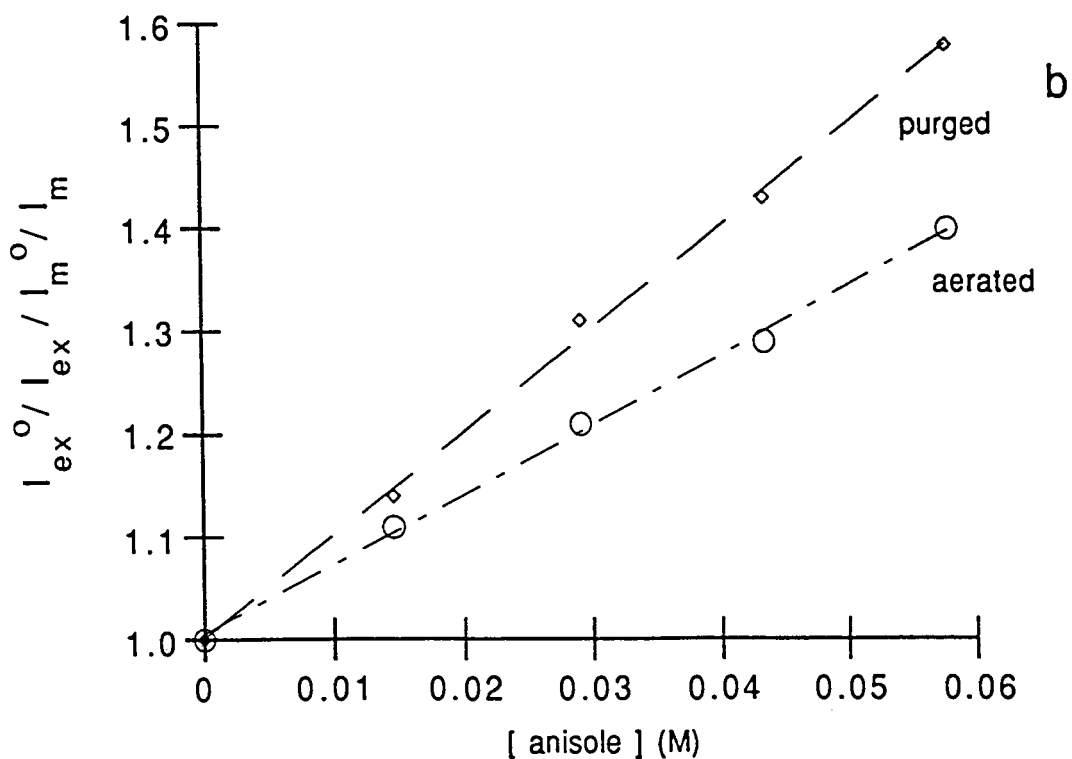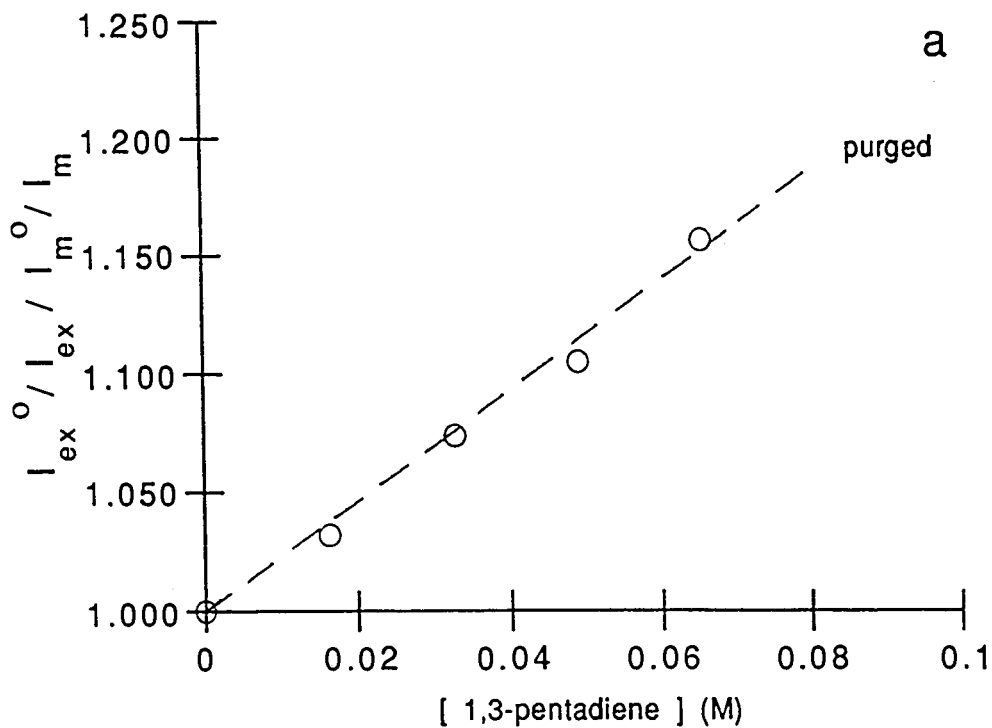
Fig. 2-12   Stern-Volmer plot for exciplex quenching; (a) Quenching by 1,3-
            pentadiene, (b) Quenching by anisole

29

2-1.7 Quantum Yield Studies in the Absence and Presence of Anisole and 1,3-pentadiene

The quantum yields for the formation of (**9**) for the photocycloaddition of PN (2.0×10^{-2} M) with AABF$_2$ (1.0×10^{-2} M) were determined using 350 nm lamps in the absence and the presence of anisole (0.0000 M - 0.3000 M). The relative quantum yield Φ_p / Φ_p^0 (Φ_p is quantum yield in presence of anisole and Φ_p^0 is quantum yield in the absence of anisole) was observed to decrease with increasing anisole concentration under air and argon (Table 2-4). The Stern-Volmer constants were estimated from equation 2-6 to give K_{sv}^{ex} = 10.7 (under Ar) and 7.0 (under air) shown in Fig.2-13. The similar quantum yield studys were also carried out using 1,3-pentadiene as quencher under argon. The photoproducts were attenuated when 1,3-pentadiene was present as shown in table 2-5. The Stern-Volmer constant K_{sv}^{ex} was 1.6.(Fig.2-13)

$$\Phi_p^0 / \Phi_p = 1 + K_{sv}\, [Q] \qquad\qquad (2\text{-}6)$$

30

Table (2-4): The Quantum Yield of Photoaddition of PN with $AABF_2$ in the Absence and Presence of Anisole[a,b,c]

Experiment #	[anisole] (M)	R_f	Φ_p	Φ_p^0 / Φ_p
purged				
1	0.000	0.107	0.0642	1.00
2	0.0300	0.0821	0.0493	1.30
3	0.0450	0.0792		
4	0.0600	0.0754	0.0453	1.42
5	0.0900	0.0531	0.0319	2.01
6	0.1500	0.0408	0.0245	2.62
7	0.3000	0.0320	0.0192	3.34
K_{sv}^{ex}		10.7 ± 1.0		
aerated				
1	0.000	0.0856	0.0472	1.00
2	0.0300	0.0826	0.0455	1.04
3	0.0600	0.0602	0.0332	1.42
4	0.0900	0.0517	0.0285	1.66
5	0.1500	0.0394	0.0217	2.18
6	0.2100	0.0352	0.0194	2.43
7	0.3000	0.0300		2.84
K_{sv}^{ex}		7.0 ± 0.6		

a. The solution containing PN (2.0×10^{-2} M), $AABF_2$ (1.0×10^{-2} M) and Various concentration of ansiole (0 - 0.3000 M) were irradiated for 15 min. in apparatus I with 350 nm lamps (16 x 24 watt).

b. Percent conversion of PN was controlled under 10 %.

c. GC were used to analysis of photolysis where n-$C_{16}H_{34}$ (1.0×10^{-2} M) was used as internal standard (I.S.).

Table 2-5: The Quantum yield of Photocycloaddition of PN with $AABF_2$ in presence of 1,3-pentadiene[a,b,c]

Experiment #	[1,3pentadiene] (M)	R_f	Φ_p	Φ_p^0/Φ_p
1	0.0000	0.172	0.104	1.00
2	0.0200	0.167	0.101	1.03
3	0.0400	0.160	0.0963	1.07
4	0.0800	0.153	0.0919	1.13
5	0.1200	0.146	0.0879	1.18
6	0.1600	0.136	0.0815	1.27
7	0.2000	0.134	0.0803	1.29
K_{sv}^{ex}		1.6 ± 0.1		

a. The solution of PN (2.0×10^{-2} M), $AABF_2$ (1.5×10^{-2} M), $C_{16}H_{34}$ (1.0×10^{-2} M) and various of 1,3-pentadiene were purged for eight min. and irradiated for14 min. in Apparatus I with 350 nm lamps (16 x 24 watt).

b. percent conversion of PN was controlled under 10 %

c. GC were used to analysis of photolysis where n-$C_{16}H_{34}$ (1.0×10^{-2} M) was used as I.S..
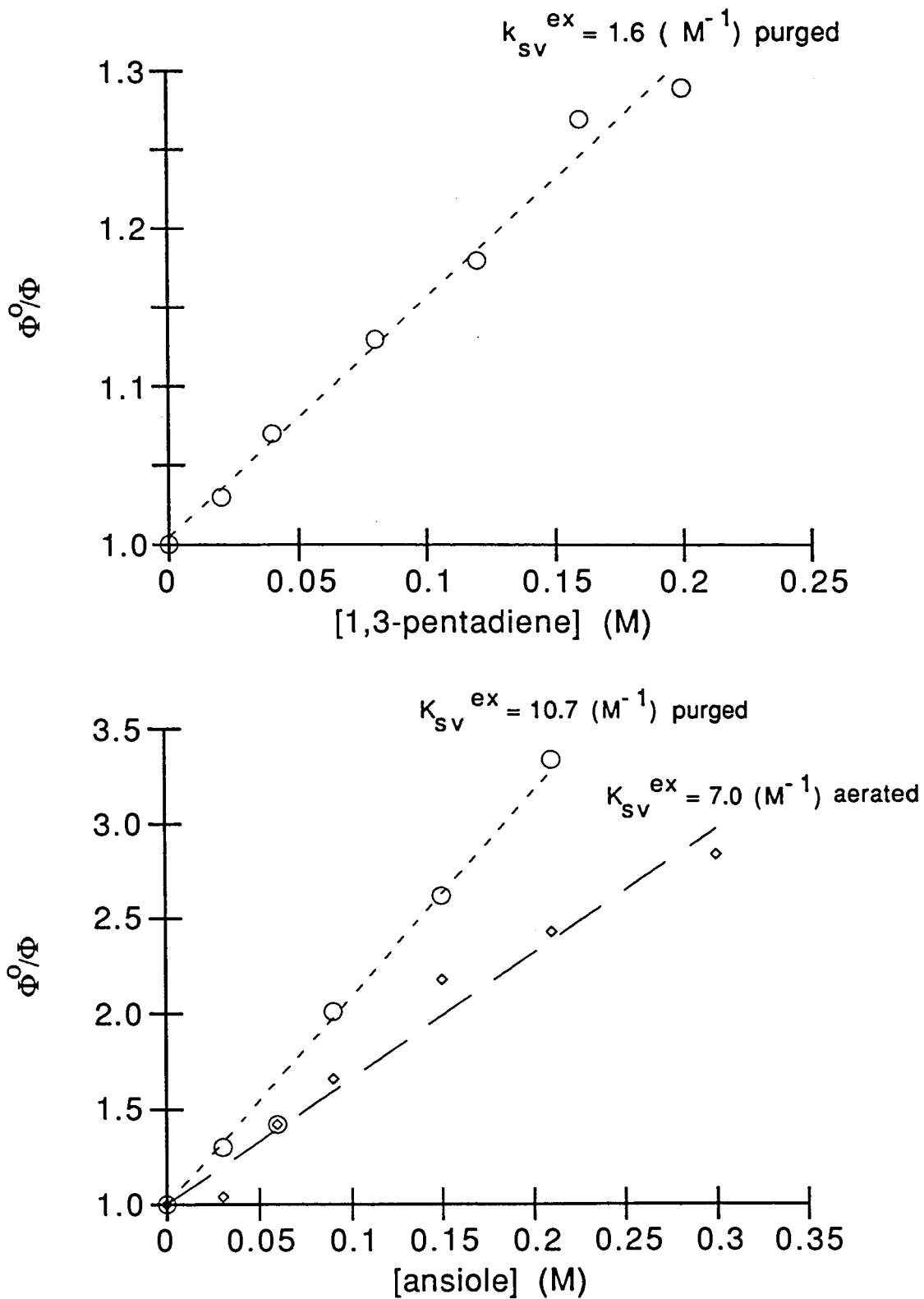
Fig. 2-13   Stern-Volmer plots for quantum yield of product formation in
the absence and the presence of quencher (Q)

2-1.8 Fluorescence Decay Kinetics[33, 34]

Based on mechanism proposed (Scheme 3-1) from the steady-state experiments, all rate constants in the scheme was further probed using time-resolved fluorescence decay study. The lifetimes of singlet excited state PN were determined in dioxane solution which gave the single exponential decay traces (Fig. 2-14) with lifetimes of 26 ns and 54 ns under air and argon, respectively. In the presence of $AABF_2$ (λex 350 nm), the decay of PN and its exciplex with $AABF_2$ exhibited biexponential behavior (Fig. 2-15). The fluorescence emission from excited PN would be comprised of a short-lived unquenched PN component and a long-lived exciplex component. The lifetimes were found to be a function of $AABF_2$ concentration. The lifetime of short-lived component (τ_1) decreased with increasing $AABF_2$ and lifetime of long-lived component (τ_2) was invariant in low $AABF_2$ concentration range (0.010 - 0.12 M) but decreased with high concentration of $AABF_2$ (greater than 0.12 M). The quantity of the biexponential fits were judged on the basis of low chi-square statistic (χ^2), autocorrelation, and Durbin-Watson (DW) parameters $\geq$ 1.7. The observed lifetimes, at various [$AABF_2$], are listed in Table (2-6). The results were analyzed using equation 3-6, 3-7 and 3-8 to give rate constants.(Table 2-7)
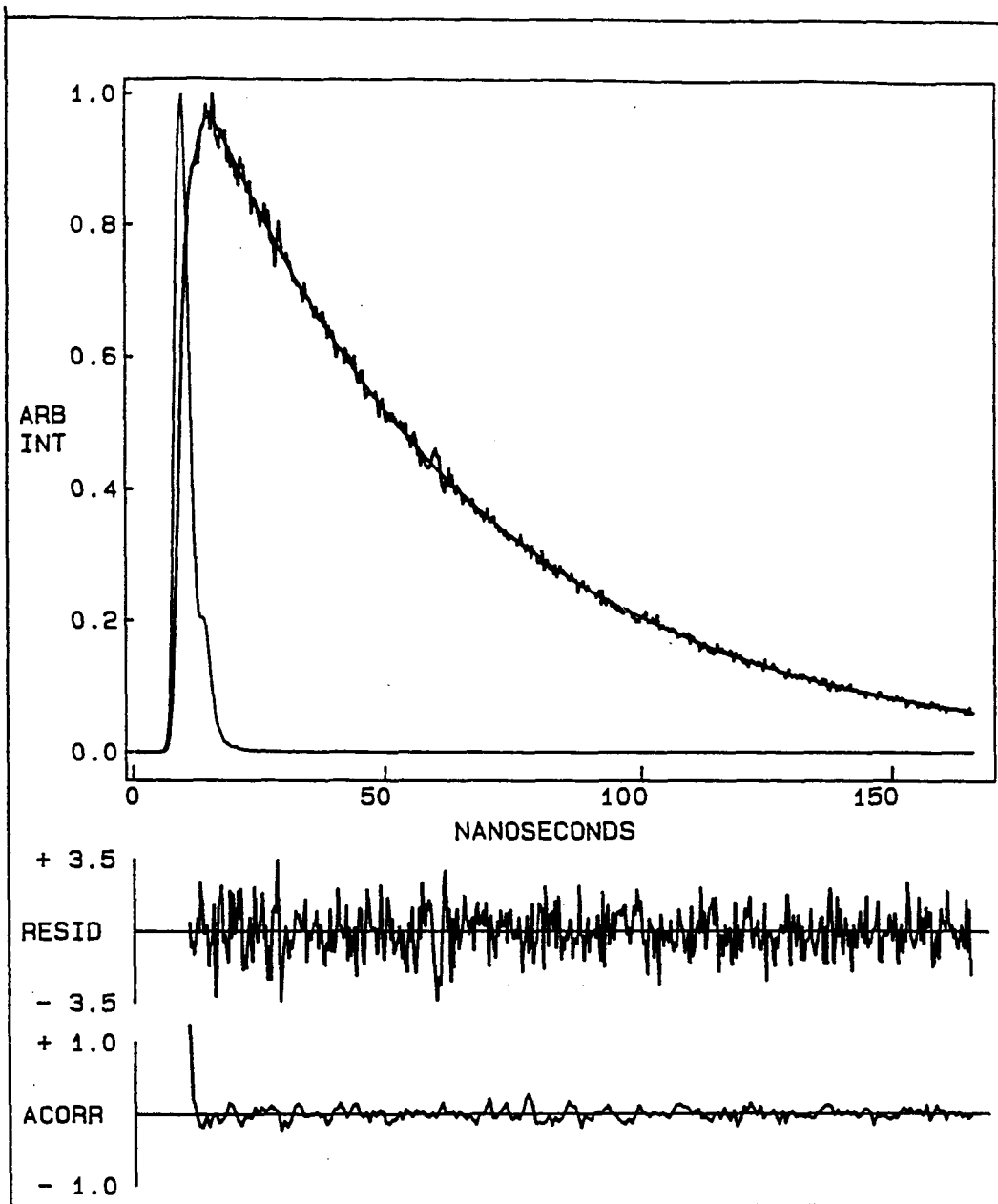
Fig. 2-14   Single exponential decay of PN, [PN] = 5.0 x 10^{-5} M in dioxane, λ_{ex}
350 nm, $\lambda_{monitor}$ 370 nm
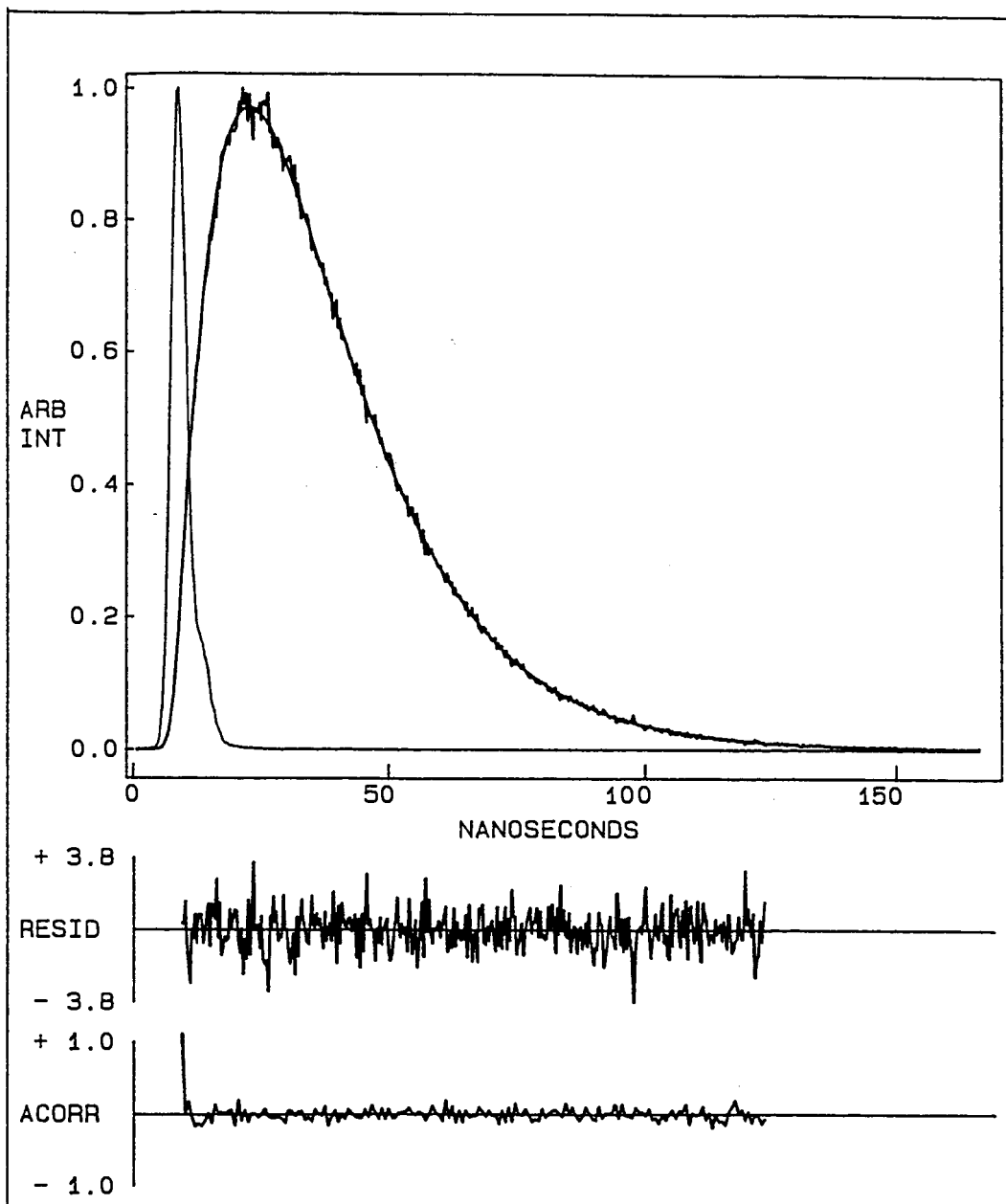
Fig. 2-15   The typical fluorescence decay for PN and PN/AABF$_2$ exciplex
emission, [PN] = 5.0 x 10^{-5} M, [AABF$_2$] = 1.0 x 10^{-2} M in dioxane,
λex 350 nm, λmonitor 470 nm

36

Table (2-6): Kinetic Parameters[a] of Singlet Excited PN And Exciplex With AABF$_2$

[AABF$_2$](M)	τ_1 (ns)	$\lambda_1 \times 10^{-7} s^{-1}$	τ_2 (ns)[b]	$\lambda_2 \times 10^{-7} s^{-1}$
0.00	53.8[c]	1.86±0.02		
0.01	11.86	8.4	17.44	5.7
0.02	7.97	12.5	17.15	5.8
0.03	5.42	18.4	18.32	5.5
0.04	4.33	23.1	17.27	5.5
0.05	3.50	28.6	17.22	5.8
0.08	1.99	50.2	17.34	5.8
0.12	1.49	67.2	16.17	6.2
0.12[d]			16.28	6.1
0.25[d]			13.29	7.5
0.30[d]			12.34	8.1

a [PN]=5 x 10^{-5} M in dioxane under argon with λ_{ex} 350 nm;

b From Eq. $\tau=\lambda^{-1}$;

c This corresponds to τ^0 and τ_1=26 ns under air;

d A separate series of experiments.

Table 2-7　　Rate constants; the interaction of *PN and exciplex with AABF$_2$ in dioxane

Σk_d	$(1.87 \pm 0.02) \times 10^7$ s^{-1}
kq	$(5.51 \pm 0.11) \times 10^9$ M^{-1}s^{-1}
	5.2×10^9 M^{-1}s^{-1}　　a
	4.6×10^9 M^{-1}s^{-1}　　b
$\Sigma k_d^{ex} + k_r$　c	$(5.7 \pm 0.1) \times 10^7$ s^{-1}
k_q^{ex}	$(7.2 \pm 0.4) \times 10^7$ M^{-1}s^{-1}
k_{-a}　　c	$(< 10^6$ s$^{-1})$
$k_{qc'}^{ex}$　d	5.7×10^8 M^{-1}s^{-1}
$k_{qc''}^{ex}$　d	1.3×10^8 M^{-1}s^{-1}

a　　Calculated from K_{sv} obtained in the static quenching experiment under argon.

b　　Calculated from K_{sv} obtained in the static quenching experiment under air and the reduced lifetime of 26 ns.

c　　Since K_{-a} is insignificant, it is omitted.

d　　The rate constants of the exciplex quenching by anisole ($k_{qc'}^{ex}$) and 1,3-pentadiene ($k_{qc''}^{ex}$) calculated from K_{sv}^{ex} in static quenching experiments, $\tau_{ex} = 19$ ns.

2-1.9 Flash Photolysis

The previous estimatation of the high dipole moment of the $PN/AABF_2$ exciplex suggested a significant charge transfer character for the $PN/AABF_2$ exciplex. Owing to the polar nature of exciplex, dissociation of exciplex to the corresponding radical-ion is believed to be the general process undergone in polar media if the free energy for electron transfer is exothermic, i.e., the formation of the radical-ion is potentially more efficient than the product formation from exciplex.[19a, 35] Flash photolysis used to prove the existence of a radical species resulting from electron transfer reactions. This method may afford a clue why neither the photocycloaddition nor exciplex emission of PN with $AABF_2$ was observed in acetonitrile. To examine the possibility of radical-ion formation in the present photocycloaddition system, the system was studied in acetonitrile with laser-pulsed flash photolysis with 355 nm excitation (YAG laser) using an apparatus available at the University of Victoria, B.C..

Irradiation of PN in dioxane solution with $AABF_2$ resulted in a transient absorption peak at 480 nm (Fig. 2-16A). This peak intensity was significantly decreased in aerated solutions and the lifetime decreased from 23 μs (degassed) to 0.5 μs (aerated). The triplet state species have long lifetime so that they are sensitive to oxygen. The sensitivity of the lifetime to oxygen implied that a triplet species, $^3PN^*$, is responsible for this absorption at 480 nm. This transients absorption was assigned as the T-T absorption of triplet excited PN by comparsion with literature spectra[36]. A similar experiment was carried out in acetonitrile solution. In acetonitrile, PN was photoexcited in the presence of $AABF_2$ to give a transients absorbing at 400 nm, 480 nm and 800 nm where the decay at 450nm was biexponential with the two lifetimes of 1.6 μs and 1.2 μs

39

under degassed (Fig.2-16B).   This suggested that there were two overlapped

transients.   The peak intensity at 480 nm was sensitive to oxygen and rapidly

dropped under air (from 1.2 to 0.5 µs), it was assigned as the T-T absorption of

triplet excited PN.   The remaining signal showed the absorption maxima at 400,

420 and 700 - 800 nm (broad) (Fig.2-16C).   Although the resolution is not very

good, these absorption maxima are very similar to the reported PN cation

radical transient absorption in acetonitrile[37].   No absorption due to the anion

radical of AABF$_2$ could be discovered.   The observation of PN cation radical in

acetonitrile is suggestive that in a polar solvent singlet excited PN underwent

photoinduced electron transfer.
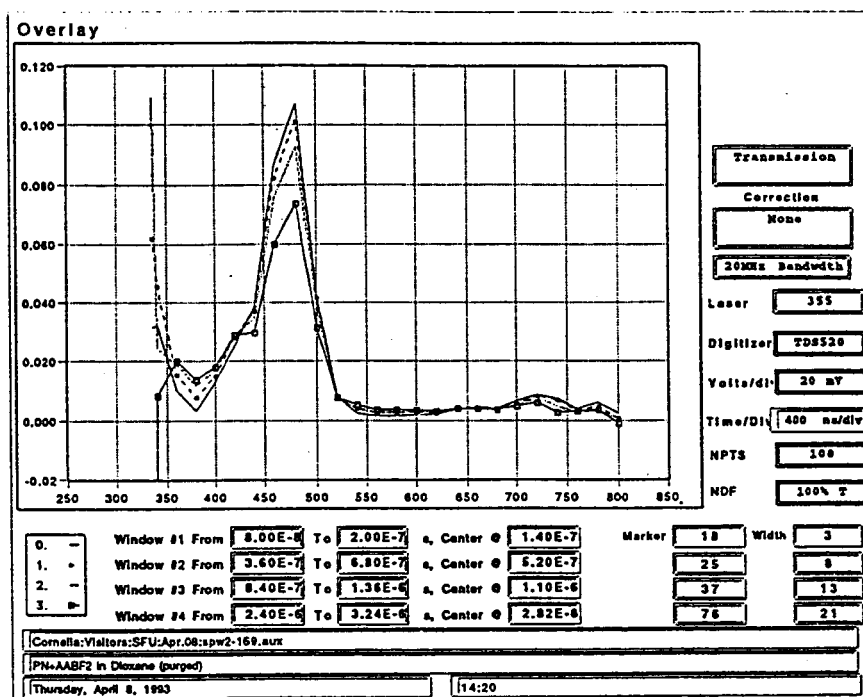
A

Fig. 2-16A   Flash photolysis of [PN] = 5.0 x 10^{-2} M and [AABF$_2$] = 2.0 x 10^{-2} M

under argon in dioxane
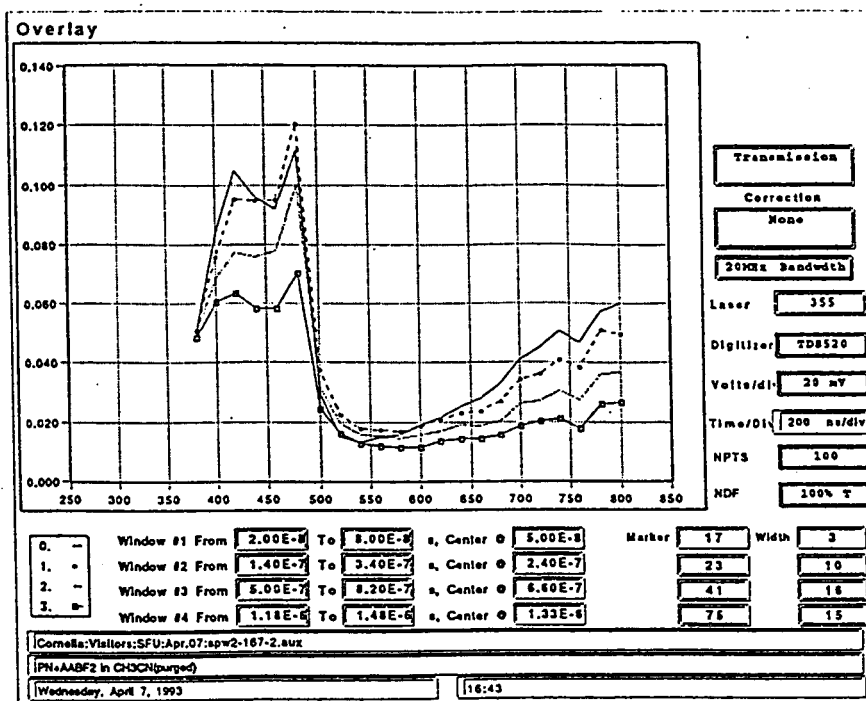
Fig. 2-16B   Flash photolysis of [PN] = 5.0×10^{-2} M and [$AABF_2$] = 2.0×10^{-2} M

under argon in acetonitrile
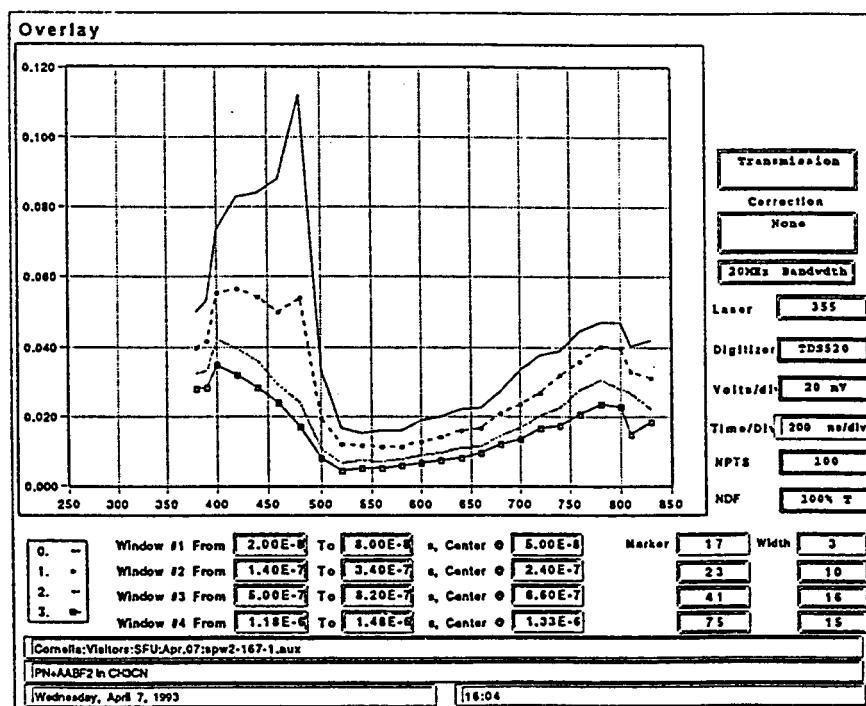
Fig. 2-16C   Flash photolysis of [PN] = 5.0×10^{-2} M and [$AABF_2$] = 2.0×10^{-2} M

under air in acetonitrile λex = 355nm

41

2-2 Spectroscopic Studies of β-Diketonatoboron Difluoride

2-2.1 Absorption and Emission Spectra

The UV-VIS spectra of $MBDBF_2$ (5 x 10^{-6} M) were recorded in various solvents (Fig.2-17) in (a) ether, (b) hexane, (c) acetonitrile and (d) dichloromethane. The fluorescence of low concentrations of $MBDBF_2$ was also recorded in various solvents. (shown in Fig.2-18) In hexane, the fluorescence of $MBDBF_2$ showed two peaks (403 and 427 nm), one peak (435 nm) in CH_2Cl_2. The 0-0 band of $MBDBF_2$ was estimated to give lowest singlet energy, E_S = 69.1 kcal/ mol at 414 nm in CH_2Cl_2.

The fluorescence intensity decreased as the concentration of $MBDBF_2$ increased (5.0 x 10^{-6} to 5.0 x 10^{-4} M) (Fig.2-19a). The new structureless emission was observed at λ_{max} = 520 nm when the concentration of $MBDBF_2$ was 5.0 x 10^{-2} M with 45° configuration.(Fig. 2-19b)

2-2.2 Quenching of MBDBF₂ Fluorescence Intensity

The fluorescence emission of $MBDBF_2$ (5.0 x 10^{-6} M) at 430nm was quenched by 1,3-pentadiene, cyclohexene, norbornylene and methyl methacrylate (Fig. 2-20 to Fig. 2-23). The Stern-Volmer plots of $I^0/$ I *versus* [quencher] gave reasonable straight lines in all cases. The corresponding $k_q\tau$ for these quenchers were 10.8, 0.0007, 9.0 and 0.0065 M^{-1}.
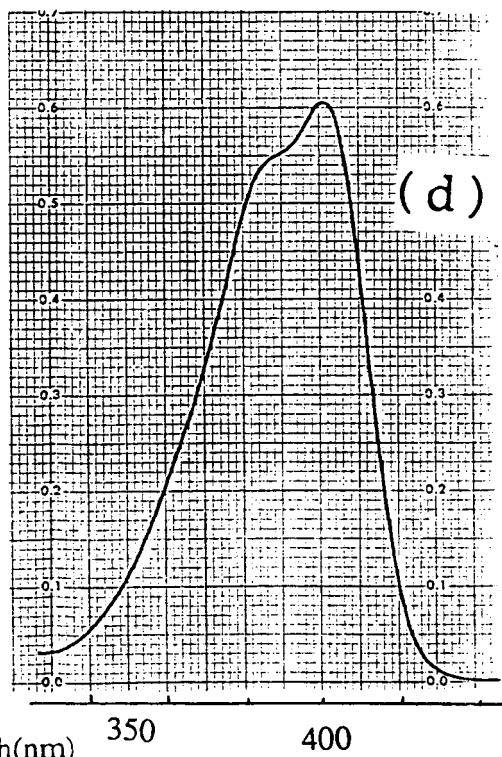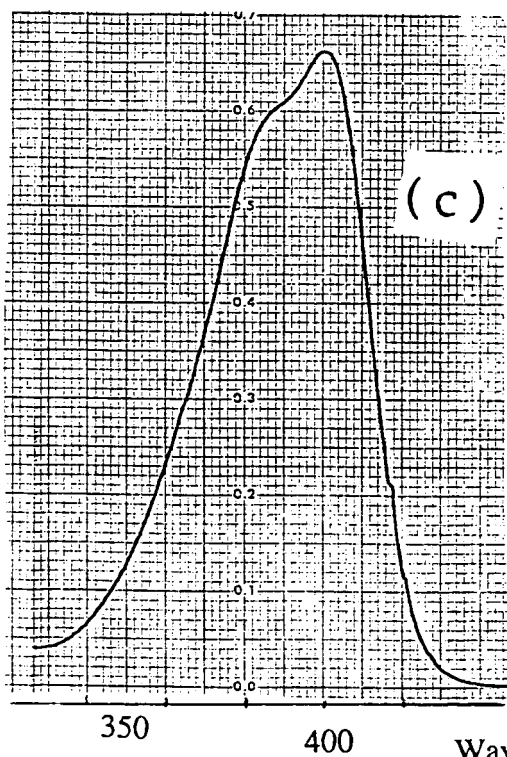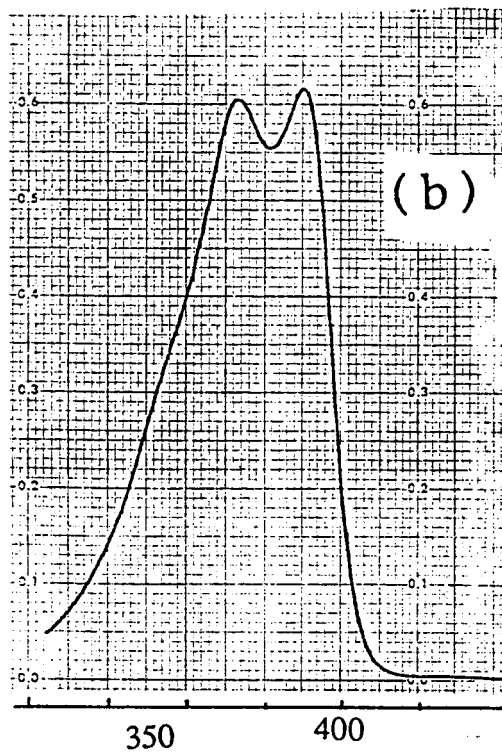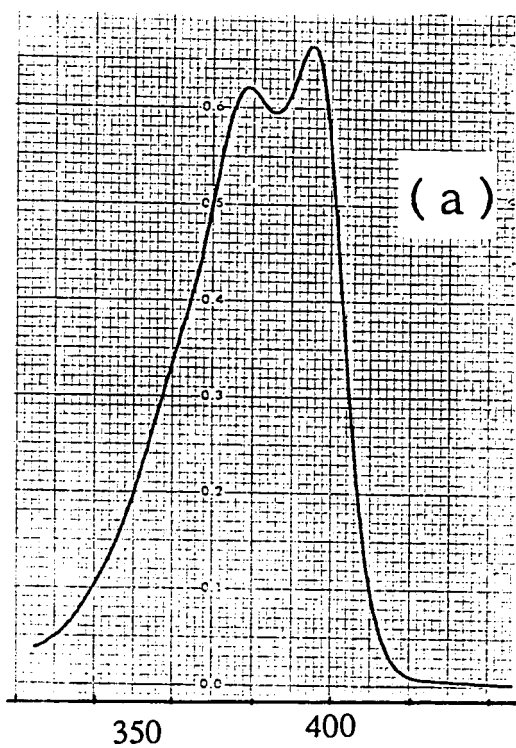
Fig. 2-17   Absorption of MBDBF$_2$ in different solvent: (a) n-hexane, (b)
diethyl ether, (c) acetonitrile and (d) dichloromethane

43

400　　　　450　　　　500

Wavelength (nm)
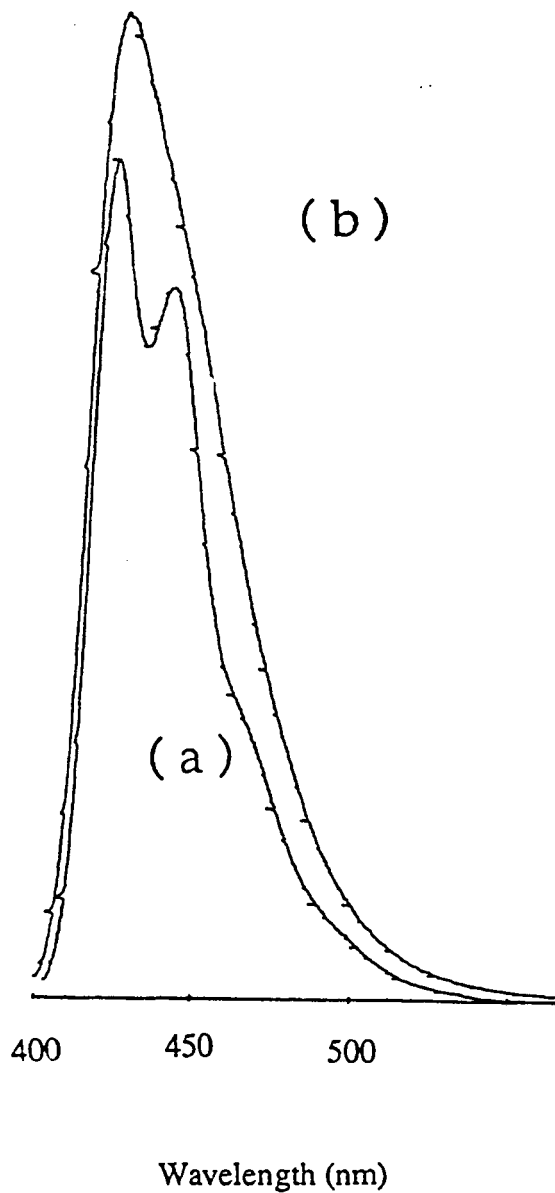
Fig. 2-18　　　Emission of MBDBF$_2$ (5.0 x 10^{-6} M) in (a) n-hexane,λ_{ex} 375 nm, (b) dichloromethane,λ_{ex} 375 nm

(a)

(b)

[MBDBF$_2$] (M)

1	5.0 x 10^{-6}
2	5.0 x 10^{-5}
3	5.0 x 10^{-4}

[MBDBF$_2$] = 5.0 x 10^{-2} (M)

400   450   500   550   410   460   510   560   610

Wavelength (nm)
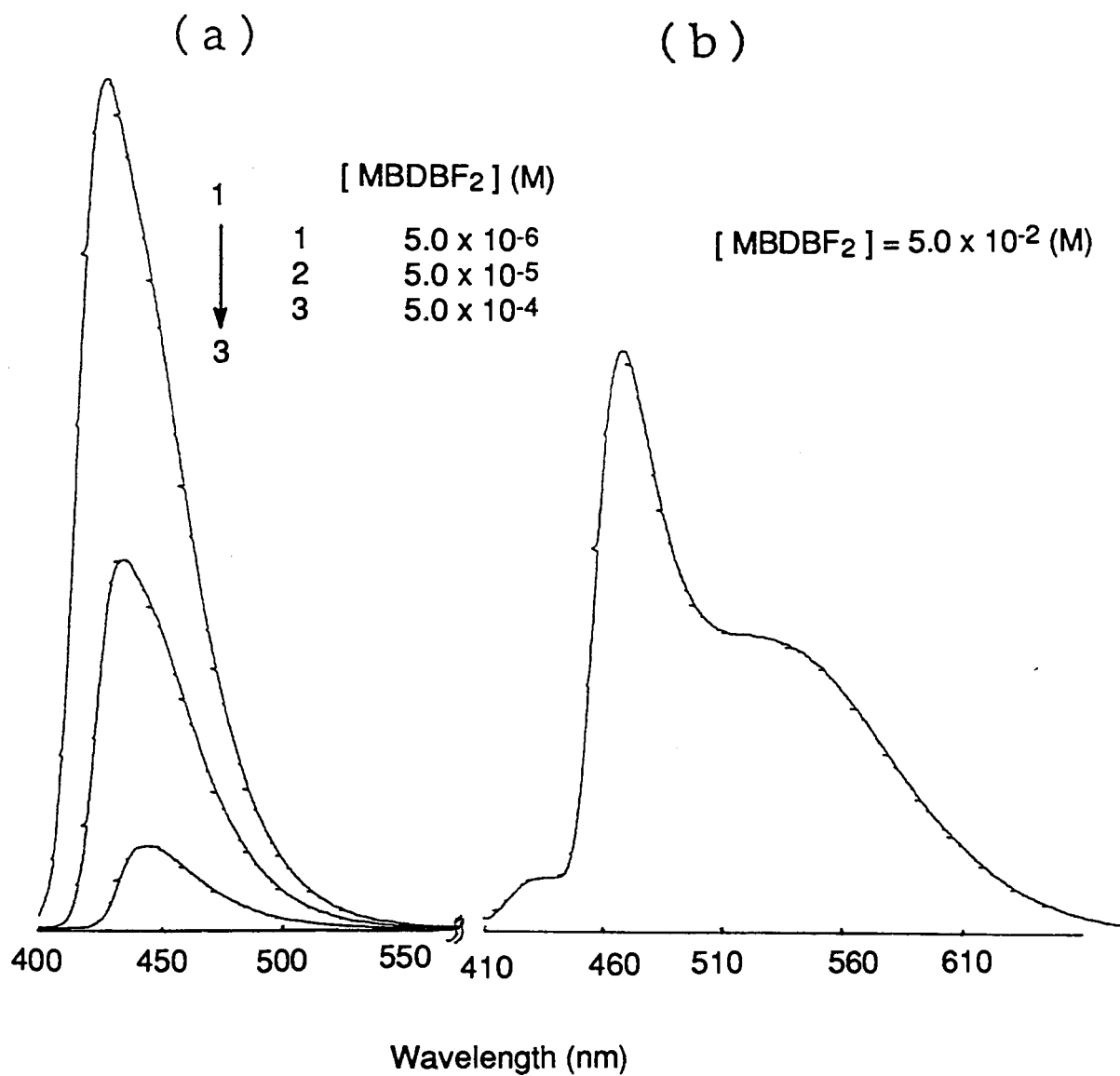
Fig. 2-19   (a) The concentration dependence of MBDBF$_2$ (b)Emission of

MBDBF$_2$ (10^{-2} M) λ_{ex} 395 nm in dichloromethane (front-face cell)

45

[1,3-pentadiene] (M)

1	1	0.0000
	2	0.0099
	3	0.0198
	4	0.0297
6	5	0.0397
	6	0.0496

405   445   485   525   565

Wavelength (nm)
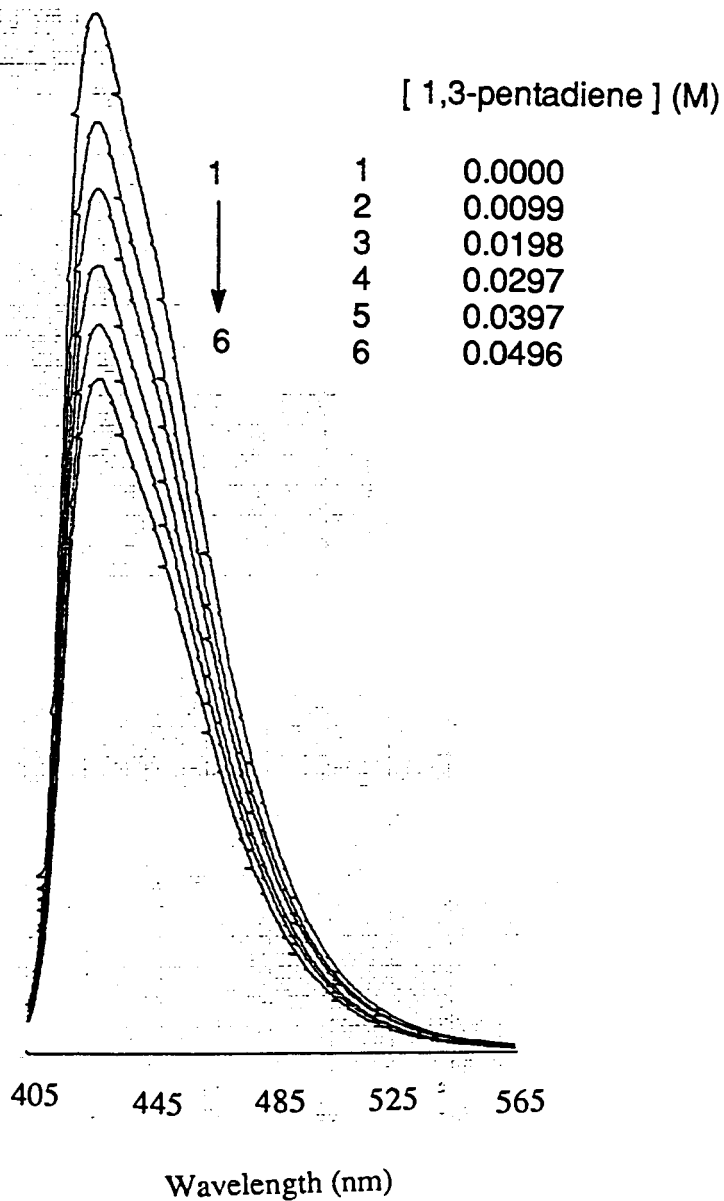
Fig. 2-20   Fluorescence quenching of MBDBF$_2$ (5.0 x 10^{-6} M) by 1,3-
pentadiene (0, 0.0099, 0.0198, 0.0297, 0.0397, 0.0496 M)
in CH$_2$Cl$_2$,λ_{ex} 395 nm
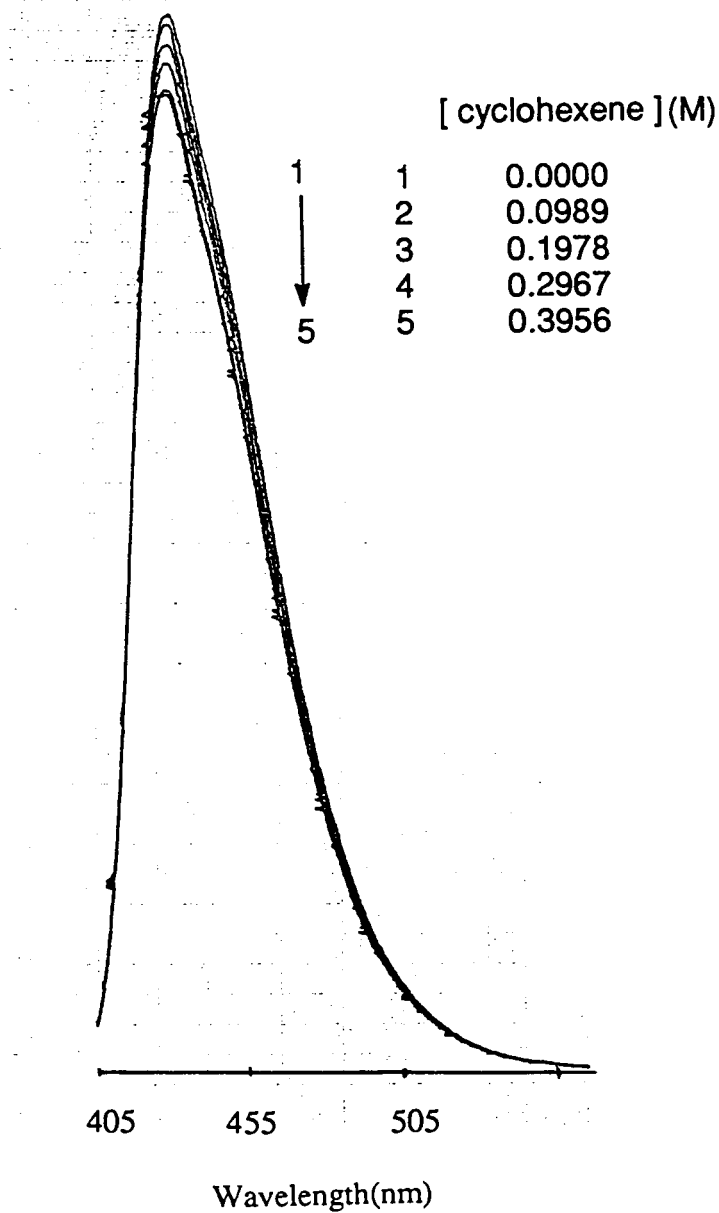
Fig. 2-21   Fluorescence quenching of MBDBF$_2$ (5.0 x 10^{-6} M) by cyclohexene

(0, 0.0989, 0.1978, 0.2967, 0.3956 M) in CH$_2$Cl$_2$,λ_{ex} 395 nm
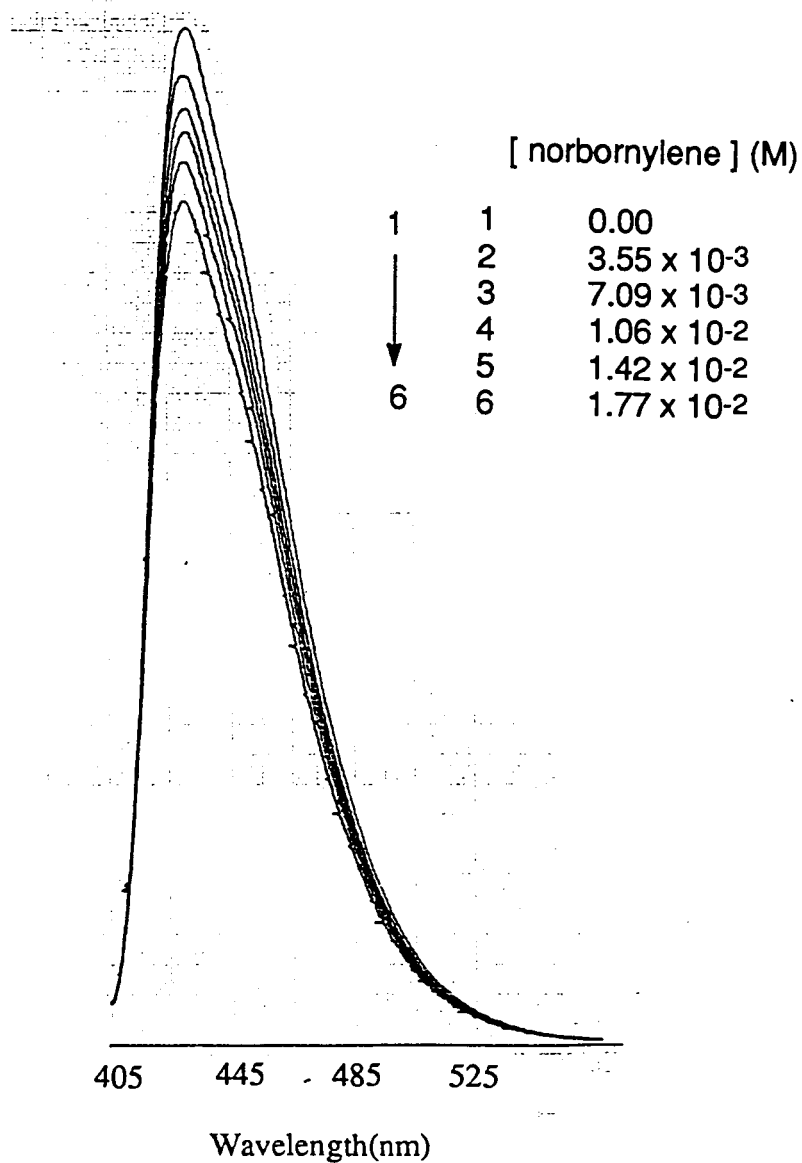
Fig. 2-22   Fluorescence quenching of MBDBF$_2$ (5.0×10^{-6} M) by norbornylene (0, 3.55×10^{-3}, 7.09×10^{-3}, 1.06×10^{-2}, 1.42×10^{-2}, 1.77×10^{-2} M) in CH$_2$Cl$_2$,λ_{ex} 395 nm
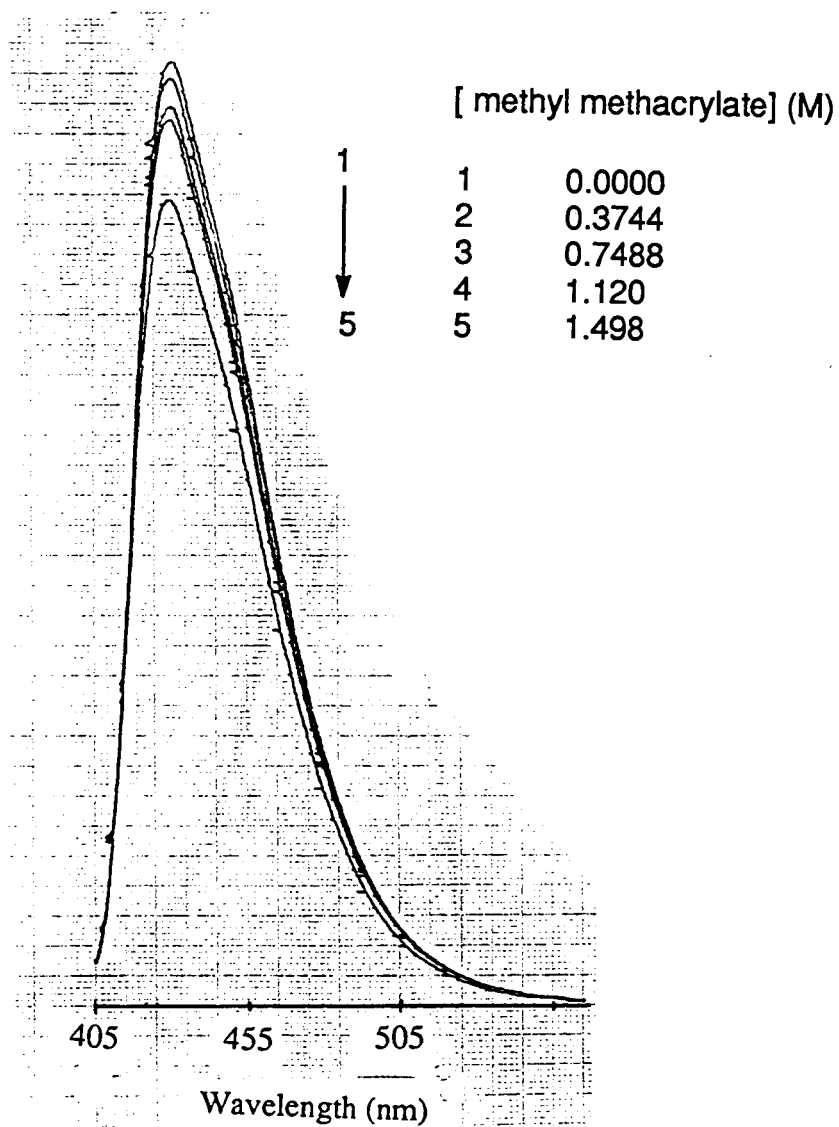
Fig. 2-23   Fluorescence quenching of MBDBF$_2$ (5.0 x 10^{-6} M) by methyl methacrylate (0, 0.3744, 0.7488, 1.120, 1.498 M) in CH$_2$Cl$_2$ λ_{ex} 395 nm

2-2.3 Photocycloaddition of BABF$_2$ and MBDBF$_2$ to Olefins

BABF$_2$ with cyclohexene:

Irradiation of BABF$_2$ (0.05 M) in the presence of cyclohexene (0.5 M) in CH$_3$CN with 350 nm lamps for 15 hours led to adduct product (**21**) which was isolated by column chromatography as a pale yellow oil (isolated yield 18.9 %).
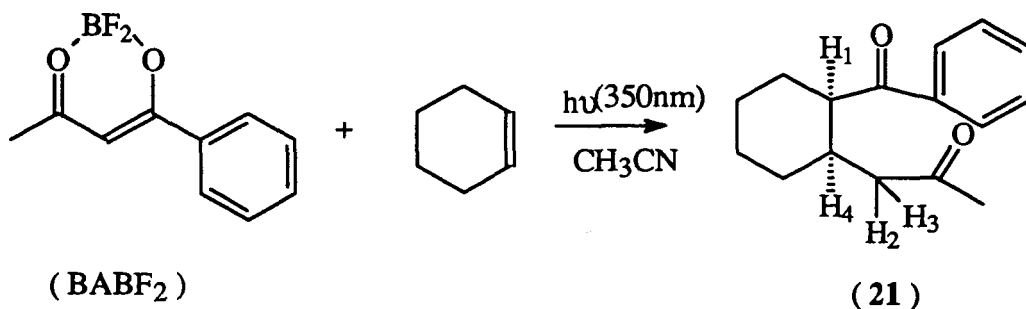
Analysis of the GC-MS spectra of **21**, under CI conditions, gave an M$^+$+1 = 245 that agrees with the 2+2 adduct of BABF$_2$ and cyclohexene. Two different carbonyl absorptions in the IR spectrum (1714 and 1675 cm^{-1}) were found, the latter one corresponds to carbonyls in acetophenone derivatives.[10a] The ^{13}C NMR spectrum gave two carbon signals at 207.85 and 203.45 ppm. The spectroscopic data are listed in Tables 4-6 to 4-9.

The stereochemistry of *vic*-disubstituted diketone could be determined to be *cis* configuration from the relevant ^{1}H coupling constant[38a,b] of 6.8 Hz. Accordingly, the spin-spin coupling constant between H$_1$ and H$_4$ of the adduct was calculated using PC model (88.0)[38c] and gave the coupling constants of J$_{1,4}$ = 6.2 Hz for the *cis* structure and J$_{1,4}$ = 12.2 Hz for the *trans* configuration.

The experiment data gave $J_{1,4} = 8$ Hz. A comparison of the experimental and the calculated value showed that the adduct (21) most likely had a *cis* configuration.

The sole adduct has the benzoyl group attached to the ring which is supported by appearance of the MS fragment (m/e = 187, M^+-CH_2COCH_3).

MBDBF$_2$ with norbornylene:

Photolysis of MBDBF$_2$ (5 x 10^{-2} M) in the presence of norbornylene (0.5 M) in CH_2Cl_2 with 350 nm lamps for seven hours led to the δ-diketone, (22), which was isolated in a 43 % yield as a yellow oil.
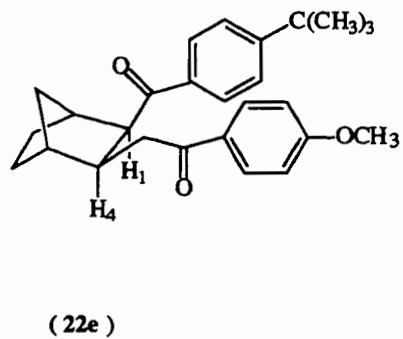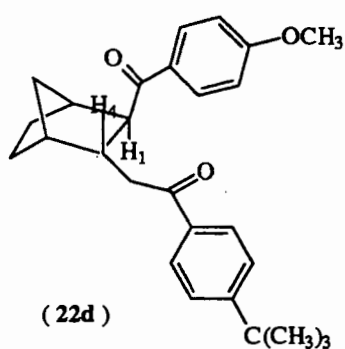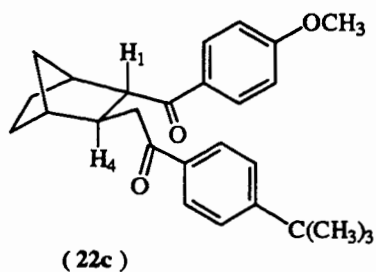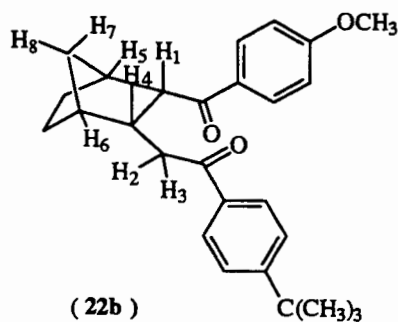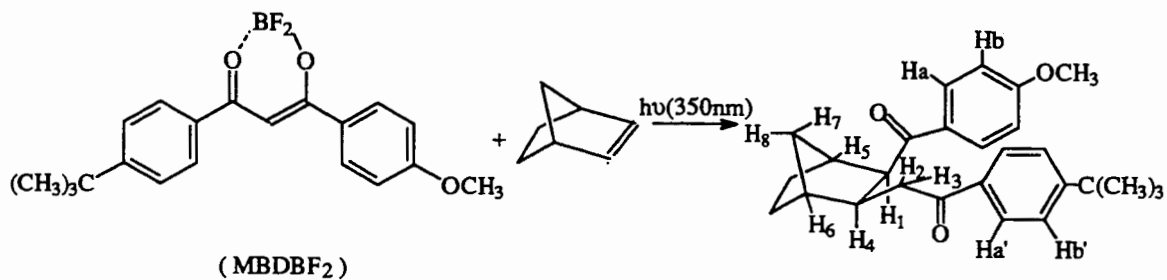
The structure was assigned using its spectroscopic data shown in Tables 4-6 to 4-9. MS (EI) gave a molecular weight of 404, which is consistent with the molecular formular of the 2+2 adduct of 4-t-butyl-4'-methoxy-dibenzoylmethane with norbornylene. The IR stretching bands at 1673 (vs) and 1601 (vs) cm^{-1} and ^{13}C NMR (in CDCl$_3$) resonances at 202.04 and 198.36 ppm supported the existence of two distinct carbonyl groups. ^{1}H-NMR decoupling experiments were able to rule out other structures. Irradiating of either H$_1$(3.57 ppm) or H$_4$ (2.79 ppm) caused the sharpening of the H$_8$ (1.25 ppm) doublet, conversely,

H_1 and H_4 sharpened when H_8 was irradiated. The long range coupling between H_1, H_4 and anti-bridge proton, H_8, is weak, therefore, further studies were conducted by ^1H nuclear Overhauser effect (nOe). ^1H noe spectra showed that 1) irradiation of H_1 resulted in an enhancement of H_4, H_5 and H_a in methyoxyphenyl, but no noe was observed in H_7, 2) irradiation of H_4 (H_2 and H_3 were also irradiated due to their close chemical shift) resulted in the enhancement of H_1, H_6, H_7,and H_{10}. It should be point out that the enhancement of H_7 was caused by irradiation H_2 and H_3. The noe effect at H_4 upon irradiation of H_1, combined with the absence of any enhancement from H_7 indicated that H_1 was located at *endo* position. Furthermore, H_1 and H_4 were in *cis* to each other, i.e., the 2+2 adduct was most likely a *cis, exo*-addition. Accordingly, the *cis, exo* adduct showed a very strong m/e 337 fragment which is arising from the MaLafferty rearrangement followed by the loss of a cyclopentenyl moiety.[39] The structures of (**22b**) and (**22c**) were safely ruled out on the basis of noe results. The structure (**22d**) was also ruled out basis on the observation of weak coupling between H_4 and H_8, and the observation of no coupling between H_4 and H_6. It was also concluded that the methoxylphenyl group was directly attached to norbornane ring by observing a noe in H_a upon irradiation of H_1, i.e., the sole adduct had a structure that corresponded to (**22a**), and not the regioisomer (**22e**)
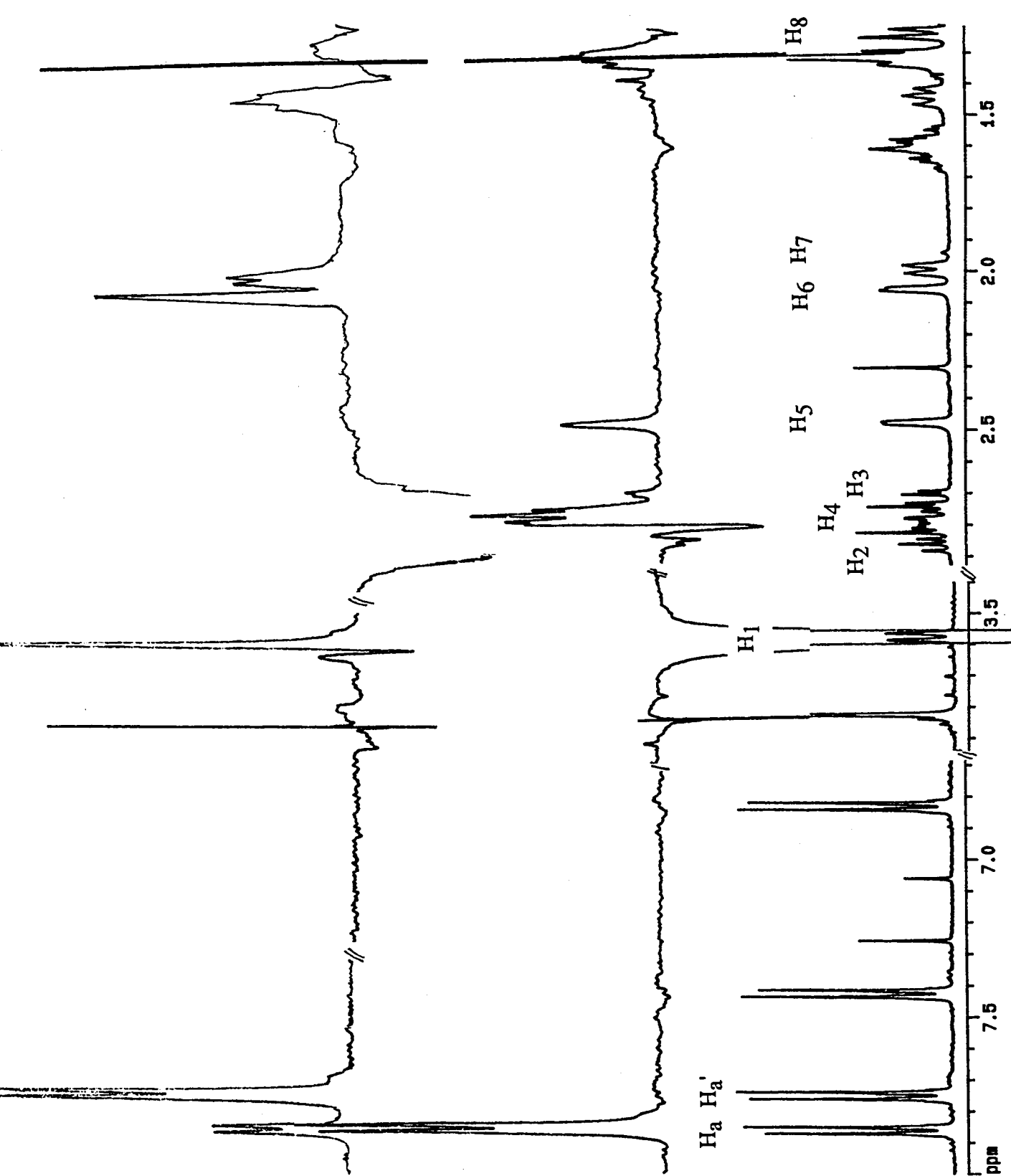
Fig.2-24   The ^{1}H NOE difference spectra of **22a** in CDCl$_3$

MBDBF$_2$ With 1,3-pentadiene:

The photolyses of CH$_3$CN solutions of MBDBF$_2$ (0.01 M) and 1,3-penradiene (0.01 M) resulted in the formation of the adduct (23) as suggested by GC-MS (EI mode, molecular weight of 378). This corresponded to a 1:1 adduct between 4-t-butyl-4'-methoxy-dibenzoylmethane with 1,3-pentadiene. The isolated products were a mixture (4:6 ratio by ^{1}HNMR) of 23a and 23b. The structures are shown below. The relative ratio of 23a and 23b was close to the cis-$trans$ ratio (4:6) in the starting material of 1,3-pentadiene. The structural assignment of 23 was based on its spectroscopic data shown in Tables 4-6 to 4-9. The ^{1}HNMR spectrum of adducts 23a and 23b showed two different allylic methyl signals at 1.69 and 1.66 ppm, respectively. Both were coupled with adjacent olefinic protons.

(MBDBF2)

(23a)

(23b)
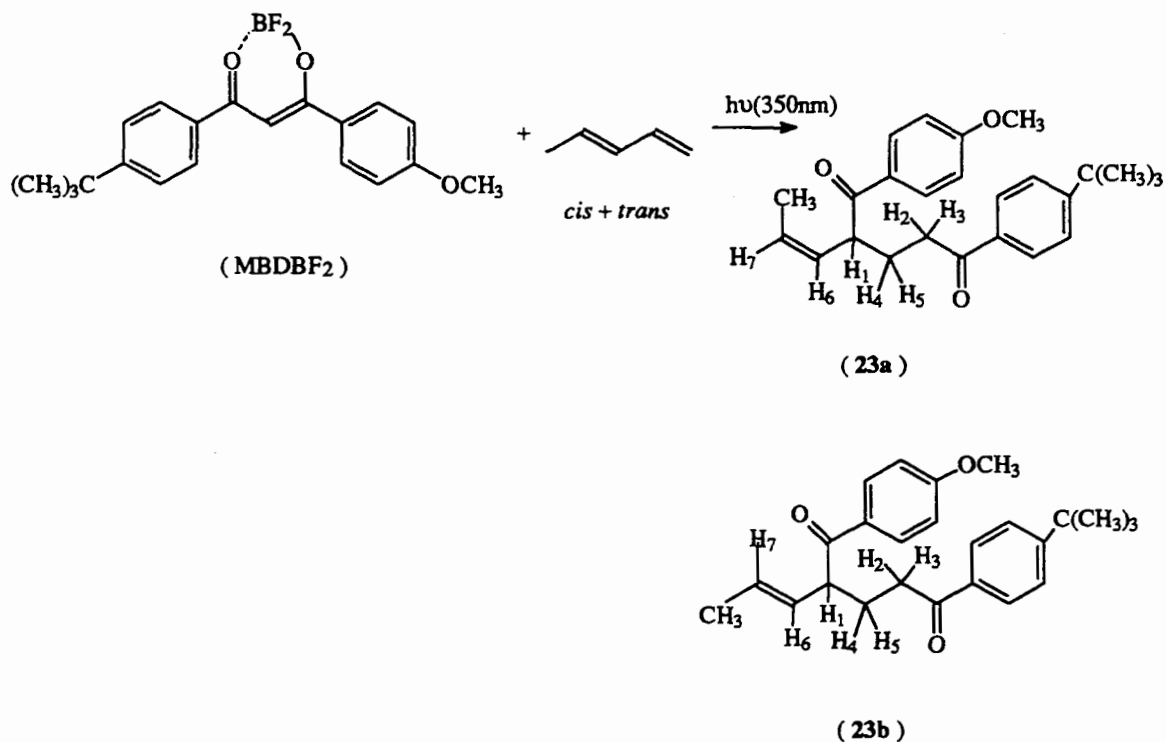
MBDBF2 With Methyl Methacrylate:

The photolyses of MBDBF$_2$ (0.05 M) in present of methyl methacrylate (0.5 M) in CH$_2$Cl$_2$ give one adduct (24) in a 44% yield. The structure (24), which could be derived from the head to head adduct, was supported by ^{1}H-NMR spectrum.

(MBDBF$_2$)

(24)
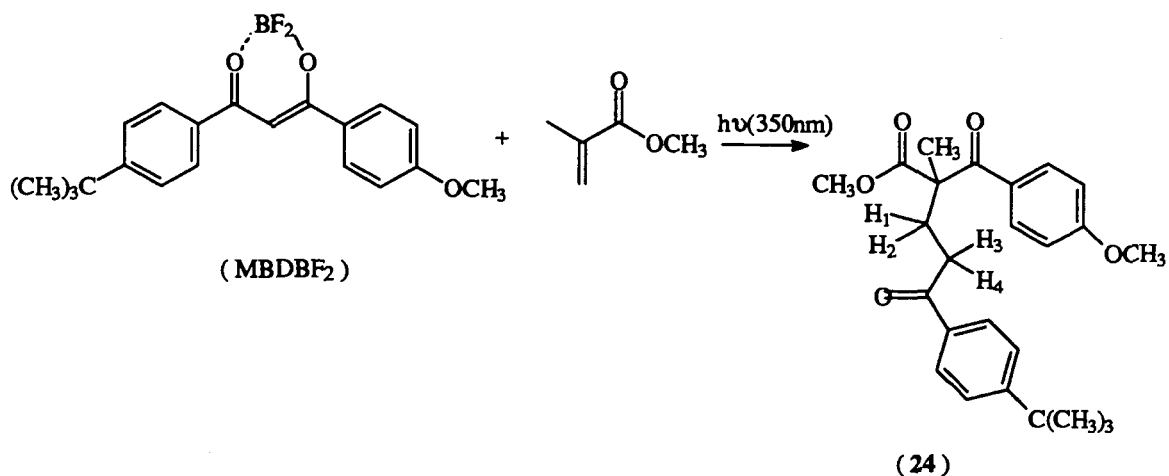
^{1}HNMR of **24** showed two groups of symmetrical multiplets at 2.45 and 2.90 ppm (2H each) that arose from the two magnetically non-equivalent methylenes on the adjacent position. It is necessary to mention that if adduct was the result of head to tail addition, the methylene protons should give an AB pattern for each methylene unit. However, this is not the case. In addition, IR, ^{13}CNMR and MS data (Table 4-6 to Table 4-9) supported the proposed structure (**24**). It should also be point out that the photocycloaddition occured with high regiospecificity.

CHAPTER 3   DISCUSSION

3-1   Mechanism Studies of Photocycloaddition of PN with AABF$_2$

3-1.1   Quantum Yield of Photocycloaddition

Both singlet state PN and AABF$_2$ are known to undergo [2 + 2] photocycloaddition with ground state olefines[16, 21], which implies that either PN or AABF$_2$ may initiate a photocycloaddition between PN and AABF$_2$. Since a wide spectral output of irradiation lamps was used for photocycloaddition experiments, and the absorption spectra of PN and AABF$_2$ overlap, we must differentiate which species initiates the reaction.

The quantum yield of product (9) increases when [AABF$_2$] is increased, but stays constant with increasing [PN]. This indicates that PN is the initiating excited state species.

3-1.2   Triplet Sensitization

PN undergoes an efficient intersystem crossing (Φ_{isc} = 0.82 in non polar solvent). Photocycloaddition of PN with maleate and fumarates demonstrates that the triplet state of PN is involved. The corresponding potential triplet state reaction was eliminated on the basis that triplet sensitization experiments show no cycloaddition products. Hence neither PN nor AABF2 triplet states are reactive. The result shows an interesting contrast to PN photoreaction with maleate and fumarates[21, 22, 30].

3-1.3 Steady-State Fluorescence Studies

Taking together triplet sensitization results, quantum yields clearly indicate that the singlet excited state of PN is the primary excited species under the experimental conditions employed.

At room temperature, PN fluorescence was efficiently quenched by the addition of $AABF_2$. The observed fluorescence quenching rate constant was found to be 5.4×10^9 M^{-1} in dioxane ($\tau = 55$ ns used in the calculation). This is near the diffusion controlled rate as suggested by pyrene excimer formation in a solvent of similar viscosity ($k_q = 6 \times 10^9$ $M^{-1}s^{-1}$)[40], which is known to be diffusion controlled. The reduction of PN fluorescence intensity by $AABF_2$ is accompanied by the appearance of a new red-shifted structureless emission band in dioxane with a λ_{max} at 480 nm. We assign this new emission as the exciplex formed from the singlet excited state of PN with the ground state of $AABF_2$. An exciplex is a relatively stable excited state species and the emission of exciplex is typically red shift and structureless band. Our experiments support the existence of the exciplex. It is expected that we should observe an isosbestic point when $AABF_2$ quenches the excited state of PN to generate the exciplex. Indeed, we observe an isosbestic point in the low concentration range of $AABF_2$ (<0.025 M). We also find that above $[AABF_2]$ = 0.035 M, the isosbestic point is lost and the intensity of exciplex emission ceases to increase regardless of further quenching of PN fluorescence. The quenching of the exciplex by $AABF_2$ is believed to cause the unfocused isosbestic point. This quenching of exciplex by $AABF_2$ is insignificant in the low concentration range of $AABF_2$, but starts to show at high concentrations of $AABF_2$. Previous steady-state fluorescence studies were conducted in fluid solutions. Under these conditions

59

the excited state of PN and ground state of AABF$_2$ could diffuse to close distances within the lifetime of the excited state PN. However, in a frozen solution of 2-propanol and ether, neither fluorescence nor phosphorescence of PN is affected by AABF$_2$ concentrations up to 0.025 M at 77K. This observation rules out the long range Coulombic mechanism for the interaction of excited state of PN with ground state of AABF$_2$. It is concluded that the interaction of singlet excited PN with AABF$_2$ must occur by close contact (about 3.5$\overset{o}{A}$) as required by the exciplex formation.

3-1.4 Exciplex Characterization

The observation of exciplex fluorescence in the PN-AABF$_2$ system raises our interest to study the nature and dynamics of this exciplex. Solvent effects on the electronic spectra (such as absorption and emission) of organic molecules are well known and have been used to characterize the dipolar nature of the absorbing and emitting species. It was observed that the maximum and intensity of exciplex emission are sensitive to solvent polarity. The polar nature of the exciplex (PN/AABF$_2$) is revealed by the bathochromic shifts of the emission maxima with increasing solvent polarity. The dipole moment of 11.6 D is attributed to charge-transfer character, where complete electron transfer would give a dipole moment of 12 -14 D[29, 41]. This means that exciplex is stabilized by the charge-transfer interaction. Further charge-transfer perturbations by the other electron donor or acceptor are utilized to study the exciplex. Caldwell and co-workers have examined several exciplexes[42]. Their study shows that exciplexes seem to have a distinct preference for quenching by either electron donors or acceptors, but not both. As we know PN

acts as electron donor, due to its lower oxidation potential, in the exciplex of PN/AABF$_2$, therefore, we chose anisole and 1,3-pentadiene, electron donors, as quenchers. Both quenchers are capable of quenching the exciplex without quenching the initial excited state of PN significantly. We have found that exciplex fluorescence and photoproduct are attenuated to the same extent when a certain amount of quencher is added to the reaction mixture. The Stern-Volmer equations of 2-5 and 2-6 are used to study the quenching process. The quenching constants, K_{SV} ($k_q^{ex}\tau^{ex}$) obtained from the exciplex fluorescence quenching study agree well with those obtained from quantum yield measurements of the cycloadditions. A comparison of the quenching efficiencies are shown in Table 3-1.

Table 3-1. Exciplex quenching efficiency (kqτ)

Quencher	kqτ	
	cycloaddition	fluorescence
Anisole	10.7 ± 1.0 (purged)	10.0 ± 0.3 (purged)
	7.0 ± 0.6 (aerated)	6.9 ± 0.2 (aerated)
1,3-pentadiene	1.6 ± 0.1 (purged)	2.1 ± 0.2 (purged)

The results can be rationlized in terms of an exciplex formation from the singlet excited state of PN with the ground state of AABF$_2$ and this eventually leads to photoaddition. It can be concluded unambiguously that the singlet emitting exciplex of PN/AABF$_2$ is the percursor of the photocycloaddion.

3-1.5 Proposed Mechanism

Based on steady-state experiments, the proposed mechanism involving the exciplex as the intermediate is shown in Scheme (3-1).

Scheme 3-1

$$PN \qquad\qquad PN + AABF_2$$

$$\uparrow k_{qc}[Q] \qquad\qquad \uparrow k_{qc}^{ex}[Q]$$

$$^*PN \; \underset{k_{-a}}{\overset{k_q[AABF_2]}{\rightleftharpoons}} \; ^*(PN\text{-}AABF2) \; \xrightarrow{k_q^{ex}[AABF_2]} \; PN + 2AABF_2$$

$$h\upsilon \;\Big\updownarrow\; \Sigma k_d \qquad\qquad \Big\downarrow\; \Sigma k_d^{ex} + k_r$$

$$PN + h\upsilon' \qquad\qquad PN + AABF_2 + h\upsilon'' + 9$$
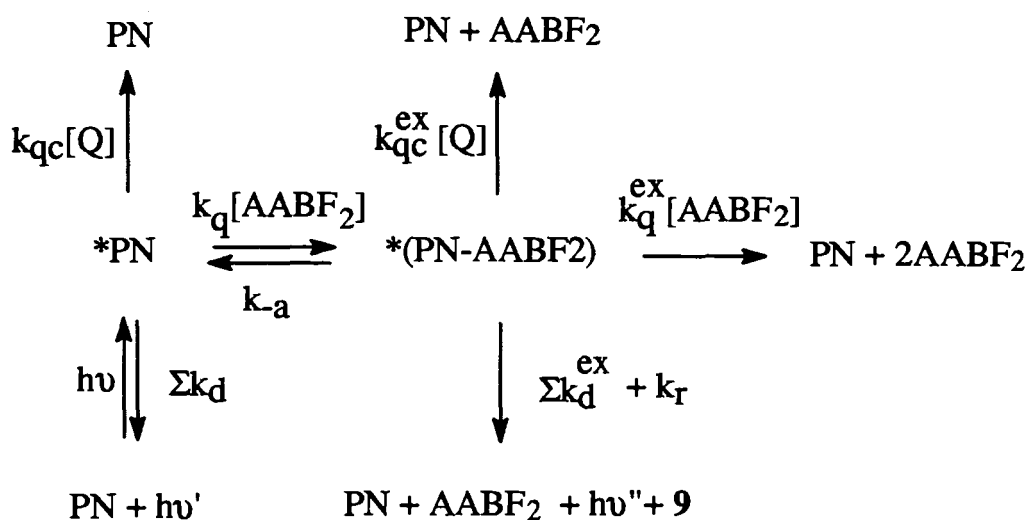
The terms $\sum k_d$ and $\sum k_d^{ex}$ represent the sum of all unimolecular reactions rates for $^*PN$ and the exciplex $^*(PN\text{–}AABF_2)$, respectively, and they involve the fluorescence decay rate (k_f , k_f^{ex}). The terms k_q and k_q^{ex} represent the rate constants for the interaction of $^*PN$ and the exciplex with $AABF_2$, respectively. k_r is the rate constant for the formation of 9 from the exciplex. k_{-a} is the rate constant of the reverse reaction. The k_{qc} and k_{qc}^{ex} are employed only when another quencher is present. Based on Scheme (3-1) under steady state conditions, the quantum yield of cycloaddition (Φ) can be derived as shown in Eq. (3-1):

$$\frac{1}{\Phi} = \frac{(\sum k_d^{\alpha} + k_{-a} + k_q^{\alpha}[AABF_2])(\sum k_d + k_q(1-f)[AABF_2])}{k_r k_q[A]}$$

$$(3-1)$$

where f is the reverse reaction efficiency, and is expressed as follows:

$$f = \frac{k_{-a}}{\sum k_d^{\alpha} + k_{-a} + k_r + k_q^{\alpha}[A]}$$

If the proposed mechanism is correct, the calculated Φ from equation (3-1) should agree with the experimental results listed in Table (2-1). A direct comparison of Φ from equation (3-1) with that of experimental values is impossible without prior knowledge of some rate constants. Therefore a quantitative analysis of the proposed mechanism concerning equation (3-1) is deemed necessary. To obtained all the rate constants steady state methods can not be easily applied, however, time-resolved fluorimetry is capable of accessing the rate constants (Scheme 3-1).

3-1.6 Kinetic Studies of Photocycloaddition of PN with AABF₂

Analysis of dynamics of exciplex formation and decay may change from simple to complex[43, 44, 45, 46]. Ware and Coworks have investigated some systems and they successful obtainted the detail kinetic analysis based on the variations in the fluorescence lifetimes of the unquenched monomer component and the exciplex with increasing the quencher concentration[47]. A similar approach is used in our studies. The formation and decay of the fluorescent

63

exciplexes were studied using transient fluorescence measurements. The time dependence of *PN and the exciplex concentrations are expected to obey the coupled differential equations (3-2) and (3-3).

$$\frac{d[^*PN]}{dt} = I(t) + k_{-a}[^*PN - AABF_2] - (\sum k_d + k_q[AABF_2])[^*PN] \tag{3-2}$$

$$\frac{d[^*PN - AABF_2]}{dt} = k_q[AABF_2][^*PN] - (\sum k_d^\alpha + \sum k_r + k_q^\alpha[AABF_2])[^*PN - AABF_2] \tag{3-3}$$

If a δ function excitation pulse is used, the solutions of Eqs. (3-2) and (3-3) are given by Eq. (3-4) and Eq. (3-5).

$$[^*PN](t) = C_1 e^{-\lambda_1 t} + C_2 e^{-\lambda_2 t} \tag{3-4}$$

$$[^*PN - AABF_2](t) = C_3 (e^{-\lambda_1 t} - e^{-\lambda_2 t}) \tag{3-5}$$

where

$$2\lambda_{1,2} = X + Y \pm \{(X-Y)^2 + 4k_q k_{-a}[AABF_2]\}^{1/2} \tag{3-6a}$$

$$X = \sum k_d + k_q[AABF_2] \tag{3-6b}$$

$$Y = \sum k_d^\alpha + k_r + k_{-a} + k_q^\alpha[AABF_2] \tag{3-6c}$$

X and Y represent the sum of the decay rate constants of *PN and *(PN-AABF₂), respectively.

From Eq. (3-6a) the relation between the observed lifetimes can be expressed by Eqs. (3-7) and (3-8) as follows:

$$\lambda_1 + \lambda_2 = \sum K_d + \sum k_d^{ex} + k_r + k_{-a} + (k_q + k_q^{ex})[AABF_2] \tag{3-7}$$

$$\lambda_1 \lambda_2 = \sum k_d (\sum k_d^{ex} + k_r + k_{-a}) + \{k_q^{ex} \sum k_d + k_q \sum k_d^{ex}\}[AABF_2] + k_q k_q^{ex}[AABF_2]^2 \tag{3-8}$$

These equations are utilized to calculate individual rate constants on the assumption that the mechanism is valid. Based on equations 3-6, 3-7 and 3-8, the plots shown in Figures 3-1 through 3-3 were used to analysis and the rate constants were obtained (shown in Table 2-7).
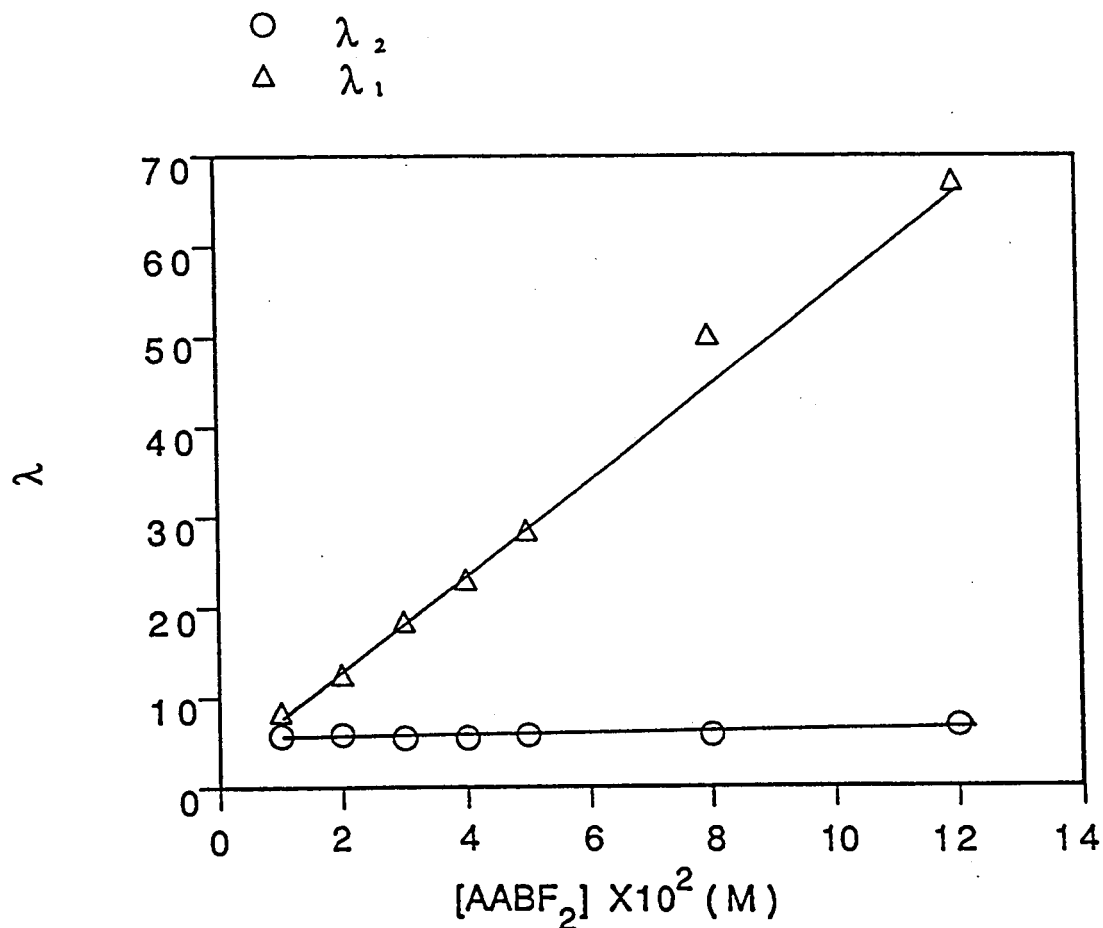
Fig. 3-1 λ_1 or λ_2 *vs* [AABF$_2$]
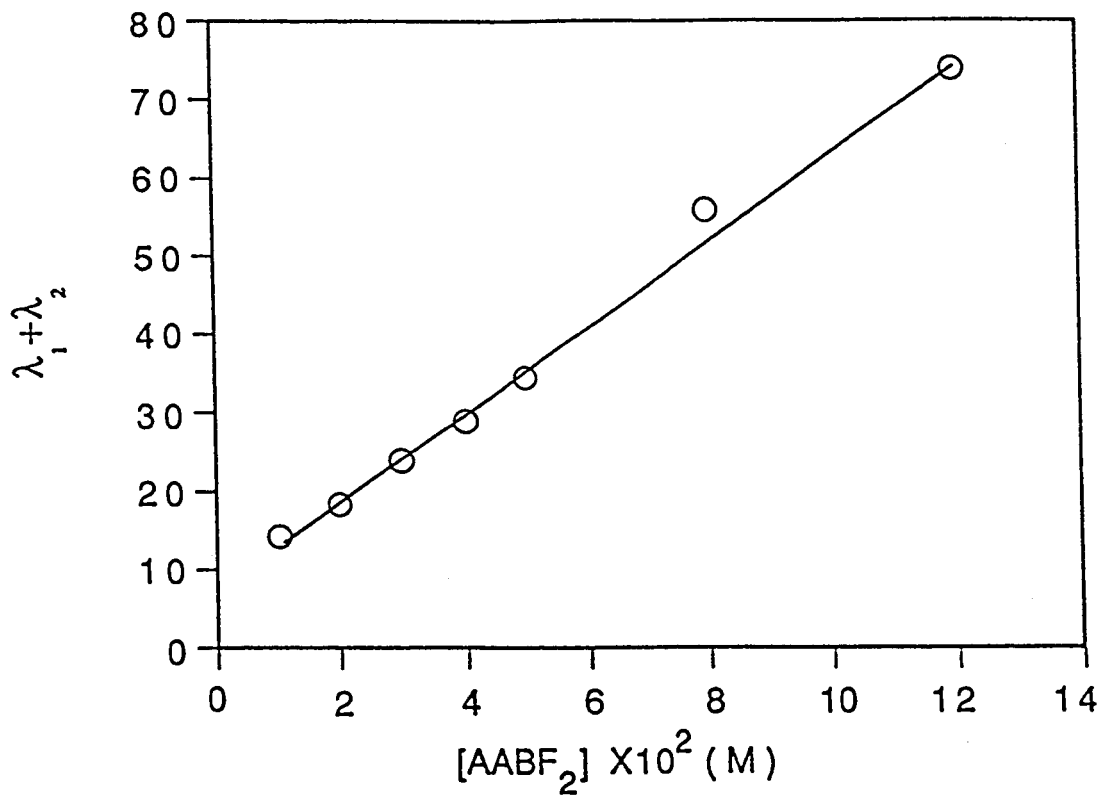
Fig. 3-2 $\lambda_1 + \lambda_2$ *vs* $[AABF_2]$
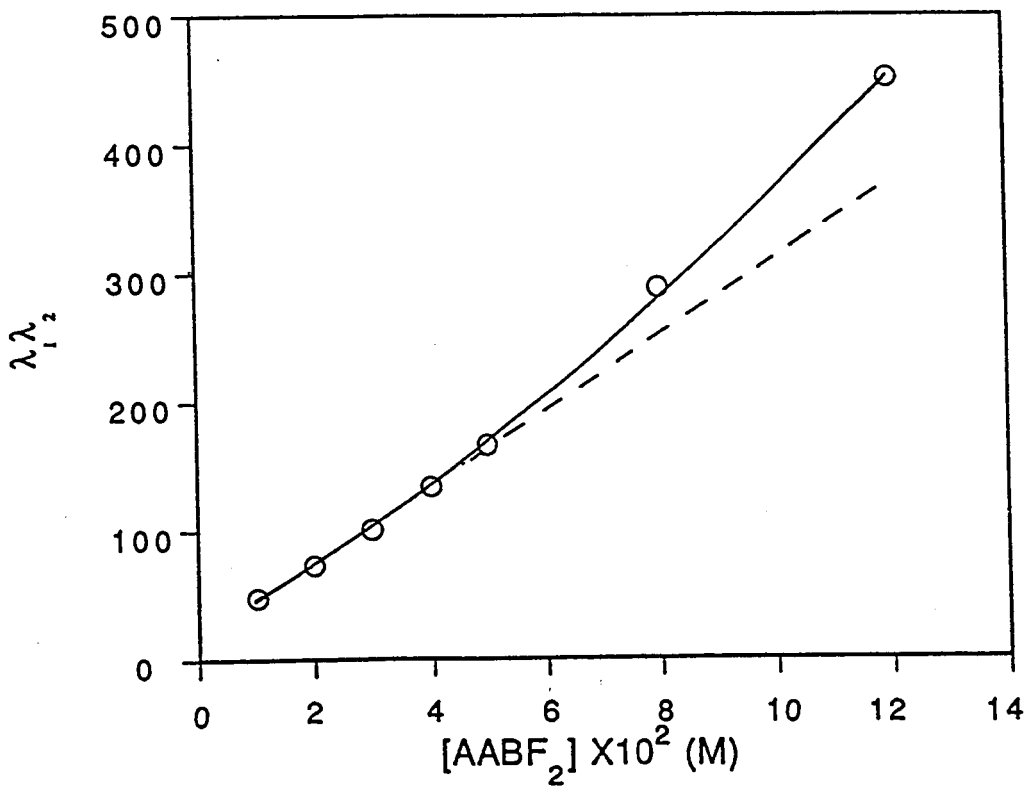
Fig. 3-3 $\lambda_1 \lambda_2$ *vs* $[AABF_2]$

The plot of λ_1 vs [AABF$_2$] (Fig.3-1) is linear, indicating the irreversible formation of exciplex. The slope from this graph give a k_q of 5.51×10^9 M^{-1}s^{-1}. The plot of $\lambda_1\lambda_2$ versus [AABF$_2$] shows a slight upward curvature indicating a contribution from the quadratic term in Eq. (3-8). That means that k_q^α does exist. These conclusions are in accord with the steady state results where quenching of *PN-AABF$_2$ by AABF$_2$ leads to scrumbling of the isoemissive point. Where the exciplex is formed irreversibly, as expected from equation 3-6a, a plot of the exciplex decay constant, λ_2 versus the concentration of AABF$_2$ yields a straight line with zero slope at low concentrations of AABF$_2$ (<0.12 M). The zero slope indicates that quenching of exciplex by the ground state of AABF$_2$ is insignificant. The intercept is used to calculated the sum of all *PN-AABF$_2$ unimolecular decay rate constants, $\Sigma k_d^{ex} + k_r + k_{-a} = 5.7 \times 10^7$ s^{-1}. When [AABF$_2$] > 0.12 M, the plot of λ_2 versus [AABF$_2$] is linear with a positive slope, which gives $k_q^\alpha = (7.6 \pm 0.4) \times 10^7$ M^{-1}s^{-1}. The plot $\lambda_1 + \lambda_2$ versus [AABF$_2$] affords a slope of (5.57 ± 0.22) $\times 10^9$ M^{-1}s^{-1} and an intercept of (7.46 ± 0.79) $\times$ 10^7 s^{-1}. Appropriate subtractions from these figures give $k_q^\alpha = (6.8 \times 10^7$ M^{-1}s^{-1}). The average of the two is 7.2×10^7 M^{-1}s^{-1}.

The lifetimes of PN under argon and air in dioxane solution are 53.8 ns and 26.1 ns, respectively. Static fluorescence quenching experiments gave rate constants (k_q) of 5.2×10^9 M^{-1}s^{-1} and 4.6×10^9 M^{-1}s^{-1} under argon and air for the interaction of *PN with AABF$_2$. The fluorescence decay kinetics demonstrate that the exciplex formed irreversibly in dioxane, i.e., $k_{-a} \ll \Sigma k_d^{ex} + k_r$. This conclusion is confirmed by the close agreement of k_q from steady and time resolved quenching results. It is now possible to use the rate constants estimated from static and dynamic fluorescence decays to evaluate the quantum yield

pattern of the product shown in Fig. (2-2). A reasonably good agreement with experimental values may be regarded as evidence for the reaction mechanism as proposed. In order to do this, it is necessary to estimate the rate constant of the product formation from the exciplex, k_r. It is carried out by using experimental point where $[AABF_2] < 0.02M$, the linear portion is extrapolated to the $1/\Phi$ axis to give intercept = 7.7 ± 2.5, which is the reciprocal of limiting quantum yield. Since the above treatment is carried out in the low concentration range where the quenching of exciplex by $AABF_2$ is unimportant, every excitation of PN leads to an exciplex followed by the formation of products. Since $k_r = \Phi \times (\Sigma k_d^{ex} + k_r)$, the value of k_r was found to be 7.4×10^6 s^{-1}. The accuracy of this value is limited owing to scatter of the data points in the linear portion. All kinetic data are used to compute the quantum yield by Eq. (3-1) under the experimental condition in dioxane, the resulting the plot of $1/\Phi$ versus $1/[AABF_2]$ agrees in the low concentration range but deviates from the experimental points as represented by a solid line in Fig. (2-2). Numerical fitting shows that the computed line agrees with the experimental points in all concentration range if k_q^{ex} is 10 times larger than that obtained from fluorescence decay study (the other rate constants remain the same). Since the quantum yield can be affected by many factors, the lifetime measurement is considered more reliable. In our study, the quantum yield determination is complicated in two respects. First, quenching of the exciplex by $AABF_2$ causes a curvature in the plot of $1/\Phi$ vs $1/[AABF_2]$. This is caused by a built in secondary dependency on $[AABF_2]$ as illustrated by eq 3-1. This contribution does not cause a drastic deviation. Second, because of the close overlap of the absorption bands of PN and $AABF_2$ in the 310-350 nm area, an increase in $[AABF_2]$ leads to an increase in the absorption of light without generating the exciplex and the product. The overall

effect artificially retards the quantum yield by an internal screen effect when [AABF$_2$] increase.

3-1.7 Flash Photolysis

The dipole moment of exciplex (11.6 D) indicates a substantial charge transfer character. Failure to observe photocycloaddition in CH$_3$CN, a polar solvent, indicates that the proposed mechanism (Scheme 3-1) requires modification. As we know, the excited donor-acceptor may form as either an exciplex (EXC) or radical ions. These radical ions may be classified as contact radical ion pair (CRIP), solvent-separated radical ion pair (SSRIP) and free-radical ions (FRI). The dominance of any of these species is strongly influenced by polarity of solvent as shown in Scheme 3-2[48, 49, 50]:

Scheme 3-2

$$A + {}^{*}D \longrightarrow ({}^{*}AD) \longleftrightarrow (\overset{..-}{A}\ \overset{.+}{D}) \rightleftharpoons (\overset{..-}{A_s}\ \overset{.+}{D_s})$$

$$\text{EXC} \qquad\qquad \text{CRIP} \qquad\qquad \text{SSRIP}$$

$$\uparrow h\upsilon \qquad\qquad\qquad\qquad\qquad\qquad \updownarrow$$

$$A + D \qquad\qquad\qquad\qquad\qquad \overset{..-}{A_s} + \overset{.+}{D_s}$$

$$\text{FRI}$$
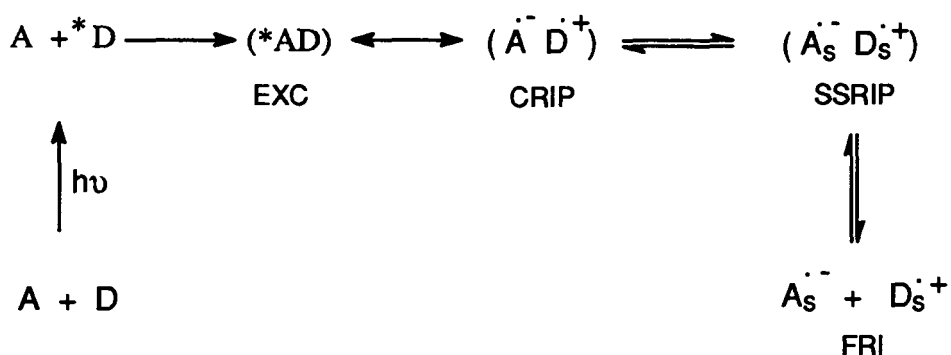
SSRIP and FRI are more solvated, therefore, it is expected to be more sensitive to solvent polarity than EXC and CRIP. We succeeded in observing the transient spectra of the PN cation radical by flash photolysis in the presence of PN and AABF$_2$ in CH$_3$CN. Presumably, the AABF$_2$ anion radical is also present but it

was not detected. This accounts for a change in mechanism in CH_3CN. Obviously, the radical ions are energetically disfavored in non-polar solvents, hence exciplex formation dominates in non-polar solvents. In polar solvent, the channel leading to radical ions is more favorable since they are stabilized through solvation. The observation of a cation radical of PN suggests that a full electron transfer occurs. This electron transfer may occur through two possible routes as shown below:

$$A + D \xrightarrow{h\upsilon} A + {}^*D \longrightarrow ({}^*AD) \xrightarrow{a} A_s^{\cdot -} + D_s^{\cdot +}$$

$$\downarrow b$$

$$A_s^{\cdot -} + D_s^{\cdot +}$$

Without further investigation, we can not distinguish between a and b. However, either route does compete with product formation. The lack of any detectable product formation from the photochemical reaction in CH_3CN suggests that the formation of the cation radical of PN occurs efficiently. It can be concluded that the opening up of the FRI pathway is , at least in part, responsible for the lack of formation of photoadduct in CH_3CN.

3-2   Photophysics and Photochemistry of MBDBF$_2$ with Olefins

3-2.1   Emission of MBDBF$_2$

At low concentration (10^{-6} M), MBDBF$_2$ shows strong emission in non-polar solvent (n-hexane) and polar solvent (CH_3CN). The emission band is

approximately the mirror image of the absorption band of MBDBF$_2$ in corresponding solvents.

3-2.2   Excimer Formation of MBDBF$_2$

MBDBF$_2$ exhibits a remarkable concentration dependence on fluorescence emission resembles that found in a pyrene solution in heptane,[51] which is a classic example of excimer formation. Raising the concentration of MBDBF$_2$ lead to quenching of the monomer fluorescence of MBDBF$_2$ and a new structureless emission band appeared at λ_{max} 520 nm, which is red shifed as compared to the monomer fluorescence.   It is concluded that the excimer is formed at high concentration of MBDBF$_2$ by a dynamic interaction of singlet excited state of MBDBF$_2$ with its ground state.

3-2.3   Photocycloaddition of MBDBF$_2$ with olefins

We have made a preliminary investigation of the photocycloaddition of MBDBF$_2$ with several olefins to see their complexity and feasibility.   All products obtained from the photolyses of MBDBF$_2$ with olefins are δ-diketones. These products result from a 2 + 2 cycloaddition reaction that gives a cyclobutane intermediate, followed by a spontaneous ring opening of the cyclobutane to give the final δ-diketone product.

Irradiation of MBDBF$_2$ to 1,3-pentadiene and methyl methacrylate only give the head to head adducts.   Thermodynamically, the formation of the sterically hindered head to head adducts is less favorable, and the reaction should be expected to yield preferentially the head to tail adduct.   The head to

head adduct obtained is explained that the 2+2 cycloaddition is likely to proceed through an exciplex intermediate. In the other words, if a reaction involves the exciplex formation step, the activation energy will be minimum for the most stable exciplex. Head to head addition can give maximum overlap between the aromatic π-orbital in MBDBF$_2$ and the π-orbital in either 1,3-pentadiene or methyl methacrylate which has minimum activation energy.[52]

The structures of BABF$_2$ and MBDBF$_2$ have unsymmetrical character. The carbon-carbon double bond may be located in two different positions as illustrated in Scheme 3-2. This unsymmetric BF$_2$ complex may result in the complexity of the photocycloaddition pattern. The results show that addition is regiospecific. The addition of BABF$_2$ and cyclohexene occurs at (a) position. The same results are observed in photocycloaddition of MBDBF$_2$ and 1,3-pentadiene, methyl methacrylate and norbornylene, which addition preferably occurs at (a) position[53].

Scheme 3-2

(a) BABF$_2$ (b)

(a) (b)

MBDBF$_2$

72
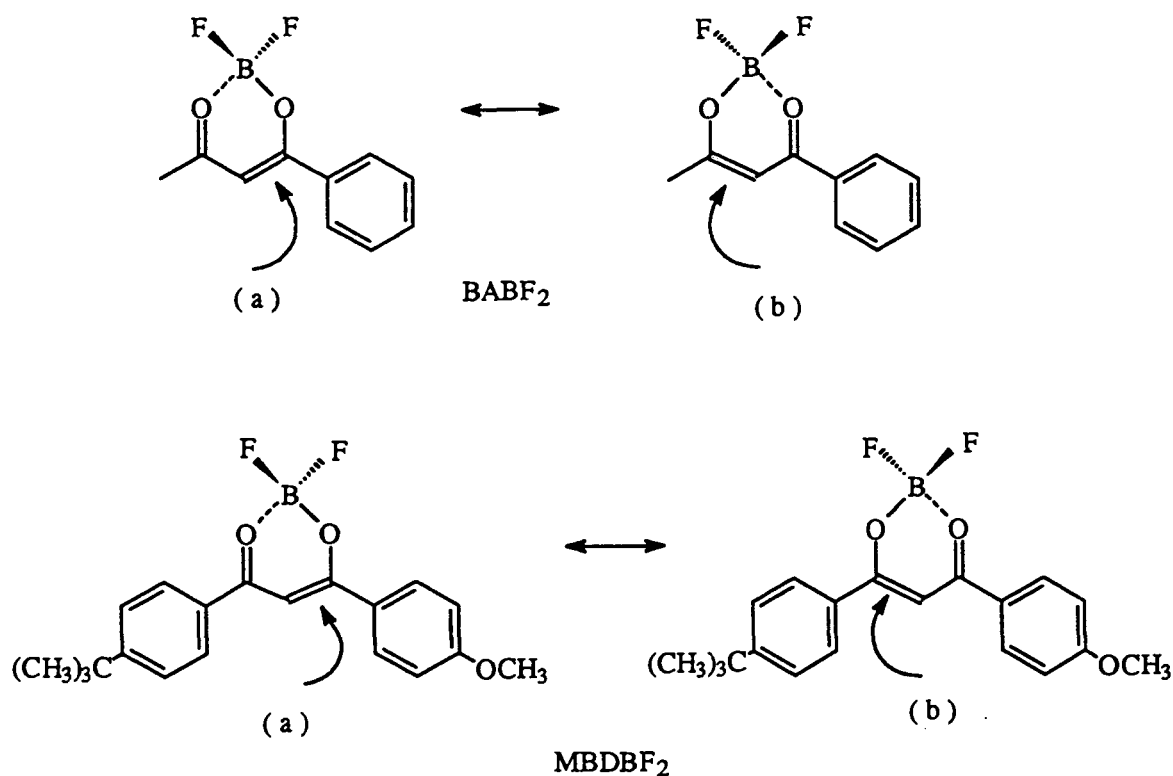
As we know the photocycloaddition of acetylacetone to norbornylene give the *cis-exo* product. This has been explained in terms of the approach of an attacking reagent on the less hindered exo-face of norbornylene[54, 55].

3-3   Concluding Remarks

In summary, a number of studies have been carried out on the mechanism of photocycloaddition of PN and $AABF_2$, the photophysics and photochemistry of $MBDBF_2$. The results from these studies lead to the following conclusions:

(1).   The photocycloaddition of PN and $AABF_2$ is solvent dependent, and it occurs in non- or medium- polar solvent, but not in CH_3CN.

(2).   No triplet state is involved in the photocycloaddition of PN and $AABF_2$.

(3).   No ground state complex of PN and $AABF_2$ was detected.

(4).   PN/$AABF_2$ exciplex fluorescence emission is found in non- and medium polar solvent, but not in polar solvent (CH_3CN). This exciplex has been estimated to have dipole moment as 11.6 ± 0.5 D which indicates a substantial electron transfer involved in exciplex.

(5).   PN/$AABF_2$ exciplex has been demonstrated to be the intermediate for the photocycloaddition reaction.

(6).   The formation of exciplex is irreversible and diffusion controlled process.

(7).   At high [$AABF_2$] the PN/$AABF_2$ exciplex is further quenched by $AABF_2$.

(8).   The curvature of double reciprocal of $1/\Phi$ vs $1/[AABF_2]$ at high [$AABF_2$] is due to simultaneous complication from quenching of exciplex by $AABF_2$ and unproductive light absorption by $AABF_2$.

(9).   The rate constants are obtained from static and kinetics fluorescence studies.

(10). The cation radical of PN has been observed in CH_3CN. It is concluded that singlet excited PN preferentially undergoes electron transfer to give the cation radical of PN without undergoing a cycloaddition in CH_3CN.

(11). $MBDBF_2$ exhibits monomer and excimer fluorescence emission.

(12). The monomer of $MBDBF_2$ is quenched by 1.3-pentadiene, norbornylene, methyl methacrylate and cyclohexene.

(13). $MBDBF_2$ photocycloaddes to 1.3-pentadiene, norbornylene and methyl methacrylate in CH_2Cl_2 to give 1,5 diketones. The additions of $MBDBF_2$ with 1.3-pentadiene and methyl methacrylate give head to head adducts. Photocycloaddition occurs at the carbon-carbon double bond next to the *p*-methoxyphenyl side of $MBDBF_2$ with high regioselectivity.

CHAPTER 4   EXPERIMENTAL

4-1   General Conditions And Material

4-1.1   Analytical Equipment

Gas chromatography (GC) analysis was performed on a Hewlett packard 5790 chromatograph equipped with a 3390 A Integrator and a 15m x 0.2 mm DB-1 capillary column.   Retention times (Rt) are reported in minutes (min). Ultraviolet and Visible (UV/VIS) spectra were obtained using a Varian Cary-210 or PU8720 spectra photometer.   Infrared spectra (IR) were recorded on a Perkin Elmer 559B or Perkin Elmer/1600 Series FTIR (neat film, KBr pellet).   The intensities of IR signals are reported as s (strong), m (medium), w (weak). Melting points (m.p.) were measured on a Fisher-Johns melting point apparatus (uncorrected).   Fluorescence and phosphorescence spectra were obtained from a Perkin-Elmer MPF 44B spectrophotometer (uncorrected).   Mass spectra (MS) and gas chromatography-mass spectra (GC-MS) were acquired using a Hewlett-Parkard 5985 GC-MC system equipped with a DB-1 capillary column.   MS spectra was obtained using electron impact ionization (EI) and/or chemical ionization (CI).   Routine nuclear magnetic resonance (NMR) spectra were obtained using a Bruker 400 MHz spectrometer.   Chemical shifts of ^{1}H and ^{13}C spectra are both reported in parts per million (ppm) and referenced to tetramethylsilane.   The splitting patterns of ^{1}H are presented as s (singlet), d (doublet), t (triplet), q (quarter), or m (multiplet).   The coupling constants are reported in Hz.   Fluorescence lifetimes were measured at room temperature on a single photon counting instrument (PTI LS-1 Spectrofluorimeter equipped with

single photon electronics) using a hydrogen spark lamp as the excitation source. Fluorescence decays were analyzed using a software supplied by PTI. Flash column chromatography was carried out using 230-400 mesh silica gel (Merch) with either dichloromethane or ethyl acetate/ hexanes as eluant.

4-1.2 Chemicals

(a) Solvents

Photochemical reactions were carried out in reagent grade solvents and they are CH_3CN, diethyl ether, ethyl acetate and hexanes (BDH); *p*-Dioxane (Anachemia); dichloromethane (Fisher). Spectroscopic grade solvents were employed in photophysical studies without further purification. These solvents are CH_3CN, diethyl ether and carbon tetrachloride (BDH); chloroform (Fisher); dichloromethane, cyclohexane and methyl alcohol (Mallicrodkt); *p*-Dioxane (Anachemia).

NMR studies were carried out using chloroform-d (MSD) which was used as supplied.

(b) Olefin, Arene and Diketone

All olefins except norbornylene (Aldrich) used in photolysis and fluorescence quenching were distilled prior to use. These olefins were cyclohexene (Aldrich), 1,3-pentadiene (Matheson, technical), 3,3-dimethylbutene (Aldrich), methyl methacrylate (Anachemia, practical), anisole (BDH). Purification of PN (Matheson) required the removal of anthracene using a published method.[19b] Acetylacetone (BDH, reagent grade), and 4-*tert*-Butyl-4'-methoxy-dibenzoylmethane (Givaudan, SA) were used as received without

purification in the preparation of BF_2 complexes. $AABF_2$ and $MBDBF_2$ were prepared using a published procedure[1] and then purified by recrystallization.

(c) Others

n-Hexadecane (Sigma) and Dodecane (Matheson, practical) were used for internal standard in GC analysis. Acetophenone (BDH), Benzhydrol (Matheson), Benzophenone (Fisher, certified) and Xanthone(Aldrich) were used as supplied.

4-1.3 Photolysis Appraratus And Quantum Yield Determination Method

Apparatus

Pyrex test tubes containing samples were placed in merry-go-round sample holder that was mounted in a Rayonet photochemical reactor equipped with either RPR-3000 $\overset{o}{A}$ lamps (16 x 21 watts) or RPR-3500 $\overset{o}{A}$ lamps (16 x 24 watts). The apparatus was equipped with a cooling fan that provided a constant temperature of approximately 31°C.

Method for quantum yield determination:

The following procedures were followed in the preparation of the actinometer solution which was used in measurements of light intensity and quantum yield.

Actinometer:

The stock actinometer solution was prepared by dissolving benzophenone (456 mg, 2.50 mmol) and benzhydrol (921 mg, 5.00 mmol) in benzene (50 ml).

The concentrations of benzophenone and benzhydrol in this solution were 0.050 M and 0.100 M. 5.0 ml of the actinometer solution was pipetted into test tubes and purged with N_2 for 7 minutes. These test tubes were irradiated for 10 minutes together with test tubes containing the sample solution in question in merry-go-round apparatus. Optical absorbances of the solutions, before and after irradiation, were measured using a cell with 0.1 cm path length. The actiometer of benzophenone and benzhydrol have a quantum yield of 0.74. The consumption of benzophenone was determined from the absorption at 340 nm. This result was employed in the calculation of the incident light intensity (in Einstein / min) was determined using Eq. (4-1):

$$I^0 = \frac{\Delta c \times v}{\Phi \times \Delta t} \quad \text{(einstein, min}^{-1}\text{)} \qquad (4\text{-}1)$$

where Δc refers to concentration change of benzophenone which was calculated from the absorbance change at 340 ± 2 nm. Δt represents the irradiation time of actinometer in minute; Φ is quantum yield of actinometer

Quantum yield measurement:

The unknown quantum yield of compound was studied under the assumption that incident light intensity was the same as actinometer. The same Eq. (4-1) was applied, but using its alternative form shown in Eq. (4-2).

$$\Phi = \frac{\Delta c \times v}{I^0 \times \Delta t} \qquad (4\text{-}2)$$

where Δc refers to concentration change of product that was obtained by GC analysed with hexadecane ($C_{16}H_{34}$) as an internal standard (I.S.) expressed by Eq. (4-3)

$$\Delta c = R_f \times f \times [I.S.] \qquad (4\text{-}3)$$

where R_f is GC peak area ratio of product to I.S. and f is a response factor for the product.

4-2   Photochemistry and Photophysics of PN With AABF$_2$

4-2.1   Purification of PN

There is anthracene(3%) in phenanthrene sample. Since anthracene and phenanthrene exhibited a similar emission character, existence of anthracene interferes PN's fluorescence study.   Recrystallization could not remove anthracene. The reported method was used to purify PN[19b]. Phenanthrene (6.0 g) was refluxed with malic anhydride (0.14 g) in o-xylene (30 ml) for 7 hours.   Malic anhydride reacts with anthracene to form anhydrides. After reaction, the solution was extracted with base, Na$_2$CO$_3$(aq.), to remove the anhydrides. Then solution was washed with 10 ml water, separated water and dried over MgSO$_4$. The residue was obtained after removed solvent.   The residue was recrystallized from Et$_2$OH.   White leaf shape crystal of PN was obtained M.P. 98 ± 1°C. After reaction, no UV-VIS absorption due to anthracene was detected.   The absorption spectra of PN are shown in Fig.4-1.
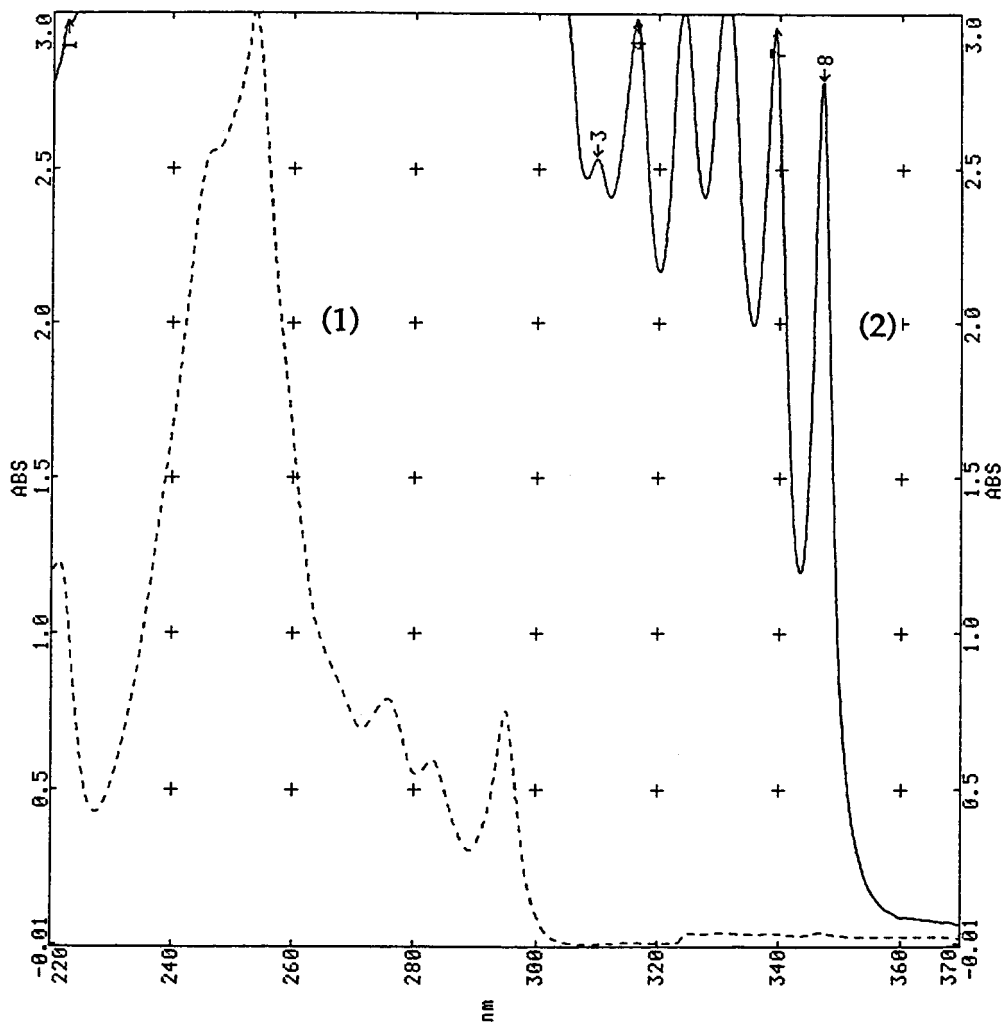
Fig.4-1　　The absorption of PN in dioxane

　　(1) [PN] = 5.0×10^{-5} M

　　(2) [PN] = 1.3×10^{-2} M

4-2.2 Acid and Base Treatment of Diketones (9)

In ether (9) was slowly isomerized to (10); the yield was only 5-6 % in 10 h stirred in heterogeneous phases with 0.1 N aqueous H_2SO_4.

0.2 N $NaOCH_3$-CH_3OH was used to treat cis product (9). After 1.5 h stirred, 40 ml water was added, and resulting solution was extract with 3 x 20 ml CH_2Cl_2. The combined CH_2Cl_2 extract was washed with saturated NaCl solution and dired with $MgSO_4$. The crude product was analysis by GC-MS which have two peaks with the similar pattern of MS 261 (M^++1) in CI mode. This agrees with adduct (9) lose water. Flash chromatography of the residue with 20% ethyl acetate in hexanes as the eluant provided (11). The structure (11) was assigned based on MS, ^1H NMR, ^{13}C NMR and IR. For the ^1H NMR spectrum in CDCl3, when the signal at 2.24 ppm (H_2, H_3) was irradiated, the CH_3 signal sharpened to a double (J = 1.0 Hz) and two methine protons (H_1, H_4) become a AB pattern of two doublets (J = 5.1 Hz). When the signal at 3.79 ppm (H_1) was irradiated, the signal at 3.48 ppm (H_4) became a broadened triplet (J = 7.5 Hz).
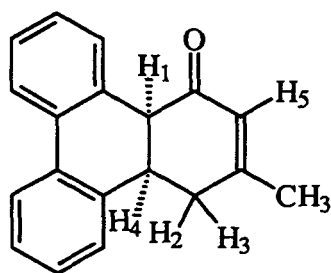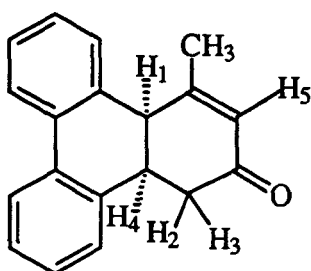
(11)   (12)

4-2.3 Determination of Quantum Yield of (9)

81

A stock solution(A) of PN (356.8 mg) and hexadecane (internal standard, 226.8 mg) in dioxane(100 ml) was prepared. This solution (50 ml) was used to dissolve 324.0 mg of $AABF_2$ to make 0.0400 M of $AABF_2$ solution(B). Ten samples were made by pipetting 5.00, 3.00, 2.50, 2.00, 1.75, 1.50, 1.30, 1.10, 1.00, 0.80 ml of solution(B) into 0.00, 2.00, 2.50, 3.00, 3.25, 3.50, 3.70, 3.90, 4.00, 4.20 ml of solution(A), respectively. The samples containing PN (2.0×10^{-2} M), hexadecane (1.0×10^{-2} M) and various concentrations of $AABF_2$ (0.0064-0.0400 M). The samples were placed in 10 pyrex tubes and purged with nitrogen. These tubes were irradiated with RPR 3500A light source for 14 minutes to cause less than 8% conversion of PN as determined by GC analysis. The yield of (9) as determined by GC was used to calculate the quantum efficiency against an actinometry of benzophenone (5.0×10^{-2} M) and benzhydrol (1.0×10^{-1} M). The plot of $1/\Phi$ against $1/[AABF_2]$ is in Fig. (2-2).

4-2.4 Triplet Sensitization

Three solutions (3.0 ml) containing PN (2.0×10^{-2} M), $AABF_2$ (2.0×10^{-2} M) and $C_{16}H_{34}$ (1.0×10^{-2} M as I.S.) were prepared in dioxane. Solution (1) was served as the control sample in which did not contain the sensitizer. Solution (2) and (3) were contained acetophenone (0.200 M) and benzophenone (0.200 M), respectively. After 10 minutes degassed, three solutions were irradiated for one and half hour with 350 nm lamps. GC analysis (at $230^{0}C$) showed that adduct (9) was only formed in solution (1) with 20% yield. No product peaks were observed in solution (2) and (3).

4-2.5 Investigation the Possibility of formation of the Ground State Complex (GSC) of PN with AABF$_2$

The dioxane solutions containing PN (5.4×10^{-4} M) and AABF$_2$ (0.0, 2.0 $\times 10^{-3}$, 2.0 $\times 10^{-2}$ M) were made. Absorptions were recorded. The absorption spectra of PN showed that no new absorption band was observed upon addition of AABF$_2$, indicating no formation of a ground state complex of PN with AABF$_2$.
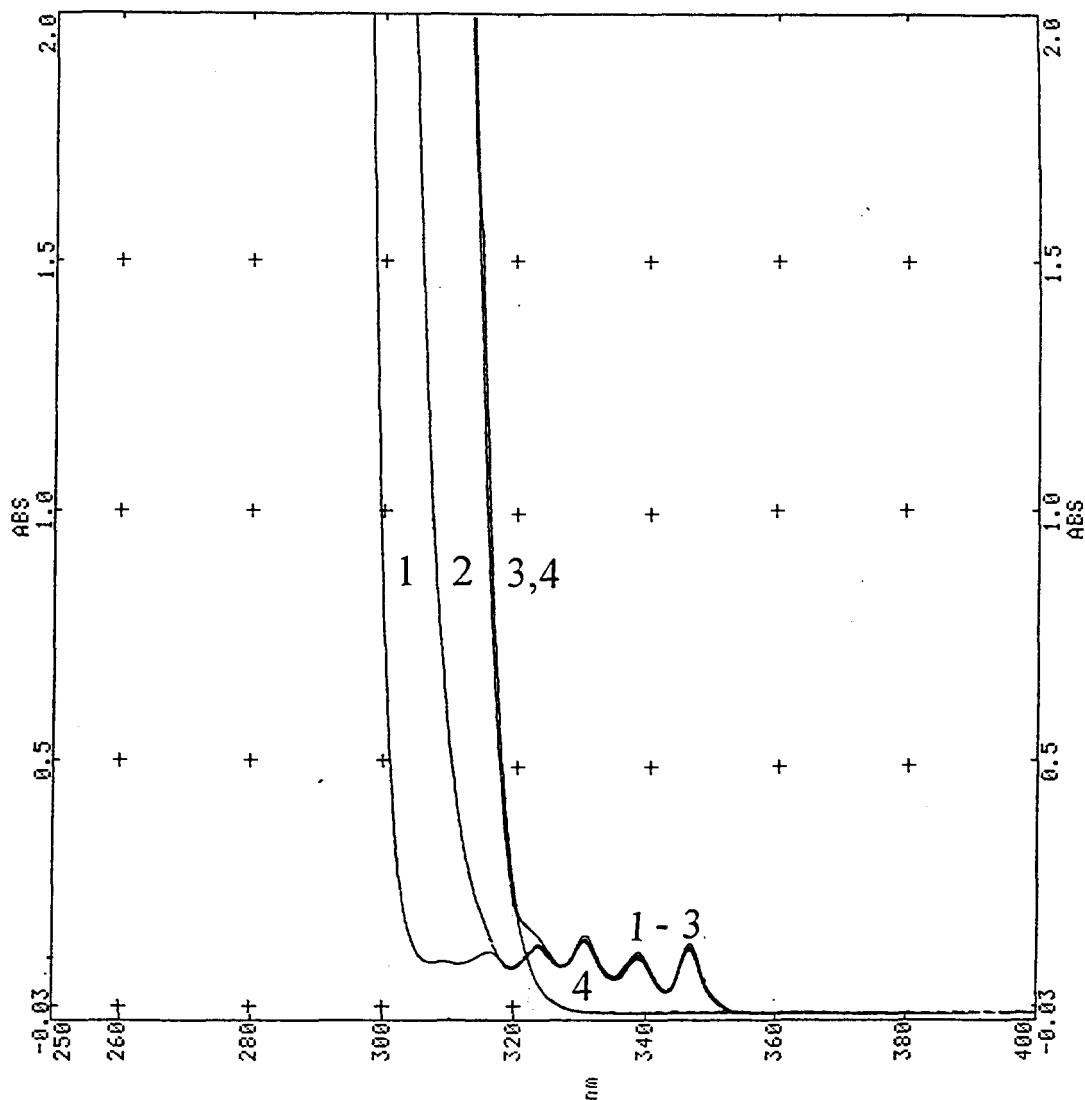
Fig.4-2 The absorption spectra of PN in dioxane with various concentration of AABF$_2$, curve 1 to 3, [PN] = 5.4×10^{-4} M, [AABF$_2$] = 0.0, 2.0 $\times 10^{-3}$, 2.0 $\times 10^{-2}$ M, curve 4 [PN] = 0.0 M, [AABF$_2$] = 2.0 $\times 10^{-2}$ M.

4-2.6 The Emission of PN and Quenching Study

(a)   Fluorescence and Phosphorescence of PN

The total emission of PN was obtained at 77°k (liq. N_2) with 1:3 ratio of i-propanol : Et_2OH as solvent without chopper.   The emission intensities were not affected by $AABF_2$ presence ($[AABF_2]$ up to 0.25M).

(b)   Quenching of PN fluorescence by $AABF_2$ at room temperature

PN solutions (2.0×10^{-3} M - 2.0×10^{-4} M) in diethyl ether or dioxane were prepared for fluorescence quenching studies.   The experiments were carried out by either direct injecting a known volume of a stock solution of $AABF_2$ into 3.0 ml of fluorescence cell or adding a known amount of stock solution of $AABF_2$ in 5.0 ml volumetric flask to make separated solution.   A correction for dilution effect was made when quencher was directly injected into fluorescence cell.   The fluorescence measurements were carried out in both aerated and deaerated condition using 1.0 cm fluorimeter cell sealed with a rubber septum.   The experimental data are listed in (Table 4-1).   The fluorescence intensities ratio, I^0/I, were plotted against the $AABF_2$ concentrations to give corresponding Stern-Volmer constants.

Table (4-1):   Quenching of PN Fluorescence by $AABF_2$ [a,b]

[$AABF_2$] aerated	I^0/I (386 nm)	[$AABF_2$] Purged	I^0/I (386 nm)
0.00	1.00	0.00	1.00
0.002	1.22	0.002	1.52
0.005	1.62	0.005	2.33
0.010	2.14	0.010	3.73
0.016	2.89	0.016	5.33
0.024	3.88		
$Ksv = 120$		$Ksv = 276$	

a.   The separated stock solution were made to avoid dilute effect in these studies.

b.   The solution were contained PN (5.0×10^{-4} M) and various concentration of $AABF_2$. Fluorescence were recorded under 350 nm excitation wavelength.

(c)   Quenching of PN Fluorescence by 3,3-dimethylbutene, 1,3-pentadiene and Anisole

A 2.0×10^{-5} M of PN in dioxane was prepared. The quenching studies were carried by injecting the necessary amount of quencher with a microsyringe, (dilution affect were corrected), I^0/I were analyzed to give Stern-Volmer constant.

85

4-2.7   Solvent Effect on Exciplex Fluorescence

The solutions of $[PN] = 4.0 \times 10^{-4}$ M and $[AABF_2] = 0.042$ M in carbon tetrachloride, dioxane, chloroform, and methylene chloride were made. Their fluorescence spectra were taken, and their exciplex peak wavenumbers (υ_{max}) were plotted against those of the $DBMBF_2/p$-xylene system (Fig. 2-7) serving as reference.

4-2.8   Quenching of Exciplex Emission by 1,3-pentadiene, Anisole

Dioxane solution containing PN (5.0×10^{-4}) and $AABF_2$ (2.0×10^{-2} M) was purged with argon to take fluorescence spectra in the absence and the presence of 1,3-pentadiene (0-0.0818 M), which 1,3-pentadiene was injected with a microsyrings. The experimental data are listed in Table 4-2. Since the total addition volume of quencher was less than 25 μl, the dilution effect was ignored. The similar experiments with a solution of $[PN] = 4.1 \times 10^{-3}$ M and $[AABF_2] = 0.1010$ M were carried out using anisole as quencher (0-0.0579 M) in both aerated and argon purged conditions. The experimental data are listed in Table 4-3.

Table (4-2): Quenching of PN/AABF$_2$ Exciplex Fluorescence intensity by 1,3-pentadiene in dioxane: (298 K) [a,b]

[1,3-pentadiene] (M)	I_{ex}^0/I_{ex}(475nm) [c]	I_m^0/I_m (365 nm) [c]	$I_{ex}^0/I_{ex} \div I_m^0/I_m$
0.00	1.00	1.00	1.00
0.0164	1.04	1.01	1.03
0.0327	1.09	1.01	1.07
0.0491	1.13	1.02	1.11
0.0654	1.19	1.03	1.16
$kq^{ex}\tau$ (M^{-1})		2.2 ± 0.2	

(a)   Solution of PN (5.0 x 10^{-4} M), AABF$_2$ (2.0 x 10^{-2} M) and 1,3 pentadiene (0 - 0.0818 M) were purged with argon.

(b)   Their fluorescence were recorded using 335 nm excitation wavelength at room temperature.

(c)   The exciplex of PN/AABF$_2$ and PN quenching were monitored at 475 nm and 365 nm, respectively.

Table (4-3)   Quenching of PN/AABF$_2$ Exciplex Emission by Anisole [a,b,c]

[anisole] (M)	I_{ex}^0/I_{ex} (480 nm)	I_m^0/I_m (368 nm)	$I_{ex}^0/I_{ex} \div I_m^0/I_m$
aerated solution			
0.00	1.00	1.00	1.00
0.0146	1.12	1.01	1.11
0.0291	1.23	1.02	1.21
0.0435	1.33	1.03	1.29
0.0579	1.46	1.04	1.40
$k_q^{ex}\tau$		6.8 ± 0.2	
Ar purged			
0.00	1.00	1.00	1.00
0.0146	1.15	1.01	1.14
0.0291	1.35	1.03	1.31
0.0435	1.50	1.05	1.43
0.0579	1.69	1.07	1.58
$k_q^{ex}\tau$		10.1 ± 0.3	

a.   The solution were contained PN (4.1 x 10^{-3} M) , AABF$_2$ (0.1010 M) and various concentration of anisole.

b.   The spectrum were recorded using 335 nm excitation wavelength.

c.   The exciplex of PN/AABF$_2$ and PN quenching were monitored at 480 nm and 368 nm.

4-2.9   Quenching of Photoaddition PN with AABF$_2$ by 1,3-pentadiene & Anisole

A solution (A) of PN (0.0200 M) and AABF$_2$ (0.0150 M) in dioxane was prepared. Either 1,3-pentadiene (136.2 mg) or anisole (324.3 mg) was dissolved in 10.00 ml solution (A) to make solution (B). Appropriate amount of solution (B) was diluted by solution (A) to give samples containing PN (0.0200 M), AABF$_2$ (0.0150 M), hexadecane (0.0100 M) and various concentration of 1,3-pentadiene (0-0.2000 M); or anisole (0-0.3000 M). The samples (5.0 ml) were pipetted in 10 ml pyrex tubes purged with N$_2$ (some cases are not purged). All tubes were mounted in the photoreaction apparatus and irradiated with 350 nm lamps for 14 minutes. Relative quantum yields ($\Phi°/\Phi$) were determined by GC analysis using C$_{16}$H$_{34}$ as internal standard.

4-2.10 Fluorescence Decay Kinetics

Fluorescence decay data of PN and exciplex (PN/AABF$_2$) were measured on a Photon Technology International (PTI) LS-1 fluorimeter using a gated hydrogen spark lamp (lamp profile typically has a fwhm of 2.2 ns) single photon counting method. The decay parameters were valued by reduced least-squares deconvolution and their quality was judged by the χ^2 values, the randomness of the weighted residuals and the autocorrelation function. The sample decay traces shown in Fig. 2-14.and Fig.2-15 The fluorescence decay profiles were fitted single exponential in pure PN existed with χ^2 value less than 1.2. The lifetimes of PN were found to be 53.8 and 26.1 ns in argon and aerated dioxane, respectively. In the presence of AABF$_2$, the fluorescence decay were fited biexponential with similar χ^2 and Durbin-Watson values. All samples were prepared individually in 5.0 ml volumetric flask with [PN] = 2.0 - 5.0 x 10^{-5} M

and various concentrations of AABF$_2$. The samples were transferred to a fluorimeter cell and either directly used or purged with Ar.

4-2.11 Flash Photolysis

Dioxane and acetonitrile solutions containing PN (~10^{-2} M) and AABF$_2$ (~10^{-2} M) were used for flash photolysis studies. The excitation sources employed was a pulsed Lumonics Nd/YAG laser (355nm, 20 mJ/pulse or less). The transient spectra were recorded by monitored 450 nm. This new system was recently completed by Dr. C. Bohne in the Chemistry Department, University of Victoria.

4-3   Spectroscopic Studies on β-Diketonatoboron Difluorides

4-3.1   Preparation   of   4-*t*-Butyl-4'-methoxy-dibenzoylmethanatoboron Difluoride (MBDBF$_2$)

The 2.8 ml (21.84 mmol) boron trifluoride etherate was injected in the 100 ml CH$_3$CN solution containing 6.10g (20.42 mmol) of 4-*t*-Butyl-4'-methoxy-dibenzoylmethane. The reaction mixture was stirred overnight at room temperature under dry nitrogen. After removed HF by purging N$_2$ and evaporated solvent by flash evaporation, the solid yellow crude product was obtained. The crude was recrystallized twice from CH$_3$CN to give 6.0g yellow-green needle crystall (yield > 85%, m.p., 241 ±1°c). MS (m/e, EI mode) 358 (M$^+$, 55), 343 (100), 135 (75), 77 (10); IR(KBr) 2972 (w), 1605 (m), 1543 (s), 1502 (s), 1462 (m), 1371 (s), 1313 (m), 1273 (s), 1244 (s), 1185 (s), 1133 (m), 1117 (m), 1094

(m), 1069 (m), 1042 (s), 953 (w), 852 (m), 794(m) cm^{-1}; NMR, δ (ppm): ^{1}H (in CDCl$_3$) 1.37(9H, s), 3.94(3H, s), 7.08(1H, s), 7.02(2H, d), 7.05(2H, d), 7.55(2H, d), 8.14(2H,d); ^{13}C (in CDCl$_3$) 31.00(3C), 35.43, 55.76, 92.23, 114.65(2C), 124.44, 126.12(2C), 128.69(2C), 129.57, 131.46(2C), 159.20, 165.60, 181.60, 181.76.

4-3.2 The Absorption Spectra And Emission of MBDBF$_2$ in Different Solvent

Solutions of MBDBF$_2$ (5.0 x 10^{-6} M) in various solvents, such as acetoritrile, dichloromethane, diethyl ether, benzene, hexanes, were prepared and absorptions of these solutions were measured. The data were listed in Table (4-4).

Table (4-4): Absorption of MBDBF$_2$ in Different Solvents

solvent	λ_{max} (nm)		ε	
CH$_2$Cl$_2$	401		60500	
CH$_3$CN	400		66000	
diethyl ether	378	395	62000	66000
hexanes	375	390	60500	61500

The emission spectra of MBDBF$_2$:

(a)   A stock solution of MBDBF$_2$ (5.0 x 10^{-2} M) in a spectroscopic grade solvent was made by weighting MBDBF$_2$ (89.5 mg) into 5 ml volumetric flask and adding CH$_2$Cl$_2$ to dissolve it. The working solutions were prepared by dilution the stock solution into different working solvents. Fluorescence of MBDBF$_2$ was recorded in different solvents and shown in Table (4-5).

Table (4-5): The Emission Date of MBDBF$_2$ in Various Solvent

solvent	[MBDBF$_2$]	λ_{ex} (nm)	λ_f^{max} (nm)	
CH$_2$Cl$_2$	5×10^{-7}	395	435	
CH$_3$CN	5×10^{-6}	400	441	
diethyl ether	5×10^{-6}	375	420	
hexanes	5×10^{-6}	375	403	427

(b)   The concentration Dependence of Emission Spectra of DBMBF$_2$

Since MBDBF$_2$ have low solubility in nonpolar solvents, concentration dependence study was carried with dichloromethane as the solvent. The right angle was used when the concentration of MBDBF$_2$ ranged from 10^{-7}-10^{-3} M. Otherwise, a front face cell (fluorescence cell arranged in the 45° geometry) was used when the concentration of MBDBF$_2$ was 5.0×10^{-2} M..

4-3.3 Quenching of MBDBF$_2$ Fluorescence Intensity in Low Concentration of MBDBF$_2$ by norbornylene, 1,3-pentadiene, methyl methacrylate and cyclohexene

The working solutions of MBDBF$_2$ (5.0×10^{-6}) in CH$_2$Cl$_2$ were prepared by adding 5 µl of 5.0×10^{-3} M of MBDBF$_2$ into 5 ml volumetric flask.   The fluorescence quenching of MBDBF$_2$ (5.0×10^{-6} M) were carried out using 395 nm excitation wavelength. The fluorescence intensity ratio, I^0/I, was determined at 430 nm. All quenchers (norbornylene, 1,3-pentadiene, methyl methacrylate and cyclohexene) were added an appropriate amount in 5ml volumetric flask. No

dilution effect was involved for those studies. The Stern-Volmer quenching rate constants can be obtained by varying the concentrations of quenchers.

4-3.4   Photcycloaddition of BABF$_2$ And MBDBF$_2$ with Olefins

General Procedures:

The following procedures were used to perform small scale photocycloaddition reaction. A solution of 1,3-diketonatokoron difluoride with olefin was irradiated in merry-go-round apparatus with 350 nm lamps (RPR3500). The reaction was monitored by either GC or UV to follow MBDBF$_2$ disappearance. After irradiation, the photolysate was washed with water, dried with magnesium sulfate and removed solvent by reducing the pressure. The residue was flash chromatographed to afford products.

BABF$_2$ With Cyclohexene:

The solution of BABF$_2$ (0.05 M, 209.8 mg) in 20 ml CH$_3$CN was distributed into 10 pyrex test tubes, cyclohexene (100 µl, 0.5 M) was injected in each tube. The solution was purged with N$_2$ for 5 minutes and irradiated for 15 hours. The photolysate showed two major GC peaks (at 190°C) at retention times (Rt) 3.60 min. (BABF$_2$), 5.91 min. (product). The product was isolated using flash chromatography (CH$_2$Cl$_2$ as eluant) to afford pale yellow oily product (21) (isolated yield: 18.9%). The spectral data of (21) are listed from Table (4-6) to Table (4-9).

MBDBF$_2$ With Norbornylene:

The acetonitrile solution (12 ml) containing MBDBF$_2$ (214.7 mg, 0.05 M) and norbornylene (564.0 mg, 0.5 M) was distributed into four pyrex tubes. These tubes were placed in merry-go-around apparatus and irradiated for seven hours. The consumption of MBDBF$_2$ was about 41% (by UV monitor). Removed the solvent, the residue was flash chromatographed to give yellow oily product (isolated yield: 43%). The spectral data of (22) are listed from Table (4-6) to Table (4-9). The decoupling experiment and ^{1}H noe experiment suggested that structure (22a) was preferable one.

MBDBF$_2$ with 1,3-pentadiene:

The solution (20 ml CH$_3$CN) of MBDBF$_2$ (71.56 mg, 0.01 M) and 1,3-pentadiene (200 µl, 0.1 M) was irradiated for one hour. The UV spectra showed that there was 95% consumption of MBDBF$_2$. Removed the solvent, the residue was flash chromatographed using CH$_2$Cl$_2$ to give 45.3 mg (63.1%) mixture of (23a) and (23b), which was implied by ^{1}HNMR to be a mixture of (23a) and (23b) in the ratio of 6:4. The spectral data of 23 are listed from Table (4-6) to Table (4-9).

MBDBF$_2$ With Methyl Methacrylate:

A solution of MBDBF$_2$ (376.0 mg) and methyl methacrylate (1.061 g) in 21 ml of CH$_2$Cl$_2$ purged with N$_2$ was irradiated for 12 hours. GC analysis (250°C) of photolysate shown that 80% of MBDBF$_2$ was consumed and one major peak

and one small peak appeared. The crude photolysate was removed solvent and the residue was chromatographed (20% ethyl acetate in hexanes) on a silica gel column. The major product (140 mg) was obtained (40%). The structure (24) was assigned based on spectral data shown form Table (4-6) to Table (4-9).

Table (4-6): IR Data of Cycloadducts of MBDBF$_2$ With Olefins

Adduct	υ (cm^{-1})			
(11)	3049 (w)	2908 (w)	2375 (w)	1661 (s)
	1650 (m)	1484(w)	1437 (m)	1378 (w)
	1290 (w)	1255 (w)	759 (m)	738 (m)
(21)	3060 (w)	2930 (s)	2857 (m)	1714 (s)
	1675 (s)	1596 (m)	1580 (m)	1448 (s)
	1410 (w)	1371 (w)	1357 (m)	1254 (m)
	1216 (m)	1178 (m)	1162 (m)	1002 (w)
	977 (w)	946 (w)	795 (w)	760 (w)
	702 (w)	661 (s)		
(22)	3075 (w)	2956 (s)	2870 (m)	2840 (w)
	1673 (s)	1601 (s)	1575 (m)	1510 (m)
	1462 (m)	1408 (m)	1366 (m)	1259 (s)
	1228 (s)	1169 (s)	1109 (m)	1032 (m)
	995 (m)	913 (w)	821 (m)	731 (m)
	696 (w)			
(23)	2963 (s)	2870 (w)	1680 (s)	1601 (s)
	1575 (m)	1510 (m)	1462 (m)	1408 (m)
	1364 (m)	1307 (w)	1260 (s)	1170 (s)
	1109 (m)	1029 (s)	980 (m)	802 (s)
	731 (w)	694 (w)		
(24)	2963 (s)	1736 (s)	1679 (s)	1602 (s)
	1576 (m)	1511 (m)	1461 (m)	1419 (w)
	1365 (m)	1306 (m)	1259 (s)	1172 (s)
	1110 (m)	1063 (w)	1029 (m)	970 (m)
	912 (w)	844 (m)	732 (m)	

Table (4-7): GC-MS Data of MBDBF$_2$ And Cycloadducts of MBDBF$_2$ With Olefins

Adduct	m/e (CI)	m/e (EI)		
(11)		261 (M$^+$+1, 1.8)		260 (M$^+$, 5.9)
		179 (14.7)		178 (100)
(21)	245 (M$^+$ + 1)	187 (15)	105 (100)	77 (35)
(22)		404 (M$^+$,9)	337 (6)	255 (25)
		229 (25)	161 (65)	150 (63)
		135 (100)	77 (13)	
(23)		378 (M$^+$,9)	310 (4)	243 (1)
		229 (2)	217 (3)	200 (3)
		161 (80)	135 (100)	
(24)		410 (M$^+$,3)	350 (3)	310 (25)
		161 (100)	135 (60)	

Table (4-8): ^{13}C Chemical Shift of Cycloadducts of MBDBF$_2$ With Olefins

Adduct	δ (ppm) in CDCl$_3$			
(11)	199.24	162.56	137.54	134.07
	133.26	130.48	128.31	128.09
	128.00	127.81	127.40	126.28
	124.34	123.68	49.38	39.98
	34.76	29.69	24.17	
(21)	207.85	203.45	136.95	132.76
	128.61(2c)	128.09 (2c)	46.15	43.97
	32.71	30.45	29.53	25.62
	23.66	22.75		
(22)	202.04	198.36	163.30	156.45
	135.68	130.42	130.20 (2c)	128.10 (2c)
	125.54 (2c)	113.52 (2c)	55.39	52.06
	43.26	41.68	40.95	39.36
	35.02	31.06 (3c)	29.56	29.38
(24)	197.65	196.65	174.66	163.47
	156.58	132.62	130.91	130.33 (2c)
	128.57 (2c)	125.55 (2c)	113.70 (2c)	56.27
	55.42	52.45	35.06	33.55
	33.28	31.02 (3c)	21.58	

Table (4-9): ^{1}H Chemical Shift of Cycloadducts of MBDBF$_2$ With Olefins

Adduct	δ (ppm) in CDCl$_3$
(11)	6.03 (H$_5$, s)　　3.79 (H$_1$, d)　　3.48 (H$_4$, dt)　　2.24 (H$_2$,H$_3$,bm) 1.89 (CH$_3$, bs)　7.05-7.81 (8H, m) J$_{1,4}$ = 5.1 Hz　J$_{5,CH3}$ = 1.0 Hz　　J$_{4,2}$ or J$_{4,3}$ = 7.5 Hz J$_{-CH2'-CH3}$ = 0.5 Hz
(21)	3.64 (H$_1$, m)　　2.55 (H$_4$, m)　　2.53 (H$_3$, dd)　　2.45 (H$_2$, dd) 2.01 (Me, s)　　1.83 (H$_5$, m)　　1.81 (H$_6$, m) 1.40-1.69 (6H, H$_7$-H$_{12}$, m) 7.44-7.92 (5H, m, phenyl) J$_{2,3}$ = 16 Hz　　J$_{2,4}$ = 5 Hz　　J$_{3,4}$ = 7.5 Hz　　J$_{1,4}$ = 8 Hz
(22)	3.82 (s, 3H, -OCH$_3$)　　3.57 (H$_1$, d)　　2.85 (H$_3$, dd) 2.79 (H$_4$, m)　　2.72 (H$_2$, dd)　　2.74 (H$_5$, d) 2.07 (H$_6$, d)　　1.98 (H$_7$, bd)　　1.58 (H$_9$, H$_{11}$, H$_{12}$, m) 1.45 (H$_{10}$)　　1.32 (9H, t-butyl, s)　1.25 (H$_8$, bd) 6.83-7.85 (8H, m, phenyl) J$_{1,4}$ = 9 Hz　　J$_{3,4}$ = 4 Hz　　J$_{2,4}$ = 8.5 Hz J$_{2,3}$ = 15 Hz　　J$_{7,8}$ = 10 Hz
(23a)	5.55 (H$_7$, dq)　　5.45 (H$_6$, ddq)　　4.52 (H$_1$, ddd) 3.85 (s, 3H-OCH$_3$)　　3.00 (H$_2$, H$_3$, m)　　2.31 (H$_5$, m) 1.95 (H$_4$, m)　　1.70 (3H, dd, Me)　　1.32 (9H,s) 6.87-8.00 (8H, m, phenyl) J$_{6,7}$ = 10 Hz　　J$_{6,1}$ = 10 Hz　　J$_{6'-CH3}$ = 1 Hz
(23b)	5.64 (H$_6$, H$_7$, m)　　4.12 (H$_1$, m)　　3.85 (s, 3H) 3.00 (H2, H$_3$, m)　　2.31 (H$_5$, m)　　1.95 (H$_4$, m) 1.65 (3H, dd, Me)　　1.32 (9H, s)　　6.87-8.00(8H, m, phenyl)
(24)	3.86 (s, 3H)　　3.65 (s, 3H)　　2.92 (H$_3$, H$_4$, 2H, m) 2.46 (H$_1$, H$_2$, 2H, m)　　1.59 (s, 3H)　　1.35 (s, 9H) 6.90-7.88 (8H, m, phenyl)

REFERENCES

[1]   Morgan, G. T.; Tunstall, R. B., *J. Chem. Soc.*, **1924**, 125, 1963

[2]   (a) Hauser, C. R.; Frostick, F.C.; Mann, E. H. *J. Am. Chem. Soc.* **1952**, 74, 3231
       (b) Hauser, C. R.; Eby, C. J. *J. Am. Chem. Soc.* **1957**, 79, 725
       (c) Crimmins, T. F.; Hauser, C. R. *J. Org. Chem.* **1961**, 746, 2427

[3]   Darst, K. B.; Lukehart, C. M.; *Organometal Chem.*, **1978**, 161, 1

[4]   Toporcer, L. H.; Dessy, R. E.; Green, S. I. E.; *Inorg. Chem.*, **1965**, 4, 1649

[5]   Hanson, A. W.; Macauly, E. W. *Acta. Cryst.* **1972**, B28, 1961

[6]   (a) Sone, K. *J. Am. Chem. Soc.*, **1953**, 75, 5207
       (b) Brown, N. M. D.; Bladon, P., *J. Chem. Soc.*, A **1969**, 526

[7]   Karasev, V. E.; Kotokikh, O. A., *J. Inorg. Chem.*, **1986**, 31, 493

[8]   (a) Chalandon, P.; Susz, B. P. *Helv. Chim. Acta.* **1958**, 41, 697
       (b) Ilge, H. D.; Birchner, E.; Fassler, D.; Kozmenko, M. G.; Kuzmin, M. V.; Kuzmin, M. G. ; Hartmann, H. *J. Photochem.* **1986**, 32, 177

[9]   Halm, J. M. , *Tappi* **1977**, 60, 90

[10]   (a) de Mayo, P.; Takeshita, H., *Can. J. Chem.*, **1963**, 41, 440
       (b) Nozaki, H.; Kurita, M.; Mori, T.; Noyori, R., *Tetrahedron*, **1968**, 24, 1821
       (c) Challand, B. D.; Hikino, H.; Kornis, G.; Lange, G.; de Mayo, P., *J. Org. Chem.*, **1969**, 34, 794

[11]   Chow, Y. L.; Cheng, X. E., *Can. J. Chem.*, **1991**, 69, 1575

[12]   Chow, Y. L.; Cheng, X. E., *J. Chem. Soc. Chem. Commun.*, **1990**, 1043

[13]   Chow, Y. L.; Cheng, X. E.; Johansson, C. I., *J. Photochem. Photobiol. A. Chem.*, **1990**, 51, 247

[14]   Chow, Y. L.; Cheng, X. E. *Can. J. Chem.* **1991**, 69, 1575

[15]   Chow, Y. L.; Cheng, X. E. *Can. J. Chem.* **1991**, 69, 1331

[16]   Cheng, X. E. *Thesis*, Simon Fraser University, **1990**

[17]   Chow, Y. L.; Ouyang, X. X. *Can. J. Chem.* **1991**, 69, 423

[18]   Caldwell, R. A.; Creed, D. *Acc.Chem. Res.* **1980**, 13, 45

[19]   (a) McCullough, J. J., *Chem. Rev.*, **1987**, 87, 811
        (b) Creed, D.; Caldwell, R. A.; Ulrich, M. M., *J. A. Chem. Soc.*, **1987**, 100, 5831
        (c) Hacker, N. P.; McOmie, F. W. *Tetrahedron*, **1984**, 40, 5249

[20]   (a) Farid, S.; Doty, J. C.; William, J. L. R., *J. Chem. Soc. Chem. Commun.*, **1972**, 711
        (b) Miyamoto, T.; Mori, T.; Odaira, Y., *J. Chem. Soc. Chem. Commun.*, **1970**, 1598
        (c) Bryce-Smith, D.; Vickery, B., *Chem. Indu.* (London), **1961**, 429

[21]   Caldwell, R. A.; Ghal, N. I.; Chien, C. K.; DeMarco, D.; Smith, L., *J. A. Chem. Soc.*, **1978**, 100, 2857

[22]   (a) Caldwell, R. A.; Smith, L. *J. Am. Chem. Soc.* **1974**, 96, 2994
        (b) Caldwell, R. A.; Maw, T.-S. *J. Photochem.* **1979**, 11, 165

[23]   (a) Ouyang, X. X. *Thesis*, Simon Fraser University, **1990**
        (b) Johansson, C.J. Unpublished Results, Simon Fraser University, Zhang, Y. H. " Private Communication with Chow, Y. L."

[24] Turro, N. J. *Modern Molecular Photochemistry* , chapter8, Benjamin/Cummings, **1991**

[25] Beens, H.; Knibbe, H.; Weller, A. *J. Chem. Phys.*, **1967**, 47, 1183

[26] Mataga, N.; Ottolenghi, M. *Molecular Association* , *Vol.* 2 Edited by Foster,R.

[27] de b. Costa, S. M.; Macanita, A. L.; Melo, E. C. C. and Prieto, *J. Photochem.* **1979**, 11, 361

[28] Johansson, C. I. Unpublished Results, Simon Fraser University, **1994.**

[29] Beens, H.; Weller, A. *Acta Phys. Polonica*, **1968**, 34, 593

[30] Caldwell, R. A.; Creed, D; DeMarco, D. C.; Melton, L. A.; Ohta, H. and Wine, P. H. *J. A. Chem. Soc.*, **1980**, 102, 2369

[31] Creed, D.; Caldwell, R. A. *J. Am. Chem. Soc.*, **1974**, 96, 7369

[32] (a) Caldwell, R. A.; Smith, L. *J. Am. Chem. Soc.*, **1974**, 96, 2994
(b) Caldwell, R. A.; Creed, D. *J. Phys. Chem.*, **1978**, 82, 2644

[33] O'Connor, D. V.; Phillps, D. *Time-correlated Single Photon Counting,* Academic Press, **1984**

[34] (a) Lewis, F. D.; Bassani, D. M. *J. Photobiol. A. Chem.*, **1992**, 66, 43
(b) Lewis, F. D.; Holman, B. III, *J. Phys. Chem.*, **1980**, 84, 2328

[35] (a) Weller, A. *Pure & Appl. Chem.* **1982**, 54, 1885
(b) Weller, A. *Zeitschrift fur Physikalische Chemie. Neue Folge*, Bd. **1982**, 130, 129

[36] (a) Lasser, N.; Feitelson, J. *Photochem. and Photobiol.* **1975**, 21, 249
(b) Selwyn, J. C.; Scaiano, J. C. *Can. J. Chem.* **1981**, 59, 663

[37]   (a) Asanuma, T.; Grotch, T.; A.; Yamamoto, M.; Nishijima, Y. *J. Chem. Soc.,Chem.Commun.* **1977**, 485
(b) Shida, T.; Iwata, S. *J. Am. Chem. Soc.* **1973**, 95, 3475
(c) Chatterjee, P. K.; Webber, S. E. *Photochem. and Photobiol* **1990**, 52, 637

[38]   (a) Pasto, D. J. ; Johnson, C. R. *Laboratory text for organic chemistry.* Prentice, Englewood Cliffs, NJ. **1979**. pp.180-264;
(b) Sternhell, S. *Q. Rev. Chem. Soc.* **1969**, 23, 236
(c) Steliou, K. PCModel, Serena Software, **1988**

[39]   Budzikiewicz, H.; Djerassi, C.; Williams, D. H. *Mass Spectrometry of Organic Compounds*; Holden-Day. Inc: San Fraccisco. **1967**, pp. 155-157

[40]   Birk, J. B.; Porter, G. Ed., *Progress in Reaction Kinetics* **1967**, Vol. 5, pp. 184, Pergamon, Oxford

[41]   Knibbe, H. *Thesis, " Charge-Transfer Complex Formation in the Excited State"*, **1969**,Free University of Amsterdam

[42]   Caldwell, R. A.; Creed, D.; Ohta, H. *J. Am. Chem. Soc.* **1975**, 97, 3246

[43]   Birks, J. B. *Progress in Reaction Kinetics* **1970**, 5, 188

[44]   Gordon, M.; Ware, W. R., *The Exciplex*, Academic Press, New York, **1975**

[45]   Stevens, B., *Adv. Photochem.* **1971**, 8, 161

[46]   Dumas, J. N. *Excited State Lifetime Measurements*, Academic Press, New York, **1983**, pp. 240

[47]   (a) Ware, W. R. *Pure Appl. Chem.* **1975**, 41, 635
(b) Cheung, S. T.; Ware, W. R. *J. Phys. Chem.* **1983**, 87, 466

(c) O'Connor, D. V.; Ware, W. R. *J. Am. Chem. Soc.* **1976**, 98, 4706

[48] Muller, F.; Mattay, J. *Chem. Rev.* **1993**, 93, 99

[49] Gould, I. R.; Farid, S. *J. Phys. Chem.* **1992**, 96, 7635

[50] Kavarnos, G. J.; Turro, N. J. *Chem. Rev.* **1986**, 86, 401

[51] (a) Forster, T.; Kasper, K. Z. *Physik. Chem.* NF, **1954**, 1, 275
(b) Forster, T.; Kasper, K. Z. *Electrochem., Ber. Bunsenges. Physik. Chem.* **1955**, 59, 976
(c) Forster, T. *Angew. Chem. Internat. Ed.* **1969**, 8, 333

[52] Kuzmin, M. G.; Soboleva, I. V. *Progress Reaction Kinetics.* **1986**, 14, 157

[53] Casals, P.-F.; Ferard, J.; Ropert, R. *Tetrahedron Lett,* **1976**, 35, 3077

[54] Magdzinski, L. J.; Chow, Y. L. *J. Am. Chem. Soc.* ,**1978**, 100, 2444

[55] Rondan, N. G.; Paddon-Row, M. N.; Caramella, P.; Mareda, J.; Mueller, P.H. and Houk, K. N. *J. Am. Chem. Soc.* , **1982**, 104, 4974

[56] Chow, Y. L.; Wu, S. P.; Ouyang, X. X. *J. Org. Chem.* **1994**, 59, 421

APPENDICES

The Derivation of Eq. 3-1

According to Scheme 3-1 under the steady-state assumption the concentrations of PN and exciplex are

$$\frac{d^*[PN]}{dt} = I_a + k_{-a} \, {}^*[PN \cdot AABF_2] - (\Sigma k_d + k_q[AABF_2])^*[PN] = 0 \qquad \text{A-1}$$

$$\frac{d^*[PN \cdot AABF_2]}{dt} = k_q {}^*[PN][AABF_2] -$$

$$(\Sigma k_d^{ex} + k_r + k_{-a} + k_q^{ex}[AABF_2])^*[PN \cdot AABF_2] = 0 \qquad \text{A-2}$$

From Eq.A-1 and Eq.A-2, the concentrations of excited state PN and exciplex ($PN \cdot AABF_2$) can be expressed as following:

$$^*[PN \cdot AABF_2] = \frac{k_q {}^*[PN][AABF_2]}{\Sigma k_d^{ex} + k_r + k_{-a} + k_q^{ex}[AABF_2]} \qquad \text{A-3}$$

The back reaction efficiency (f):

$$f = \frac{k_{-a}}{\Sigma k_d^{ex} + k_r + k_{-a} + k_q^{ex}[AABF_2]} \qquad \text{A-4}$$

The *[PN] is substituting Eq.A-3 and Eq.A-4 in to Eq A-1, we obtain Eq.A-5,

$$^*[PN] = \frac{I_a}{\Sigma k_d + (1-f) \, k_q[AABF_2]} \qquad \text{A-5}$$

By definition, the quantum yield of the cycloaddition (Φ_p) is expressed as follows,

$$\Phi_p = \frac{k_r*[PN.AABF_2]}{I_a}$$

$$= \frac{k_r \dfrac{k_q*[PN][AABF_2]}{\Sigma k_d^{ex} + k_r + k_{-a} + k_q^{ex}[AABF_2]}}{\Sigma k_d + (1-f)\, k_q\, [AABF_2]}$$

$$= \frac{k_r\, k_q\, [AABF_2]}{(\Sigma k_d^{ex} + k_r + k_{-a} + k_q^{ex}[AABF_2])(\Sigma k_d + (1-f)\, k_q\, [AABF_2])} \qquad \text{A-6}$$

Then Eq.3-1 is obtained as Eq.A-7 by rewritted Eq.A-6.

$$1/\Phi_p = \frac{(\Sigma k_d^{ex} + k_r + k_{-a} + k_q^{ex}[AABF_2])(\Sigma k_d + (1-f)\, k_q\, [AABF_2])}{k_r\, k_q\, [AABF_2]} \qquad \text{A-7}$$

The Derivation of Eq.2-6

According to Scheme 3-1 under steady-state assumption in the presecnce of the second quencher, the concentrations of PN and exciplex are

$$d*[PN \cdot AABF_2] / dt = k_q*[PN][AABF_2] -$$
$$(\Sigma k_d{}^{ex} + k_r + k_{-a} + k_q{}^{ex}Q_2 + k_q{}^{ex}[AABF_2]*[PN \cdot AABF_2] = 0 \qquad \text{B-1}$$

$$\frac{d*[PN]}{dt} = I_a + k_{-a}*[PN \cdot AABF_2] - (\Sigma k_d + k_q[AABF_2] + k_{q'}Q_2)*[PN] = 0 \qquad \text{B-2}$$

From Eq.B-1 and B-2, *[PN] and [PN.AABF2] can be expressed as followings:

$$*[PN \cdot AABF_2] = \frac{k_q*[PN][AABF_2]}{\Sigma k_d{}^{ex} + k_r + k_{-a} + k_q{}^{ex}[AABF_2] + k_{q'}{}^{ex}[Q_2]} \qquad \text{B-3}$$

$$*[PN] = \frac{I_a}{\Sigma k_d + k_q[AABF_2] - f\, k_q[AABF_2] + k_{q'}[Q_2]} \qquad \text{B-4}$$

Where:

$$f = \frac{k_{-a}}{\Sigma k_d{}^{ex} + k_r + k_{-a} + k_q{}^{ex}[AABF_2] + k_q{}^{ex}[Q_2]}$$

By definition, the quantum yield of the cycloaddition (Φp) is expressed as followings,

In the presence of the second quencher, Φp:

$$\Phi p = \frac{k_r^* [PN \cdot AABF_2]}{Ia}$$

$$= \frac{k_r k_q [AABF_2] / \Sigma k_d{}^{ex} + k_r + k_{\text{-}a} + k_q{}^{ex}[AABF_2] + k_{q'}{}^{ex}[Q_2]}{\Sigma k_d + (1\text{-}f) k_q[AABF_2] + k_{q'}[Q_2]} \qquad \text{B-5}$$

In the absence of the second quencher, Φp:

$$\overset{o}{\Phi p} = \frac{k_r k_q [AABF_2] / \Sigma k_d{}^{ex} + k_r + k_{\text{-}a} + k_q{}^{ex}[AABF_2]}{\Sigma k_d + (1\text{-}f) k_q[AABF_2]} \qquad \text{B-6}$$

When the concentration of $AABF_2$ is fixed, the $k_q{}^{ex}[AABF_2]$ is constant.

where : $X = \Sigma k_d{}^{ex} + k_r + k_{\text{-}a} + k_q{}^{ex}[AABF_2]$

$\quad\quad\quad Y = \Sigma k_d + (1\text{-}f) k_q[AABF_2]$

$$\Phi p^o / \Phi p = (X + k_{q'}{}^{ex}[Q_2])(Y + k_{q'}[Q_2]) / XY \qquad \text{B-7}$$

As we know the second quenchers (such as 1,3-pentadiene, anisole) only quench exciplex without quenching PN significantly.

$\quad\quad\quad k_{q'}{}^{ex} >> k_{q'}$

Eq.2-6 is obtained from Eq.B-7

$\Phi p^o / \Phi p = 1 + K_{sv}[Q_2]$ \qquad\qquad\qquad B-8